

UCLA

UCLA Electronic Theses and Dissertations

Title

Investigation of Multi-Modal Haptic Feedback Systems for Robotic Surgery

Permalink

<https://escholarship.org/uc/item/3zt786q3>

Author

Abiri, Ahmad

Publication Date

2017

Peer reviewed|Thesis/dissertation

UNIVERSITY OF CALIFORNIA

Los Angeles

INVESTIGATION OF MULTI-MODAL HAPTIC FEEDBACK
SYSTEMS FOR ROBOTIC SURGERY

A dissertation submitted in partial satisfaction of
the requirements for the degree Doctor of Philosophy
in Bioengineering

by

Ahmad Abiri

2017

© Copyright by

Ahmad Abiri

2017

ABSTRACT OF THE DISSERTATION

INVESTIGATION OF MULTI-MODAL HAPTIC FEEDBACK SYSTEMS FOR ROBOTIC SURGERY

by

Ahmad Abiri

Doctor of Philosophy in Biomedical Engineering

University of California, Los Angeles, 2017

Professor Warren Grundfest, Chair

The advent of minimally invasive surgery (MIS) led to significant benefits for patients at a cost of increase technical difficulty for surgeons. Robotic minimally invasive surgery (RMIS) was introduced to help eliminate some of the outstanding challenges by introducing improvements such as enhanced 3D vision and additional degrees of freedom. Unfortunately, RMIS resulted in a complete loss of haptic feedback, a problem that has persisted even after more than a decade of technology development.

The limitations introduced by the loss of feedback in robotic surgery gave birth to innovations and significant research on haptic feedback systems (HFS). These systems aimed to provide an artificial sense of touch. Researchers have focused on many varieties of feedback technologies, most often relying on one specific feedback modality to help improve performance in a few, limited robotic surgical procedures.

This research project set out to investigate multi-modal haptic feedback systems capable of providing benefits for many different robotic surgical applications. Having inherited an existing tactile feedback system designed for reducing crush injuries in robotic surgical procedures, this project implemented various critical enhancements for pneumatic normal force tactile feedback. Improvements to the sensing technology such as design of shear sensing mechanisms helped expand the application of haptics beyond grip force reduction.

The development and integration of additional modalities of feedback including kinesthetic force feedback and vibration feedback, and design of a highly configurable software architecture allowed the application of the multi-modal HFS in several different RMIS applications. Evaluation of the system for knot tying in robotic surgery showed significant benefits in reducing suture breakage and improving knot quality. Application of the multi-modal HFS for palpation in robotic surgery helped improve detection non-compressible structures such as tumors and vessels in soft tissue phantoms. Finally, the system improved upon the previously developed unimodal tactile feedback systems with regards to reduction of grip force in RMIS.

The results of these investigations highlight the importance of developing multi-modal haptic feedback systems that are able simulate the synergistic relationship between the various feedback modalities involved in real human touch. Robotic surgical systems have long been held back by their lack of comprehensive haptic feedback solutions. Multi-modal haptic feedback systems hold the promise of eliminating this long-standing problem and helping expand the application of robotics in surgical sciences.

The dissertation of Ahmad Abiri is approved.

Erik P. Dutson

Peyman Benharash

Robert N. Candler

Shyam Natarajan

Tzung K. Hsiai

Warren Grundfest, Committee Chair

University of California, Los Angeles

2017

Dedicated to my beloved parents and
my brother and sister

TABLE OF CONTENTS

1	Introduction	1
2	Background	5
2.1	Minimally Invasive Surgery (MIS)	5
2.1.1	Laparoscopic Surgery	5
2.1.2	Robotic Surgery	7
2.2	Clinical Implications Of Robotic Surgery Without Haptic Feedback.....	8
2.3	Feedback Modalities	10
2.3.1	Sensory Substitution	10
2.3.2	Haptics & Sensory Augmentation	11
2.3.3	Biology of Touch	11
2.4	Haptic Feedback Systems.....	12
2.4.1	Sensing Technologies	13
2.4.2	Actuation and Feedback Technologies	17
2.4.3	CASIT’s Tactile Feedback System.....	19
2.4.4	Limitations & Drawbacks of CASIT’s Tactile Feedback System	20
2.4.5	Multi-Modal Haptic Feedback System	21
3	Research Objectives	23
4	Investigation of Inter-Subject Variations in HFS Studies	25
4.1	Visual-Perceptual Mismatch	26
4.1.1	Methods.....	29
4.1.2	Results.....	32
4.1.3	Discussion.....	33

4.2	Sensory Adaptation	34
5	Improving CASIT's Tactile Feedback System.....	36
5.1	Task A: Development of a New Sensor Board	36
5.2	Task B: Improving the Pneumatic Normal Force Feedback Actuators	38
5.2.1	Design of Depressed-Membrane Pneumatic Actuators	38
5.2.2	Evaluation of Depressed-Membrane Pneumatic Actuators	42
5.3	Task C: Improving the Normal Force Sensing Mechanism.....	45
5.4	Task D: Development of Shear Sensors.....	48
5.4.1	Design of Shear Sensors	48
5.4.2	Calibration of Shear Sensors.....	51
5.5	Summary of Tactile Feedback System Improvement	52
6	Developing A Multi-Modal Haptic Feedback System	54
6.1	Multi-Modal HFS Design Criteria	55
6.2	Low Latency Wireless Communication.....	55
6.2.1	Programming of ESP8266 WiFi Module.....	56
6.2.2	Evaluation of WiFi Module Response Time	58
6.3	System Architecture	58
6.4	Haptics Manager Software.....	60
6.4.1	Sensor Data Processor.....	63
6.4.2	Logic Engine.....	63
6.4.3	Statistical Analysis.....	74
6.5	Pneumatic Tactile Feedback.....	79
6.6	Vibration Feedback	80

6.7	Kinesthetic Force Feedback	81
6.7.1	Kinesthetic Force Feedback Using Raven II Console	82
6.7.2	Pneumatic Kinesthetic Force Feedback	83
6.8	Multi-Modal HFS Control Hardware	87
6.9	System Delay Measurements	90
6.9.1	Sensor Board Delay	90
6.9.2	Total System Delay	91
6.9.3	Haptics Manager Software Processing Time Delay	92
6.10	Multi-Modal HFS Summary	93
7	Evaluation of Multi-Modal HFS	94
7.1	A Suture Breakage Warning System	94
7.1.1	Suture Failure Loads in Robotic Surgery	95
7.1.2	Evaluation of a Suture Breakage Warning System	103
7.2	A Hybrid Vibro-Tactile HFS for Tissue Palpation	109
7.2.1	Vibro-Tactile Hybrid HFS	109
7.2.2	Vibro-Tactile Hybrid HFS using Normal Force Sensing Array	115
7.3	Kinesthetic-Tactile Hybrid HFS for Grip-Force Reduction	121
7.3.1	Kinesthetic-Tactile Hybrid HFS	121
7.3.2	Pneumatic Kinesthetic-Tactile Hybrid HFS	128
7.3.3	Ex-Vivo Studies	132
7.4	A Tri-Modal Haptic Feedback System	138
7.4.1	Methods	139
7.4.2	Results	140

7.4.3	Discussion	141
8	Conclusion	142
9	Future Work.....	145
9.1	Adaptive Haptic Feedback	145
9.2	Bi-Axial Shear Sensing	146
9.3	Tri-Axial Tactile Feedback Actuators	147
9.4	Pre-Clinical Evaluation of Multi-Modal HFS	147
10	References	149

LIST OF FIGURES

Figure 1: Minimally invasive surgery performed using laparoscopic instruments ³²	5
Figure 2: Laparoscopic Liver Surgery ³³	6
Figure 3: Intuitive Surgical's da Vinci IS1200 Surgical System ²⁰	7
Figure 4: Focal Hemorrhage in Muscularis Propria caused during a bowl run in porcine model ²⁰ 9	
Figure 5: Mechanoreceptors involved in tactile and kinesthetic force feedback in humans	12
Figure 6: Sensors Mounted on da Vinci Instruments.....	14
Figure 7: Tekscan Flexi-Force Sensors.....	15
Figure 8: Capacitive Shear Sensor Design Concepts.....	16
Figure 9: Tactile Feedback Actuators	18
Figure 10: Commercially available robotic surgical systems with Kinesthetic Force Feedback technology.....	18
Figure 11: CASIT Tactile Feedback System (2013).....	19
Figure 12: CASIT Tactile Feedback System (2013) Installed on da Vinci IS1200 Surgical System	20
Figure 13: Variations in effectiveness of HFS during in-vivo robotic studies.	21
Figure 14: Aligned and Misaligned Conditions Caused by Utilization of the Clutch Operation .	28
Figure 15: Visual-Perceptual Mismatch Study Setup.....	29
Figure 16: The results of the visual perceptual mismatch study.....	32
Figure 17: Flat, Silicon-Based Pneumatic Actuators While Inflated.....	35
Figure 18: Sensor Board Packet Format	37
Figure 19: Newly Designed Sensor Board.....	37
Figure 20: Calibration of Tekscan FlexiForce 1lb Sensor	38

Figure 21: Depressed Membrane Actuator Design Concept	39
Figure 22: Design of 3D-Printed Depressed-Membrane Actuators.....	41
Figure 23: Side-by-side view of depressed-membrane actuator and silicone-based actuator	42
Figure 24: FlexiForce Sensors Installed on Da Vinci Prograsp Forceps	43
Figure 25: Results of Actuator Comparison Study	45
Figure 26: Traditional Sensor Mounting Mechanism vs. Sensor Installed on 3D Printed Mounting Plate.....	47
Figure 27: Uni-axial Shear Sensor Design.....	48
Figure 28: Shear Sensors Installed on Cadere Graspers	50
Figure 29: Mark-10 Series 3 Digital Force Gauge.....	51
Figure 30: Shear Sensor Calibration	52
Figure 31: Abstract View of Multi-Modal HFS Architecture	54
Figure 32: ESP8266 Module.....	56
Figure 33: Multi-Modal HFS System Architecture	59
Figure 34: Haptics Manager Software Architecture Using WiFi for Sensor and Control Board Communication.....	61
Figure 35: Logic Engine Configuration Page	64
Figure 36: Data Filter Collection Configuration Page	64
Figure 37:Sensor Definition in Haptics Manager Software.....	66
Figure 38: Configuration of Advanced Deterministic Logic Engine (Generation 7 Decision Engine Used in Haptics Manager)	68
Figure 39: Used Sensor Selection During Feedback Rule Configuration	70
Figure 40: Feedback Profiles File Stored in Json Format.....	71

Figure 41: Haptics Manager Main Interface	73
Figure 42: Hierarchical Data Structure for Storing HFS Experimental Data	73
Figure 43: Haptics Manager Study Analyzer Main Interface	77
Figure 44: Vibration Motors Installed on 3D Printed Pneumatic Actuators	80
Figure 45: RAVEN II Surgical Robot	82
Figure 46: Feedback Motor on the Raven Surgical Console ¹¹³	83
Figure 47: Placement of Pneumatic Tube Between the Console Graspers to Provide Feedback During Grasping.....	84
Figure 48: Modified 3D Printed Actuators with Pneumatic Tube Installed for Providing Kinesthetic Force Feedback.....	84
Figure 49: Pressure Overshoot in Sentronic D Valve Seen in Green. Plot Shown in Asco’s Data Acquisition Software.	86
Figure 50: Dual-Valve Pressure Regulation System	87
Figure 51: Multi-Modal HFS Control Hardware	88
Figure 52: Schematic of the Multi-Modal HFS Control Board	89
Figure 53: Haptics Control Board Packet Format.....	89
Figure 54: Measurements of Sensor Board-Haptics Manager Software Communication Delay .	91
Figure 55: Haptics Manager Benchmarking Information Displayed Above the Real-Time Sensor Plot.....	92
Figure 56: Comparison of Suture Mounting Mechanism on da Vinci Forceps vs. Tytron System	96
Figure 57: USSC Suture Force Gauge	97
Figure 58: USSC Force Gauge Modified Using 3D Printed Components	97

Figure 59: Failure Load of Sutures when Pulled at Different Rates Using the Tytron System..	100
Figure 60: Control System of the Suture Breakage Warning System	103
Figure 61: Uniaxial Shear Sensor Installed on the Right Side of the Grasper and A Similar Mechanism Without the Sensing Component Installed on the Left Side of the Grasper	104
Figure 62: Experimental Set-up for the Suture Breakage Warning System Study Including Four Loose Knots that were Tightened by the Subject	105
Figure 63: Peak Shear Force of Trials with and without Suture Breakage Compared	106
Figure 64: The Average Number of Suture Failures/Faults and Knot Slippage (in millimeters) Per Subject.....	107
Figure 65: Control System of the Hybrid Vibro-Tactile HFS	110
Figure 66: Normal Force Sensor Installed on da Vinci Fenestrated Bipolar Forceps	111
Figure 67: Phantom Made of a Polyurethane Tube Hidden Inside a Soft EVA Foam	111
Figure 68: Comparison of Correctness Score (Number of Correct Detections) and Number of Faults (False Positives and Not Detected) in Detecting Non-Compressible Structure in Soft Tissue, Under Different Feedback Conditions	113
Figure 69: Comparison of Time-to-Completion for Localization of Non-Compressible Tubular Structure Under Different Feedback Conditions	114
Figure 70: Normal Force Sensor Array Installed on a 3D-printed Support for Palpation in Robotic Surgery	116
Figure 71: Control System of Vibro-Tactile Hybrid HFS using Normal Force Sensor Array ...	117
Figure 72: Soft Sponge Phantom with Spherical Tumor-Like Structures Hidden Inside, Palpated Using Normal Force Sensor Array	118

Figure 73: Comparison of the Number of Faults and Correctness Score (Number of Correct Detections) for Artificial Palpation in Robotic Surgery, Under Different Feedback Conditions	119
Figure 74: Control System of the Kinesthetic-Tactile Hybrid HFS Utilizing the Raven Console Motor for Kinesthetic Force Feedback	122
Figure 75: Comparison of Time-to-Completion and Number of Faults (Number of Peg Drops) Under Different Feedback Conditions Using the Raven Surgical System	124
Figure 76: Comparison of Average Grip Force Under Different Feedback Conditions Using the Raven Surgical System	125
Figure 77: Series of Event Leading to Subject Dropping the Peg When Kinesthetic Feedback is Provide on the RAVEN	126
Figure 78: Control System of the Pneumatic Kinesthetic-Tactile Hybrid HFS.....	129
Figure 79: Comparison of Average and Peak Grip Force Under Different Feedback Conditions When Utilizing the da Vinci IS1200 for Peg Transfer Tasks	130
Figure 80: Comparison of Number of Faults Under Different Feedback Conditions When Utilizing the da Vinci IS1200 for Peg Transfer Tasks	131
Figure 81: Ex-Vivo Porcine Large Intestine Handled Using da Vinci IS1200 Cadere Forceps	133
Figure 82: Comparison of Average and Peak Grip Force Between No Feedback and Kinesthetic- Tactile Feedback Condition During a Porcine Bowel Run.....	135
Figure 83: Variation in Effectiveness of Kinesthetic-Tactile HFS Among Novice Subjects in Ex- Vivo Porcine Bowel Run Study	135
Figure 84: Comparison of Average Grip Force Between No Feedback and Kinesthetic-Tactile Feedback Condition During a Porcine Bowel Run and the Variation in Effectiveness of HFS in Expert Subjects in the Same Study	136

Figure 85: Control System for a Tri-Modal HFS..... 139

Figure 86: Comparison of Average and Peak Grip Force in a Peg-Transfer Study Using Bi-Modal
and Tri-Modal HFS..... 140

Figure 87: Bi-Axial Shear Sensing Concept Based on Differential Sensing Methods..... 146

LIST OF TABLES

Table 1: Pneumatic Tactile Feedback Pressure Levels..... 79

Table 2: Comparison of 2013 Variant of CASIT's Tactile Feedback System and the Newly Developed Multi-Modal HFS 93

Table 3: Suture Failure Load and Tensile Strength Measurements Using Tytron System. Data is reported as Mean (Std. Dev.) 99

Table 4: Comparison of Failure Loads when Sutures are Pulled at Different Rates. Data is reported as Mean (Std. Dev.) 99

Table 5: Comparison of Mean Suture Failure Loads Recorded Using Tytron System and USSC Sutures Force Gauge 100

Table 6: Comparison of Suture Failure Loads Recorded Using USSC Force Gauge when Pulled Under Different Conditions with da Vinci Micro-Needle Driver. Data is reported as Mean (Std. Dev.)..... 101

ACKNOWLEDGEMENTS

I would like to thank my advisors, Dr. Warren Grundfest and Dr. Erik Dutson, for their extraordinary support and guidance these past few years, and for making my graduate experience a truly rewarding and memorable one. I truly appreciate the intellectual freedom I was given in my work, the continuous support for attending various conferences, and the encouragement I received to push forward and build upon new ideas. I would also like to thank my committee members, Dr. Robert N. Candler, Dr. Tzung K. Hsiai, Dr. Shyam Natarajan and Dr. Peyman Benharash for their valuable feedback and interest in my work.

I would also like to thank everyone at the Center for Advanced Surgical and Interventional Technology (CASIT), specifically, Ashkan Maccabi, Nathan Francis, Shijun Sung, Harrison Cheng, William Yao, George Saddik, Neha Bajwa, Zachary Taylor, Zach McKinney, Jonathan Chrin, Cheryl Hein, Alan Edwards, and Christina Hanna.

I would also like to thank the CASIT alumni Christopher R. Wottawa, Chih-Hung Aaron King, and Miguel Franco, who worked on this project and helped make this investigation possible. I would also like to thank Dr. Bryan Nowroozi for initially welcoming me into this lab and helping make it possible to pursue this research for the past four years.

I would like to thank my lab-mates, colleagues and friends for their continuous support throughout the years and for providing valuable feedback and assistance at every step of the way. Particularly I would like Dr. Alan Priester, Dr. Shyam Natarajan, Rory Geoghegan, and James Garritano who patiently listened to my ideas and helped make the CASIT laboratory into an amazing workplace. This research project has always been a collaborative effort and I would like to thank everyone who has contributed to the ongoing efforts. I would thank the great people of the Sensors and Technology Laboratory, particularly Dr. Robert N. Candler, Yuan Dai, and Dr. Omeed Paydar

who have been amazing to work with and have contributed immensely to the development of the sensor technologies used in this research project. Great thanks also go to the members of the Bionics laboratory, particularly Dr. Jacob Rosen and Dr. Ji Ma for their collaborative spirit and their valuable contribution to the work performed on the RAVEN system. I would also like to thank Dr. James Bisley in the department of Neurobiology for his assistance and guidance in experimental design and statistical analysis. Special thanks also go to the members of the Department of Medicine Statistical Code for the consulting on various statistical methods through the project.

I would like to acknowledge the generous funding provided by the National Institutes of Health (NIH)/ National Institute of Biomedical Imaging and Bioengineering under award R21-EB-013832-01A1 and R01-EB019473-01 and the John Bent Foundation.

VITA

- 2009 – 2013 Software Engineer, PredictionProbe Inc.
- 2011 University of California Irvine
B.S. Computer Engineering, B.S. Neurobiology
- 2013 University of California Irvine
M.S. Electrical and Computer Engineering
- 2013 – 2014 Sr. Development Engineer, Canon Information and Imaging Solutions Inc.
- 2013 – 2017 Graduate Student Researcher, Center for Advanced Surgical and
Interventional Technology (CASIT), UCLA, Warren Grundfest
- 2014 – 2017 Sr. Software Engineer, PredictionProbe Inc.
- 2016 M.S. Biomedical Engineering, University of California, Los Angeles

PUBLICATIONS AND PRESENTATIONS

- A. Abiri**, A. Tao, M. LaRocca, X. Guan, S. J. Askari, J. W. Bisley, E. P. Dutson, and W. S. Grundfest, “Visual--perceptual mismatch in robotic surgery,” *Surg. Endosc.*, pp. 1–8, 2016.
- A. Abiri**, O. Paydar, A. Tao, M. LaRocca, K. Liu, B. Genovese, R. Candler, W. Grundfest, and E. Dutson, “Tensile strength and failure load of sutures for robotic surgery,” *Surg. Endosc.*, 2017.
- A. Abiri**, O. Paydar, B. Genovese, U. Khrucharoen, R. Candler, E. P. Dutson, and W. Grundfest, “Suture Strength for Robotic Surgery,” in *SAGES 2015*, 2015.
- E. Dutson, C. Wottawa, B. Genovese, B. Nowroozi, J. Bisley, S. Hart, O. Paydar, U. Khrucharoen, **A. Abiri**, and W. Grundfest, “Evaluating Tactile Feedback in Robotic Surgery for Potential Clinical Application using an Animal Model,” in *SAGES 2015*, 2015.

Y. Dai, O. Paydar, **A. Abiri**, Z. Xiao, X. Guan, E. P. Dutson, W. Grundfest, and R. Candler, “Miniature Multi-Axis Force Sensor for Haptic Feedback System in Robotic Surgery,” in EMBC 2016, 2016.

A. Abiri, X. Guan, Y. Dai, A. Tao, Z. Xiao, E. P. Dutson, R. Candler, S. Member, and W. S. Grundfest, “Depressed-Membrane Pneumatic Actuators for Robotic Surgery,” in EMBC 2016, 2016.

O. Paydar, **A. Abiri**, B. Genovese, R. Candler, W. Grundfest, and E. Dutson, “Capacitive Sensors to Prevent Suture Breakage in Robotic Surgery,” in SAGES 2016, 2016.

Y.-Y. Juo, A. Mantha, **A. Abiri**, and E. Dutson, “Diffusion of Robotic-Assisted Laparoscopic Technology 2008-2013: A National Study,” in SAGES 2017, 2017.

Y.-Y. Juo, **A. Abiri**, A. Tao, J. Pensa, H. Christina, S. J. Askari, W. S. Grundfest, and E. P. Dutson, “Artificial Palpation with da Vinci Surgical Robot Using a Novel Haptic Feedback System,” in SAGES 2017, 2017.

Yuan Dai, **A. Abiri**, S. Liu, O. Paydar, H. Sohn, E. P. Dutson, and R. C. Warren S. Grundfest, “Grasper Integrated Tri-Axial Force Sensor System for Robotic Minimally Invasive Surgery,” in EMBC 2017, 2017.

1 INTRODUCTION

Since its introduction in the 1980s, Minimally Invasive Surgery (MIS) has changed the face of surgical sciences. Laparoscopic procedures have led to decreased incision size, reduced risk of infection, reduced patient trauma and shorter hospital stays¹⁻¹⁰. Despite their benefits, laparoscopic procedures placed additional burdens on surgeons, requiring extensive training to deal with limitations such as loss of degrees of freedom, 2D as opposed to 3D visual input, amplification of hand tremors and loss of tactile feedback¹¹⁻¹⁸. Robotic Minimally Invasive Surgery (RMIS), introduced in the early 2000s, attempted to address some of these shortcomings with better depth perception, increased dexterity, and reduction of hand tremors. But these benefits came at a cost. Robotic surgical systems suffered from an even more severe loss of haptic feedback, a problem that has persisted despite many advances in the field.

For more than a decade, researchers have attempted to alleviate this problem through various means of providing feedback in robotic surgical systems¹⁹⁻²⁴. A tactile feedback system was previously developed by the Center for Advanced Surgical and Interventional Technologies (CASIT), the primary research center under which this investigation took place²⁰. CASIT's tactile feedback system was designed primarily with the goal of reducing crush injuries caused by excessive grip force. By installing force sensors on the robotic on the robotic instruments, and pneumatic actuators on the robotic controls, it allowed surgeons to detect how much grip force was being applied to the tissue. In vivo investigations using this system showed that it could help reduce excessive grip force and the number of damaged sites in the tissue²⁵.

The purpose of this research project is to build upon the inherited tactile feedback system and expand it beyond its single-modality pneumatic normal force feedback design. The goal of this

research is to investigate a feedback system capable of conveying multiple modalities of feedback and through this multi-modal feedback solution, also expand the applications of haptic feedback beyond grip-force reduction. To this end, this work focuses on the design and development of a Multi-Modal Haptic Feedback System (HFS) that aims to mimic three major components of touch: Kinesthetic/Force Feedback, Tactile Feedback and Vibration Feedback.

Based on the results of in-vivo studies performed on the 2013 version of CASIT's tactile feedback system as well as additional bench top testing, a series of necessary enhancements were identified as preliminary steps prior to integration of additional feedback modalities. Furthermore, analysis of data from prior experiments led to investigations into the variations that exist between subjects in robotic surgical tasks. This work, therefore, encompasses both the implementations of the enhancements and investigations into the underlying cause of inter-subject variation in robotic studies.

A series of improvements were also identified as critical for enhancing the haptic feedback system's sensing technology, both with regards to the reliability and the manufacturing of the sensors. Beyond these enhancements, this work also introduces design and development of shear sensors, and their potential application in a suture breakage warning system for RMIS.

In addition to the aforementioned changes in the sensing technology, enhancements for the pneumatic tactile actuators were also investigated. These improvements were particular targeted at elimination of sensory desensitization occurring as a result of long-term usage of traditional flat, PDMS-based actuator.

To expand the application of haptics beyond single-modality feedback, the HFS architecture was built from the ground up with new design criteria. This work focuses on several changes critical to the implementation of multi-modal haptic feedback, which includes enhancements in

communication protocols, remote site teleoperation, low latency communication and processing, and a more flexible and configurable feedback controller.

In addition to the normal force tactile feedback, two other modalities of feedback have been investigated as part of this research project: vibration and kinesthetic force feedback. Kinesthetic force feedback has been studied in an attempt to provide a more natural sense of touch for grasping tasks in robotic surgery. More specifically, this work encompasses implementations of kinesthetic force feedback both for the RAVEN II and the da Vinci surgical systems. Vibration feedback has also been studied through various enhancements in the feedback controllers and the console-installed actuators.

This work focuses on the evaluation of the multi-modal HFS through four major investigations. The first set of experiments focus on vibration as a feedback modality and its effectiveness in reducing suture breakage in robotic surgery. The second set of studies focus on using our multi-modal HFS to allow palpation in RMIS, with the goal of assisting in detection of hidden structures such as nerves, vessels or even tumors in soft tissue. The third investigation focuses on comparison of multi-modal HFS with single-modality, normal force, tactile feedback for application in grip force reduction. These studies are designed to assist in identification of the potential benefits of a multi-modal feedback over single-modality feedback solutions. Finally, study of a tri-modal HFS was also performed with the goal of investigating the potential benefits of such a solution for reducing peak grip forces.

Together, the work performed throughout this project focuses not only on the engineering aspects of a multi-modal haptic feedback system, but also its potential benefits in several relevant clinical applications. Loss of haptic feedback has without a doubt been one of the most persistent issues in robotic surgical systems. This work aims to serve as the foundation for further investigation into

optimizations of multi-modal HFS with the goal of bringing us closer to simulating real touch and therefore expanding the application of robotics in surgical medicine.

2 BACKGROUND

2.1 MINIMALLY INVASIVE SURGERY (MIS)

The growth of minimally invasive surgery as an alternative to traditional open surgery can be largely attributed to fast patient recovery time, shorter hospital stays, and lower risks of infection as a result of the smaller incisions^{1-12,26-31}. Unlike traditional open surgeries in which large incisions are made in order to exposed the target area for treatment, MIS involves small incisions (typically less than 2cm) through which instruments, along with an endoscope are inserted (Figure 1). In MIS, the surgeon uses these instruments to gain access to the internal anatomy without inducing significant trauma to the nearby tissue. This in turn reduces the risk of infection and leads to shorter hospital stays as these small wounds quickly heal without further complications.

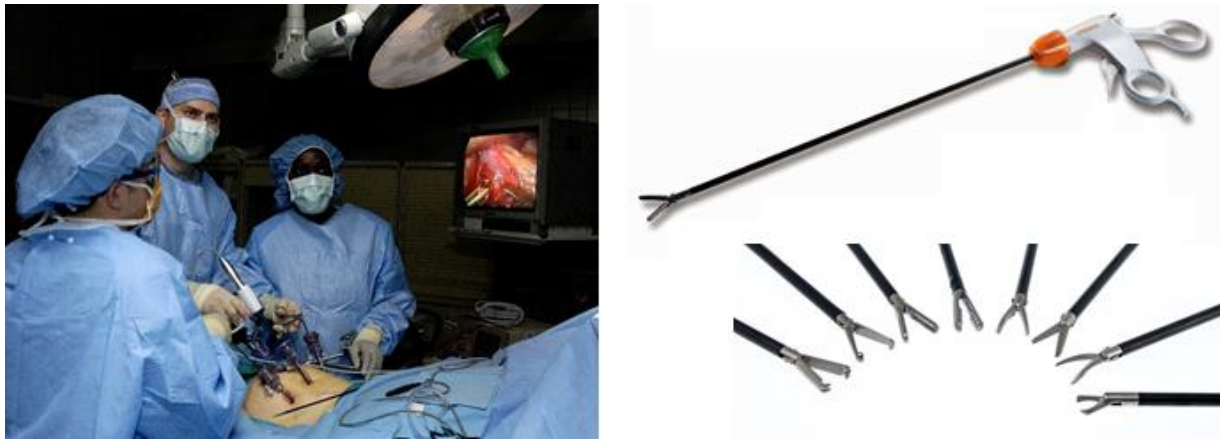


Figure 1: Minimally invasive surgery performed using laparoscopic instruments³²

2.1.1 LAPAROSCOPIC SURGERY

Laparoscopic surgery is a subset of MIS which involves procedures performed within the abdominal area. In these procedures, small incisions are created in the abdominal region and small tube-like place holders called trocars are inserted to keep the incision open (Figure 2). Instruments

are then inserted through these trocars to gain access to the internal anatomy. During a laparoscopic procedure, carbon dioxide is generated injected into the abdomen to increase the area available for performing the necessary operation using the laparoscopic tools. While many different laparoscopic tools exist, most share some basic characteristics which include, a handle for the surgeon to manipulate the tool, a long shaft and the tip of the instrument which varies depending on its function (Figure 1).

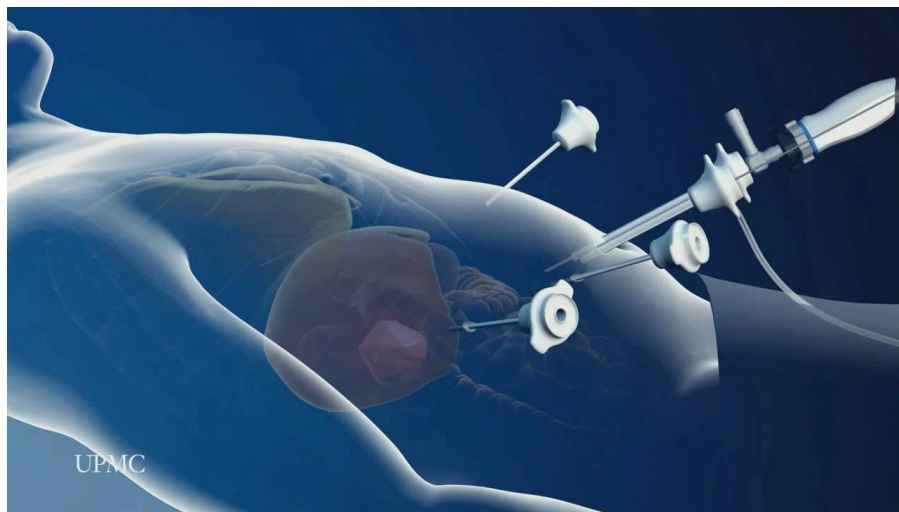


Figure 2: Laparoscopic Liver Surgery³³

Due to its benefits, laparoscopic surgery is always seen as the better alternative to laparotomy (i.e. open surgery), and due to the many advancements in this field, most surgeries can now be performed in this fashion. In fact, nearly 7.5 million laparoscopic surgeries are performed annually worldwide and this number continues to grow as new surgical techniques and minimally invasive instruments are developed^{11,12,26-31,34}.

Despite the many benefits of MIS, laparoscopic surgical techniques do suffer from certain limitations. In most cases, instruments are limited to only four degrees of freedom whereas the human hand, through wrist motion, can provide six degrees of freedom. Furthermore, the

monoscopic endoscope¹⁴, leads to a loss of depth perception. And finally, while laparoscopic instruments provide some kinesthetic force feedback, the lack of direct contact between the surgeon's hands and the tissue leads to a complete loss of tactile feedback.

2.1.2 ROBOTIC SURGERY

Research on robotic surgical systems gained attention in the 1990's with mainstream use beginning in the early 2000s^{6,35-40}. Robotic surgical systems aimed to resolve the outstanding problems with laparoscopic surgery. Improved depth perception was achieved through stereoscopic video displays, and additional degrees of freedom were provided through implementation of wrist motion on the robotic instruments and the surgical console (Figure 3). Finally software scaling and filtering algorithms allowed robotic systems to also reduce the impact of hand tremors during the procedure⁴¹⁻⁴⁴.

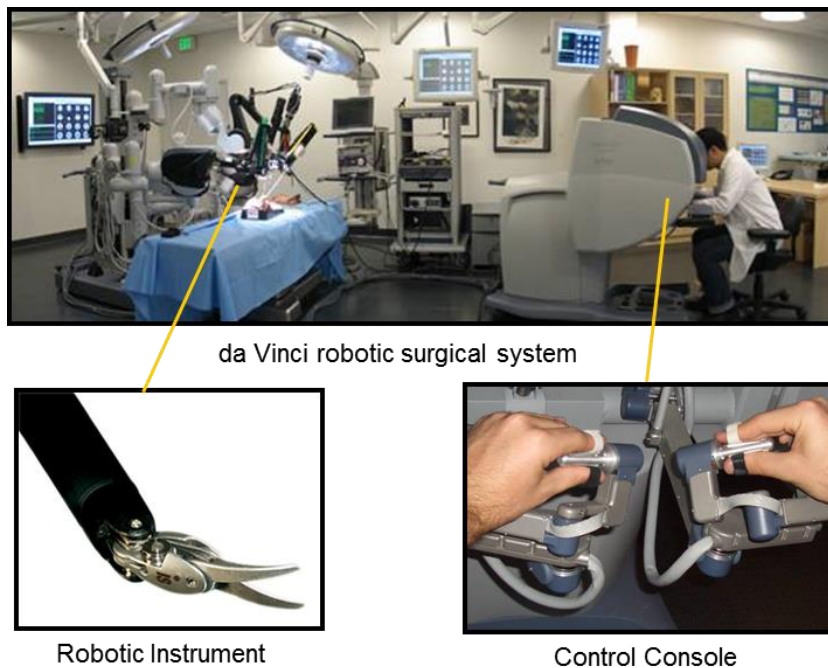


Figure 3: Intuitive Surgical's da Vinci IS1200 Surgical System²⁰

Robotic surgical systems were initially designed for only a handful of procedures^{8,9,31}, however they quickly gained popularity. In fact, since 2002, nearly 1.75 million robotic procedures have been performed in the U.S., and this number is projected to continue to increase in the next decade⁴⁵.

Just as laparoscopic surgery had faced a series of challenges, so did robotic system. Among these were high equipment costs, limitations in size and positioning of the robot⁴⁶⁻⁴⁸, lack of accessibility in large area surgeries⁴⁹, the need for additional training, limited function and arm collision in non-standard positions such as Trendelenburg⁵⁰⁻⁵³ and the complete loss of haptic feedback^{21,54-59}.

The loss of haptic feedback has been one of the most persistent issues plaguing robotic surgical systems. Despite the many improvements in robotic surgery, a complete and effective haptic feedback system remains out of reach. This is in large caused by technical challenges involving force sensing and actuation. Since robotic controls which the surgeon interacts with. have no mechanical connections to the robotic instruments that are in contact with the tissue, any effective feedback system must not only be able to sense all relevant forces on the instruments, but also convey that information to the surgeon through a simulated touch.

2.2 CLINICAL IMPLICATIONS OF ROBOTIC SURGERY WITHOUT HAPTIC FEEDBACK

Despite the lack of haptic feedback in laparoscopic and robotic surgery, these surgical techniques have been in use for many decades. Therefore, it is critical to understand the clinical impact and limitations that lack of haptic feedback has placed on laparoscopic and robotic surgeries.

During open surgery, the availability of tactile sensation allows surgeons to manipulate soft tissue without applying excessive forces. In laparoscopic and robotic surgery, metal instruments are

constantly grasping and manipulating soft tissue without the surgeon being able to easily perceive the extent of forces being applied. Research has shown that these forces can often be excessive and to lead to instances of tissue crush injury, particularly in less experienced surgeons²⁰ (Figure 4). In fact, excessive grip force is not the only performance related impact. Research has also shown that other aspects of the operation such as number of errors and total time to completion are impacted as well⁶⁰⁻⁶², leading to higher overall costs.

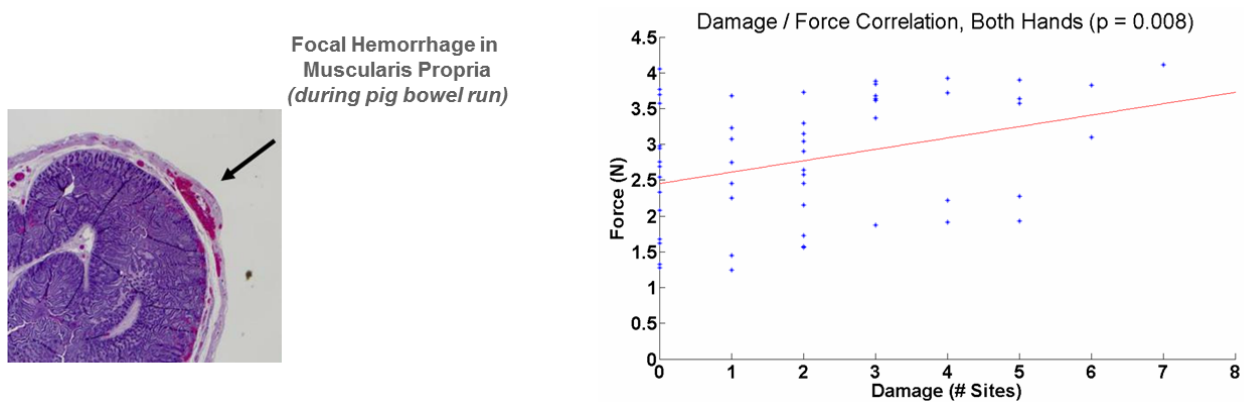


Figure 4: Focal Hemorrhage in Muscularis Propria caused during a bowl run in porcine model²⁰

Application of excessive force is not always just limited to grip forces. Excessive shear forces resulting from unnecessarily large and/or rapid displacements of the robotic arms can also lead to injuries such as tissue tearing and even suture breakage during knot tying tasks⁶³.

Another limitation that arises from the loss of haptic feedback is the loss of palpation as a means of locating various structures such as nerves, vessels and even tumors²³. Normally, palpation allows the surgeon to easily identify changes in tissue softness/hardness and therefore find various structures in soft tissue even if they are not visually identifiable. Palpation in robotic and even laparoscopic surgery can prove quite challenging since the surgeon is forced to rely purely on visual cues for identification of tissue characteristics.

Despite the growing popularity of robotic surgery, many critics have long referenced the rate of conversion of robotic procedures to laparotomy, with conversion rates ranging from 1% - 30% depending on patient comorbidities, procedure type and operator skill. Some of these conversions which can result from tissue injuries, suture breakage and operator error can be completely avoided if sense of touch could be restored through implementation of a haptic feedback system.

2.3 FEEDBACK MODALITIES

Feedback systems can utilize several different mechanisms to convey tactile information to the user. In their most abstract form, feedback technologies in surgical robotics can be categorized into two categories, sensory substitution, and sensory augmentation through haptic feedback.

2.3.1 SENSORY SUBSTITUTION

Sensory substitution is one of the most common methods for providing feedback. Sensory substitution is the process of mapping/converting data originally aimed for one sensory modality to a different sensory modality. An example of sensory substitution is sensing normal forces applied to tissue from robotic graspers and displaying it to the user as visual stimuli (ex. force vs. time plot). Feedback through sensory substitution can involve auditory, visual, electrical and even thermal stimuli. Extensive research has been done with regards to the effectiveness of sensory substitution and its ability to convey tactile information. In nearly all cases, particularly with regards to application in surgical environments involving complex tasks, it has been found that sensory substitution can lead to additional mental load and is less ideal than haptic feedback^{24,64-}

67.

2.3.2 HAPTICS & SENSORY AUGMENTATION

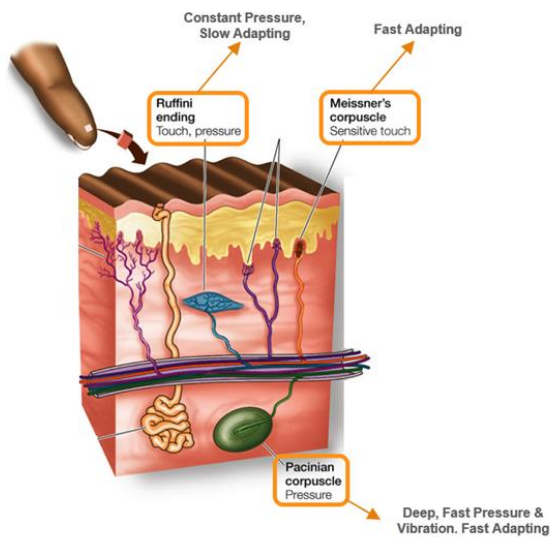
Haptics is focused on providing information to the user through a sense of touch. Its goal is to convey information to the user through simulate touch, the same way that tactile information would normally be processed in the human neurosensory pathways. An example of this type of feedback is detecting normal forces applied to tissue from robotic graspers and providing normal force feedback on the operator's fingertips.

Haptics in of itself consists of two sub-categories of feedback, tactile and kinesthetic. The reason for this breakdown is that the sense of touch involves not only the mechanoreceptors in the skin and muscles, but also the proprioceptive and attention centers of the brain.

2.3.3 BIOLOGY OF TOUCH

The effectiveness of any haptic feedback system depends largely on its ability to integrate with existing human neurosensory pathways. This has made understanding the biology of human somatosensory system critical to the engineering of effective haptic feedback systems.

Tactile Feedback



Kinesthetic Force Feedback

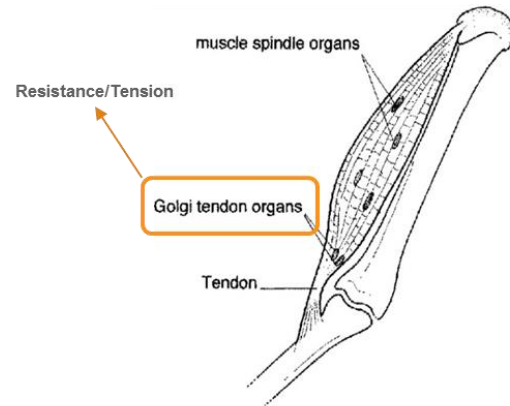


Figure 5: Mechanoreceptors involved in tactile and kinesthetic force feedback in humans

Figure 5 shows the primary mechanoreceptors involved in conveying the sense of touch. Sense of touch involves two major groups of mechanoreceptors, those in the skin and those in the muscles. In its most basic form, tactile feedback results from activation of mechanoreceptors in the skin, while kinesthetic force feedback, which provides a sense of resistance, utilizes mechanoreceptors in the muscles. The data from these sensory receptors, when combined with proprioceptive and attention centers of the brain, help control and fine tune muscular response, and drive the user's attention to critical events⁶⁸⁻⁷⁰.

2.4 HAPTIC FEEDBACK SYSTEMS

Haptic Feedback Systems are often broken down into three abstract layers: Sensing, Filtering & Control, and Actuation.

Sensing technologies which focus on detection of forces applied to the tissue can vary significantly, ranging from piezoresistive sensors installed on end effectors, to complex models

describing vibration of motors within the robot's arms^{56,71,72}. Actuation technologies on the other hand depend largely on the type of feedback that one is attempting to provide. Each actuation method usually targets a specific type of mechanoreceptor. It is therefore possible to develop multimodal feedback systems that utilize a multitude of actuators to target more than one mechanoreceptor at the same time.

Filtering & Control largely depends on the type sensor and actuator that is utilized. These components are tasked with retrieving sensor data and identifying the appropriate type and level of feedback that is to be produced.

2.4.1 SENSING TECHNOLOGIES

Development of methods for sensing forces applied to the tissue at the end effector of a robotic surgical system has been one of the most challenging problems for haptic feedback system, particularly those focused on applications in surgical robotics. This is largely due to size and biocompatibility constraints⁹.

Because of the small size of incisions in MIS, robotic and laparoscopic instruments are generally designed to move through trocars with diameters less than 12mm. This means that any sensor that is designed to be installed on either the end effector or the shaft of the tool must be significantly smaller than 12mm wide (Figure 6).



Figure 6: Sensors Mounted on da Vinci Instruments

(Left) da Vinci Cadiere grasper measuring 5mm x 14mm (Top Right) Cadiere graspers with pressure sensors installed (Bottom Right) 12mm Trocar⁷³⁻⁷⁵

In addition to size constraints, sensors positioned inside the body must be biocompatible and able to function within a wet environment without any impact on resolution and dynamic range.

Finally, the range of forces applied by different instruments can vary significantly, from 0 – 5N for instruments such as the Cadiere forceps to more than 20N for the da Vinci Prograsp forceps.

2.4.1.1 Piezoresistive Force Sensing

Piezoresistive sensors rely on the properties of semi-conductive materials such as silicon whose electrical resistance increases in response to mechanical strain. These sensors are available commercially in a variety of different sizes and dynamic ranges. Unfortunately, piezoresistive sensors often do not behave linearly within their full dynamic range. This is a design consideration that must be taken into account when utilizing this type of sensor.

In the past, CASIT’s tactile feedback system has relied on a piezoresistive force sensor (FlexiForce) from Tekscan which has a dynamic range of 0 – 4.4N.

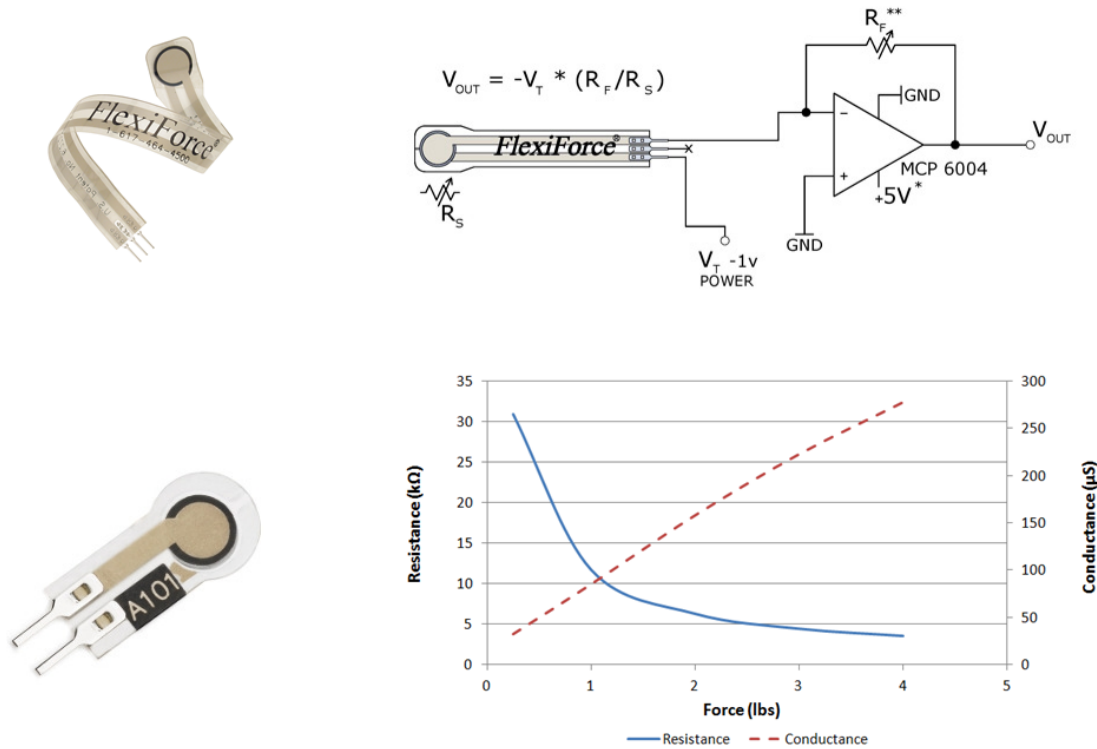


Figure 7: Tekscan Flexi-Force Sensors

(Top Left) 11lb FlexiForce Sensor - 14mm diameter (Bottom Left) 10lb FlexiForce Sensor - 7.6mm diameter (Top Right) Basic read-out circuitry. Alternatively, a simple voltage divider circuit can also be used (Bottom Right) Non-linear behavior of the FlexiForce 10lb sensors⁷⁶⁻⁷⁹

2.4.1.2 Capacitive Force Sensing

Capacitive sensors are generally designed as two conductive layers, separated by a compressible dielectric. Normal force applied to the surface of the sensor causes compression of the dielectric material, thereby decreasing the distance between the plates, and changing the capacitance^{80,81}. A capacitance to digital converter (CDC) is then used to retrieve capacitance data from the sensor for further processing. Capacitive sensors can also be used to detect shear forces by changing the overlapping area of the two plates when shear is applied to the surface of the sensor (Figure 8)^{82,83}.

Researchers have also been able to develop sensors consisting of multi-part surface electrodes. This design when combined with differential capacitance readings has led to the development of miniature tri-axial sensors capable of detecting normal force and bi-axial shear forces⁸⁴.

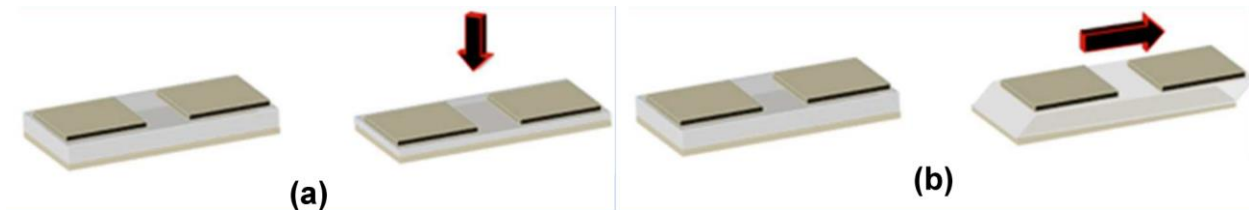


Figure 8: Capacitive Shear Sensor Design Concepts

(a) Change in capacitance caused by compressive force (b) Change overlap area caused by shear force leads to change in capacitance⁸²

2.4.1.3 Other Sensing Technologies

A variety of other force sensing technologies have also been investigated in a limited capacity for applications in surgical robotics. Among these are strain gauges which have been installed directly on the shaft of instruments in order to detect bending of the instrument due to forces applied at the end effector⁶³. This approach while effective, requires significant modification of the instrument shaft. Other groups have attempted to detect high frequency vibrations within the robotic motors and instruments to provide feedback⁵⁶. While this approach has provided information about instrument interaction with the tissue, there is no model that can map these interactions with quantitative measurement of the forces involved. More recently researchers have developed multimodal sensors (ex. BioTac) utilizing impedance electrodes engulfed in a conductive fluid as a means of detecting pressure, vibration and temperature⁸⁵. Unfortunately, this sensing technology leads to very large sensors that do not meet the necessary size constraints for application in surgical robotics. Finally, most similar to the piezoresistive sensors, are piezoelectric sensors, which are

designed to generate varying voltage depending on extent of compression of a ferromagnetic material. Researchers have used these sensors on laparoscopic graspers as a means of measuring forces applied to the tissue by the laparoscopic grasper^{71,86,87}. While these sensors are effective in detecting dynamic forces, their output quickly decays under constant load. This behavior has made piezoelectric sensors less than ideal for application in robotic surgery.

2.4.2 ACTUATION AND FEEDBACK TECHNOLOGIES

Conveying forces to the user in haptic feedback systems involves activation of various mechanoreceptors in the skin and muscles. In general, feedback technologies can be grouped into two categories, tactile feedback and kinesthetic force feedback.

Tactile feedback targets mechanoreceptors in the skin and can include vibration feedback, skin deformation feedback and normal force tactile feedback (Figure 9)^{19,22,88}. Research has found that skin deformation feedback as an independent feedback modality is ineffective and must always be coupled with force feedback⁸⁸. Vibration feedback is effective in conveying forces, however since the brain perceives vibration as a warning mechanism, it is not the ideal type of feedback for conveying graded information and if used improperly can lead to increased mental load and reduced task performance^{22,68,89}. Normal force tactile feedback which relies largely on activation of slow adapting mechanoreceptors in the fingertips has been shown as an effective actuation method, particularly for applications targeting reduction of grip force in robotic surgery^{19,58}. The effectiveness of this type of actuation is largely because pressure sensors in the skin play an important role in the fine tuning of grip force in humans^{90,91}.

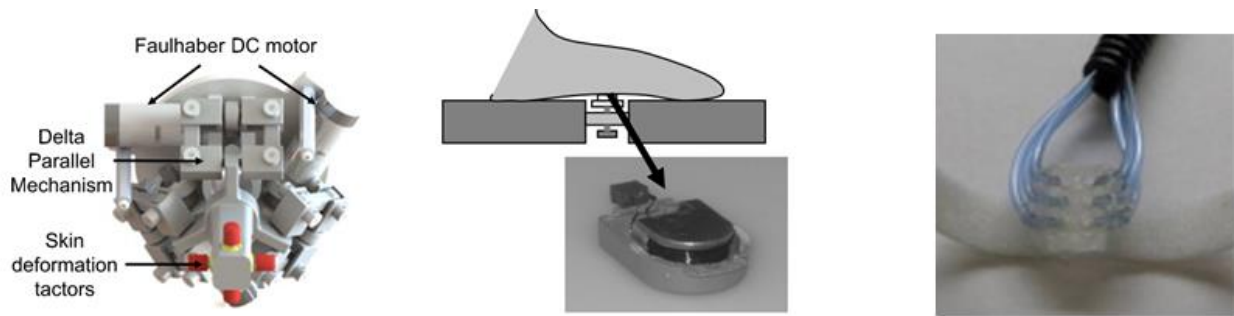


Figure 9: Tactile Feedback Actuators

(Left) Skin Deformation Actuator (Middle) Vibration Actuator (Right) Pneumatic Normal Force Actuator^{20,22,92}

Kinesthetic Force Feedback (KFF) targets mechanoreceptor in the muscles, particularly the Golgi tendon organ. Kinesthetic force feedback actuators attempt to create a sense of resistance, similar to that of real touch. KFF is most often implemented using motors installed on the hinges of robotic surgical consoles. This type of actuation modality is the most commonly studied type of haptic feedback and is used in many commercial robotic surgical systems (Figure 10)⁹³⁻⁹⁷.

Robotic Systems w/ KFF	Force Feedback Technology
TransEnterix ALF-X	Force Feedback @ Fingertips and Joystick Arms
Titan Medical SPORT	Force Feedback in Joystick Arms
MiroSurge	Force Feedback in Joystick Arms
SOFIE	Force Feedback in Joystick Arms
RAVEN II	Force Feedback @ Fingertips and Joystick Arms

Figure 10: Commercially available robotic surgical systems with Kinesthetic Force Feedback technology

2.4.3 CASIT'S TACTILE FEEDBACK SYSTEM

The CASIT tactile feedback system was initially developed in 2008. The goal of CASIT's tactile feedback system was to develop a haptic feedback system that would not only advance research in the field of haptics but also impact the clinical environment. More specifically, CASIT's tactile feedback system was aimed at reducing crush injuries caused by application of excessive grip force during MIS and RMIS procedures.

To this end, a feedback solution was designed, utilizing piezoresistive sensors capable of being installed on laparoscopic (Figure 11) and robotic (Figure 12) instruments, and functioning within the body. Through collaboration with department of neuroscience, pneumatic actuators were developed that would effectively convey tactile information to the surgeon's fingertips. The system underwent multiple enhancements through 2013 and was evaluated through several different studies, including an in-vivo porcine bowel run.

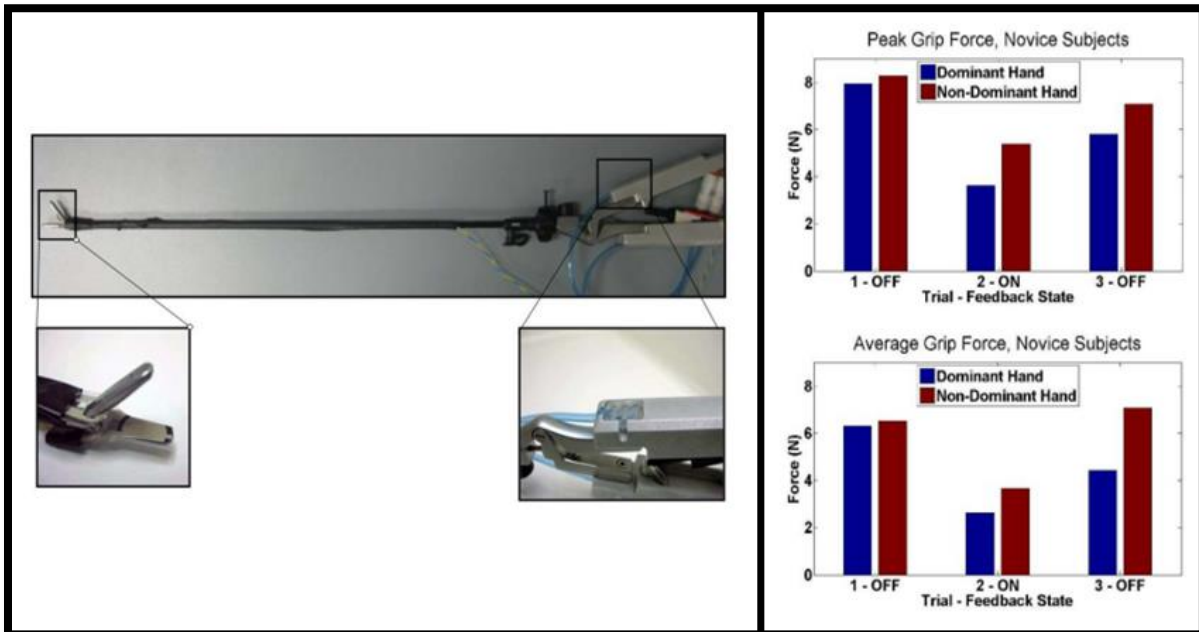


Figure 11: CASIT Tactile Feedback System (2013)

(Left) CASIT's Tactile Feedback System Install on Laparoscopic Instruments. (Right) Results of peg-transfer studies using this haptic feedback system.²⁰

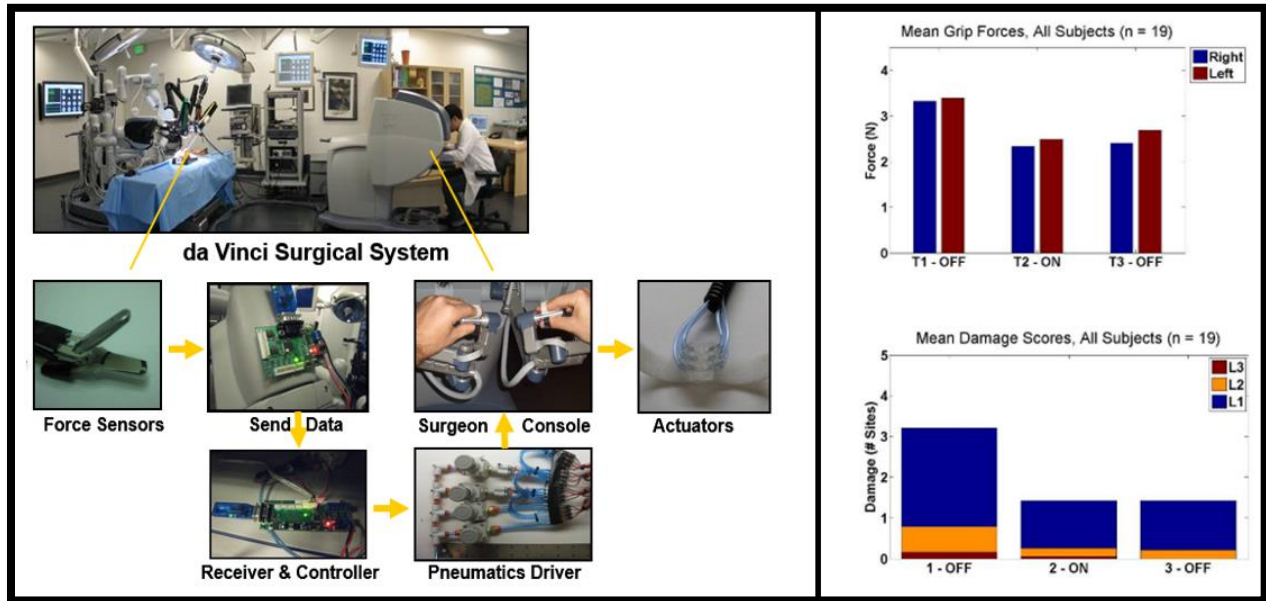


Figure 12: CASIT Tactile Feedback System (2013) Installed on da Vinci IS1200 Surgical System

(Left) CASIT's Tactile Feedback System Installed on da Vinci Surgical System. (Right) Results from an in-vivo porcine bowel run using this haptic feedback system.²⁰

The results of these studies confirmed the effectiveness of CASIT's tactile feedback system in reducing grip force and tissue damage²⁰. More importantly, this work laid out the foundation for further research in this area and the development of more complete haptic feedback systems.

2.4.4 LIMITATIONS & DRAWBACKS OF CASIT'S TACTILE FEEDBACK SYSTEM

Despite the effectiveness of CASIT's Tactile Feedback System, the 2013 variant of the system still suffered from several fundamental limitations. These shortcomings included several sensor and actuator design and manufacturing issues which needed to be addressed for further system development to be possible. Furthermore, analysis of data from the robotic and laparoscopic studies raised questions about uncontrolled factors that may have been effecting subject performance in HFS trials. More specifically, large amount of inter-subject variation was observed

with regards to the effectiveness of HFS in robotic surgical tasks (Figure 13). Finally, and most importantly, the CASIT HFS was developed as a single-modality feedback system. This unimodal design not only limited its effectiveness in grip force reduction but also prevented the application HFS to other robotic surgical tasks such as tissue palpation and knot tying.

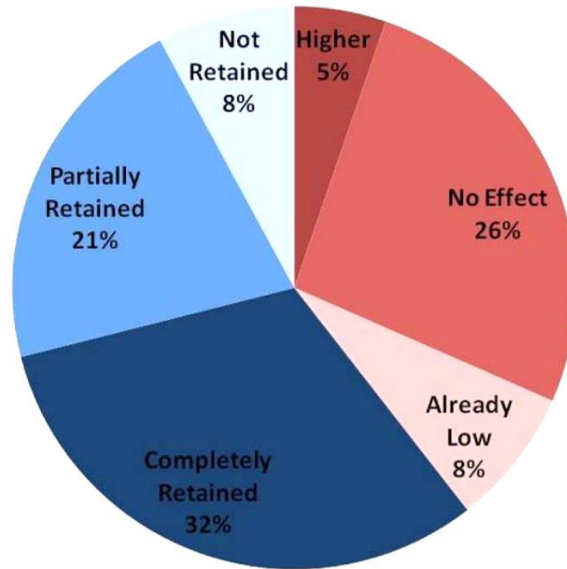


Figure 13: Variations in effectiveness of HFS during in-vivo robotic studies.

Some subjects experienced no benefit from HFS while the benefits of feedback were retained even after HFS was turned off, indicating that a learning effect may have contributed to reduction of grip forces.²⁰

2.4.5 MULTI-MODAL HAPTIC FEEDBACK SYSTEM

Multi-Modal Haptic Feedback System refers to an HFS that seeks to sense and convey more than one aspect of touch. By targeting multiple mechanoreceptors in the skin and muscles, and conveying both tactile and proprioceptive information, a more natural sense of touch can be simulated⁹⁸. In open surgery, the sense of touch allows surgeons to perform tasks such as palpation, knot tying and tissue manipulation with little risk of tissue damage or error. The goal of a multi-modal HFS is to bring us closer to that real touch and thereby expand the application of haptics beyond only a single surgical task. Due to the engineering challenges that arise from attempting to

integrate multiple sensing and feedback modalities, while still maintaining small footprints necessary for applications in surgery, multi-modal HFS has not been extensively studied. In more recent years, some attempts have been made on the development of bi-modal haptic feedback systems for surgical applications, however while some trends have been present, conclusive outcomes have not yet been achieved⁹².

3 RESEARCH OBJECTIVES

This research sought to accomplish three main engineering objectives:

- 1) Improving Sensing & Actuation in the Tactile Feedback System
- 2) Enhancing HFS Architecture: Creating A More Versatile & Adaptable Control System
- 3) Multi-Modal HFS: Providing Additional Modalities of Feedback to Better Simulate Real Touch

These objectives were achieved as part of four research aims:

AIM I – Investigate Inter-Subject Variations in Haptic Feedback Studies for RMIS: The result previous of in-vivo robotic studies performed using CASIT’s tactile feedback system showed significant variation in effectiveness of haptics for grip-force reduction among different subjects. The purpose of this investigation is to identify the main factor contributing to this effect in robotic surgical tasks.

AIM II – Improving the CASIT’s Tactile Feedback System: The purpose of this research aim was to analyze various aspects of the original tactile feedback system, and identify elements that hindered its application in grip-force reduction and other clinical task such as palpation and knot tying. This task was therefore focused on engineering of several improvements for both sensing and actuation within the tactile feedback system.

AIM III – Develop A Multi-Modal Haptic Feedback System: Based on the multi-modal sensory and feedback nature of human touch, it was hypothesized that a multi-modal haptic feedback system would be more effective in conveying tactile and proprioceptive information to the user than a unimodal one. The goal of this research aim was to engineer a multi-modal haptic feedback system, utilizing CASIT’s previous tactile feedback system as a single modality for conveying

light touch information, while implementing additional modalities of feedback through vibration and kinesthetic force feedback.

AIM IV – Evaluate the Multi-Modal Haptic Feedback System for Potential Clinical Applications in RMIS: The engineered multi-modal feedback system was designed as a flexible platform capable to being configured for application in several different tasks. Modifications in the configuration of the software control system allowed for utilization and evaluation of the multi-modal HFS for several different applications in robotic surgery. The goal of this research aim was twofold. First, these investigations would shed light on the effectiveness of haptics in improving outcomes for robotic surgical tasks where tactile sensory information can be beneficial. The second was to determine whether multi-modal haptic feedback is in fact any more effective than single-modality feedback for RMIS applications.

The rest of this dissertation will disclose and discuss the methods and findings resulting from investigations based on each of these four research aims.

4 INVESTIGATION OF INTER-SUBJECT VARIATIONS IN HFS STUDIES

Evaluation of haptic feedback systems often faces a significant problem when it comes to subject variability. In general, subjects have significantly different skill levels and even in completely novice subjects, life experiences can lead to largely different performance patterns. It is therefore critical to try to control for all variables that may impact the data but are unrelated to the effectiveness of a haptic feedback system. Of course, in nearly all cases, increasing the number of subjects enrolled in a study helps eliminate some of these effects but also creates recruitment challenges for researchers. An alternative approach is utilizing a repeated measures design, where a single subject performs a task multiple times, thereby controlling for most variables arising from variability subjects' skill level. Unfortunately, this study design can often suffer from variability in the rate at which an individual can learn a skill. Randomizing the order of trials in a repeated measures design can help reduce the impact of this effect, but not completely eliminate it. A carefully controlled subject population can also help reduce this effect. Still, it is extremely important to take these factors into consideration when evaluating haptic feedback systems. As major inter-subject variability can appear in study results, particularly in those with small number of enrollees.

Of course, in some cases, variability in results of a study can also point out fundamental issues in study design, or the engineering of the system. It is therefore critical to further analyze results from haptic feedback studies that show high inter-subject variability, and identify potential engineering and experimental design issues.

The data from studies performed by C. R. Wottawa on evaluation of a tactile feedback system for robotic surgery indicate significant inter-subject variability (Figure 13)²⁰. Since this research

project aims to build upon some of design parameters of the previous tactile feedback system, it is critical to further investigate and understand this inter-subject variability.

An overview of the inter-subject variation and the data on the evaluation of the aforementioned tactile feedback system, can be summarized into four major observations:

- Variations are less apparent in laparoscopic tasks
- Variations exist even within the same subject (different trials)
- Variations are more apparent in novices/beginners
- Some subjects report that balloon inflations become more difficult to feel over time

Based on these observations, and a series of benchtop tests, two hypotheses were developed for explaining this inter-subject variation:

Hypothesis I: Variations result from utilization of the Clutch operation, and a phenomenon referred to as Visual-Perceptual Mismatch

Hypothesis II: Sensory adaptation causes deformation in the flat pneumatic balloons to become less noticeable over time.

4.1 VISUAL-PERCEPTUAL MISMATCH

Nearly all robotic surgical systems consist of a control console, and, one or more robotic arms which are in contact with the patient. The robotic arms are driven by control signals from the master console where the surgeon uses joystick-like controls to direct the movements of the robot's arms and end effectors. This physical separation of the robotic console and the robotic end effectors is the key feature that allows for robotic systems to support teleoperation and motion scaling. Unfortunately, this same characteristics leads to space constraints. The movement of the joystick-like controls in the console is limited by the available space in the console area and the reach of

the surgeon's arms. Whereas in laparoscopic and open surgery the surgeon can physically move around to extend his/her reach, in robotic surgery, the surgeon is sitting down behind the controls and is limited to the confines of the master console. A simple example these limitations is when the robotic arms are capable of moving beyond a certain extent on one axis, but the control in the console may have reached the limits on that same axis due to effects of motion scaling.

In general, robotic surgical systems such as Intuitive Surgical's da Vinci attempt to resolve this issue by adding a "Clutch" operation. The clutch operation disconnects the robotic arms from the console so that the joystick-like controls can be repositioned without inducing any movements in the arms. In essence, the clutch operation is similar to lifting a computer mouse and repositioning it when space constraints become an issue.

The clutch operation is so often used during the procedure, that nearly all robotic surgical simulators, have some training tasks specifically designed, to improve the skill of the surgeon with the clutch. Despite its importance however, its effect on overall operator performance have not been extensively studied.

Based on understanding of the way the human brain integrates visual and proprioceptive information, it is feasible to foresee neuroprocessing mismatches arise from utilization of the clutch. In fact, this operation can lead to a phenomenon referred to as Visual-Perceptual Mismatch (VPM).

The human brain maintains a perception of the location of one's limbs in space at all times. This is referred to as the sense of Kinesthesia^{99,100}. This sense, when combined with tactile sensory information allows individuals to perform many tasks without any type of visual aid. As an example, it is possible for a healthy individual to pick up an object with one hand and pass it to the other hand without any visual aid (i.e. eyes closed) and with little difficulty. Furthermore, this

mapping of the location of the limbs in space is normally in agreement with what the visual system reports as the location of the hands in space.

The utilization of the clutch operation can create a mismatch between the brain's awareness of the location of the hands in space and what the brain sees through the eyes. In other words, it is possible that while the brain is receiving visual stimuli through an endoscope about robotic end effectors being in contact with each other, the proprioceptive centers of the brain are receiving data indicating that the surgeon's hands are many inches away from each other. Figure 14 shows an example of this misalignment in one-axis.

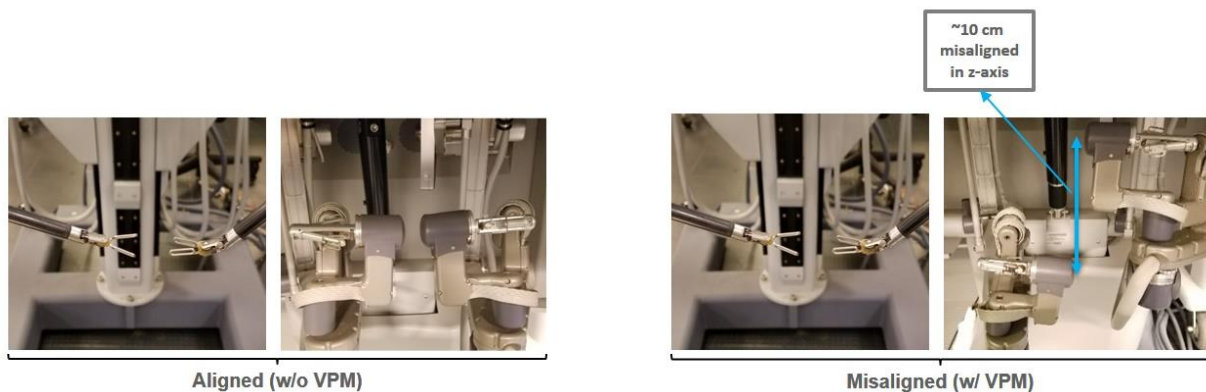


Figure 14: Aligned and Misaligned Conditions Caused by Utilization of the Clutch Operation

In certain surgical tasks where coordination between the two arms is critical, this mismatch, coupled with the lack of haptic feedback can introduce additional cognitive load, thereby reducing the surgeon's performance. The goal of this study is to determine the impact of this effect on performance, and how it may contribute to inter-subject variations observed in previous HFS studies.

4.1.1 METHODS

A series of tests were designed with the goal of studying the impact of VPM in robotic surgical tasks. The performance of novice subjects in performing a two-handed peg-transfer tasks was evaluated using quantitative measurements of grip-force, number of faults (i.e. number of times the subject drops a peg), and time-to-completion. Peg-transfer tasks were adopted from the standard peg transfer test in the Fundamentals of Laparoscopic Surgery (FLS) education module developed by the Society of American Gastrointestinal Endoscopic Surgeons (SAGES)¹⁰¹. All studies were performed using an Intuitive Surgical da Vinci IS 1200 system with Fenestrated Bipolar forceps as the instrument of choice (Figure 15b). The tasks required that a subject pick up a peg with one of the robotic arms, rotate it along the z-axis (one side of the peg was marked), pass it to the other arm, and place back down on the opposite side of the field (Figure 15a). In cases where the subject dropped the peg, the protector would reset the peg to its original position, thereby controlling for the impact of the dropped position on time-to-completion of the task. Force sensors were installed on the forceps to allow measurement of grip force during the study (Figure 15c).



Figure 15: Visual-Perceptual Mismatch Study Setup

Since the study did not utilize a repeated measures design, controlling for variables among the subject population was critical. Furthermore, a larger number of subjects was necessary to achieve the necessary power for conclusive results. To this end, 45 subjects (age 16-30 years), were

enrolled in the study. Subjects were novices with no prior experience with the da Vinci system. Each subject was given 2-minute training period prior to the first trial, in order to gain familiarity with the basic controls of the da Vinci system. Each subject performed the same tasks 5 times as part of five separate trials with 30-second break intervals between each trial. During the break, the subject was not allowed to operate the robot or get up from his/her seat. More importantly, subjects were not allowed to use Clutch or the Camera operations of the da Vinci. The camera position and zoom were adjusted to be identical for all trials. Subjects were asked to grab the peg from the side and to grab at least half of the peg before picking it up. This allowed for more consistency of sensor readings during the trial.

As part of written instructions provided to the subjects prior to the experiment, the goal of each individual was to perform the tasks with three priorities in mind, (1) not to drop the peg, (2) reduce the time-to-completion and (3) reduce the applied force to the peg without sacrificing the first two goals.

The study broke down the 45 subjects into three groups, Aligned, Misaligned and Haptics-Misaligned. For the Aligned Group, the proctor configured the robotic arms and controls using the clutch such that no mismatch would exist between visual and proprioceptive information in any of the axis. For the Misaligned group, a z-axis mismatch was created by aligning the robotic end effectors directly in-front of each other and then using the clutch to create a 10-cm misalignment in the master control console (z-axis only). The Haptics-Misaligned group had the same configuration as the Misaligned group with the difference that haptic feedback was provided using pneumatic tactile actuators¹⁰². The goal of this third group was to evaluate the benefit of introducing an additional sensory modality as a way to help compensate for any limitations induced by VPM.

The grip-force during the task was recorded for all subjects of all groups. This was done using a custom software that retrieved data from FlexiForce sensors (at 50Hz) installed on the instruments²⁰. The same software was used for recording the number of times the participant drops the peg. Finally, with regards to measuring the time-to-completion, the proctor marked the beginning of each trial with the subject approaching the first peg and marked the end of the trial as soon the participant placed the last peg down.

During data analysis, only gripped-data was measured. Gripped-data was identified as the times when the peg was being held by the graspers. All other times when the subject was not handling a peg was ignored during average grip force calculations. Gripped data was measured by only considering times when the grip force was above a certain minimum threshold. This threshold highly depends on the type of sensor and the amount of baseline noise. For this study, the threshold was identified to be 20% of the minimum detectable force recorded by the sensors.

In addition to the aforementioned metrics, time-to-completion of a single successful peg transfer was also measured. This time which was independent of the number of times the subject dropped the peg helps point out any differences that exists between the groups when the subject was able to properly pass the peg.

For all trials, data analysis was performed on the mean of all five trials for a subject. All statistical analysis was performed using one-way ANOVA followed by post-hoc analysis using Math.Net and R statistics packages. If normality or equal variance assumptions were not met, Log2 transformation was used prior to running one-way ANOVA. For analysis of the number of faults, square root transformation was used to achieve homogeneity of variance. This was followed by a non-parametric Kruskal-Wallis ANOVA and post-hoc analysis using Holm method.

4.1.2 RESULTS

Figure 16 shows the number of faults and the time to completion for the different groups in this study. The data shows that the misalignment in the z-axis, contributing to the visual-perceptual mismatch, caused an increase in the number of times subjects dropped the peg ($p < 0.05$, Kruskal-Wallis ANOVA).

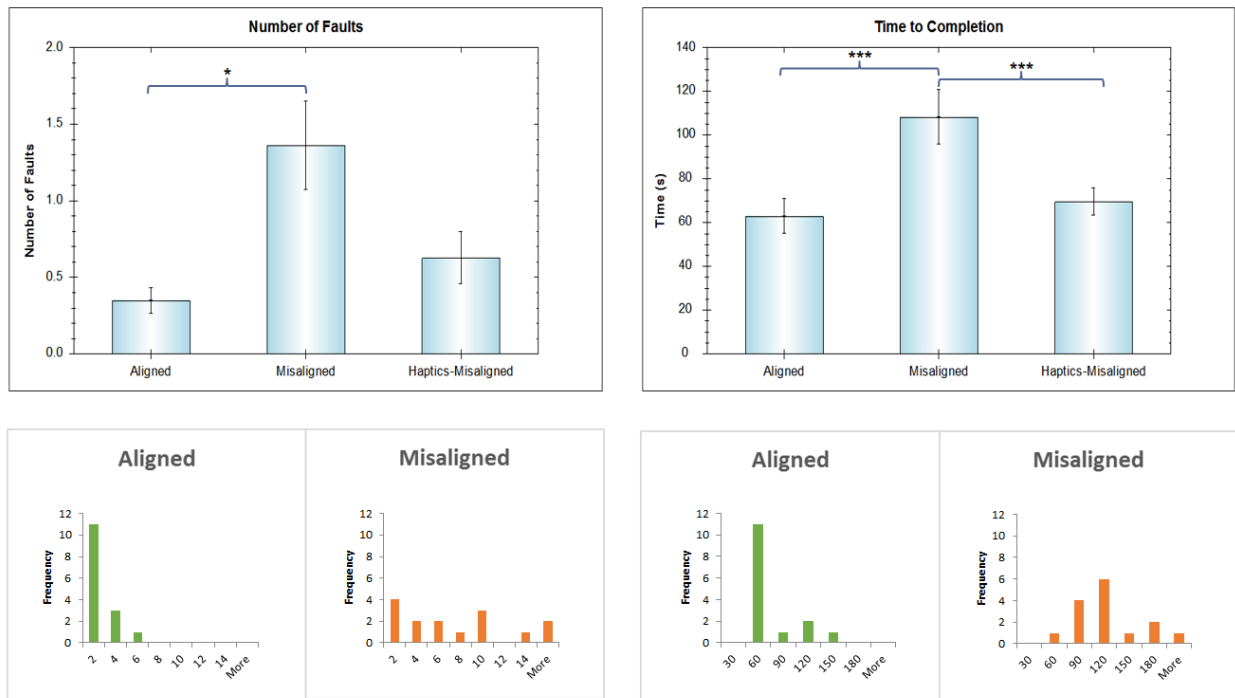


Figure 16: The results of the visual perceptual mismatch study

The subjects in the misaligned group (no HFS) dropped the peg more often than the aligned group ($p = 0.011$), but more interestingly, when haptic feedback was enabled (Haptics-Misaligned group), a reduction in number of faults/drops was observed. It is worth noting that the decrease in the number of peg drops from the haptics misaligned group was not significant ($p = 0.088$), though a trend was present which may indicate that a larger number of subjects was necessary to achieve significance.

There also exists a significant difference between groups with respect to the time-to-completion of the task ($p < 0.001$). The visual-perceptual mismatch resulted in the participants of the misaligned group taking significantly longer to complete the task ($p = 0.0006$). In this case however, it can clearly be observed that haptic feedback helped compensate for the handicap caused by VPM ($p=0.008$). No difference was observed between the Aligned and Haptics-Misaligned groups ($p=0.309$).

The pie charts in Figure 16 also lay out the variations that exists among subjects with regards to both the number of faults and the time-to-completion. It can be seen that subjects in the misaligned group showed more variation in performance than those in the aligned group, indicating that VPM is causing increase in inter-subject variation.

No statistical significance was observed with regards to the time-to-completion for a single successful peg transfer ($p = 0.13$). A similar trend followed with regards to the average grip force ($p = 0.87$) and average grip-force during a single successful peg transfer.

4.1.3 DISCUSSION

Despite extensive research in the field of surgical robotics, the effect of relative coordinate systems on surgeon performance have not been studied. Considering that nearly all surgical robotic systems utilize a clutch-like mechanism during operation, a better understanding of this behavior is necessary. Furthermore, understanding variabilities that may result from these coordinate systems can play an important role when evaluating new features, such as haptic feedback. Without proper control of such variables, evaluation of new features can become plagued by large inter-subject and even intra-subject variation.

In this study¹⁰³, the impact of the clutch operation on the performance of subjects using the da Vinci surgical system was investigated. Despite the fact that these experiments created only a small single-axis mismatch, the results clearly showed the negative impact that visual-perceptual mismatch can have on subject performance.

Additionally, while previous experiments have focused on the direct benefits of haptics such as grip force reduction, the results of this investigation point out another benefit of haptics. It can be seen how the addition of this sensory modality can provide performance benefits, allowing the brain to use additional sensory information to compensate for limitations inherent to robotic surgical operations.

Finally, these experiments provide necessary insight for the design of future haptic feedback studies. Considering that VPM can introduce inter- and intra-subject variability, any study that attempts to evaluate the effectiveness of HFS, must control for the usage of clutch.

4.2 SENSORY ADAPTATION

Another factor that could potentially contribute to variation among subjects is sensory desensitization. Some subjects in previous HFS studies reported that inflations of pneumatic balloons were difficult to notice, particularly after long periods of using them²⁰. This effect is most likely caused by desensitization of mechanoreceptors in the skin. Under normal circumstances, the sense of touch involves simultaneous retrieval of light touch and deep pressure sensors. This is because the skin is not normally in contact with any object and low pressure (i.e. light touch) contact is made only when some grasping action is initiated. This contact is then followed quickly by increase in pressure which in turn activates deep pressure sensors in the skin.

While the normal force, tactile feedback actuators attempted to recreate this effect, in reality, these actuators only target slow adapting pressure sensors in the skin. This is because the flat design of the PDMS actuators (Figure 17) causes light touch to be present at all times. In fact, depending on how tightly the subject is holding on to the robotic controls, even deep pressure sensors may remain activated.



Figure 17: Flat, Silicon-Based Pneumatic Actuators While Inflated

This effect can lead to adaptation in the mechanoreceptors of the skin and in turn, dampen the effect of the pneumatic actuators, particularly at lower pressures. Of course, this dampening effect varies among subjects due to different subject skin types, how often the subject lifts his/her hand off of the controls, and even the length and complexity of the task. Considering that real life surgical procedure can span many hours, this can lead to ineffectiveness of HFS for clinical settings. Resolving this issue is therefore critical, but requires significant modifications to the pneumatic tactile actuators. This engineering task was focused on as part of a series of enhancements made to CASIT's tactile feedback system in Aim II of this investigation (Chapter 5).

5 IMPROVING CASIT'S TACTILE FEEDBACK SYSTEM

The current tactile feedback system suffers from a series of shortcomings primarily due to the limitations of existing sensing and actuation technologies.

Therefore, the presented work on enhancements for a novel tactile feedback system were broken down into the following three major tasks:

Task A: Development of New Sensor Board

Task B: Improving the Pneumatic Normal Force Feedback Actuators

Task C: Improving the Normal Force Sensing Mechanism

Task D: Development of Shear Sensors

5.1 TASK A: DEVELOPMENT OF A NEW SENSOR BOARD

The haptic feedback system developed in this research project utilizes a variety of piezoresistive sensors from Tekscan. These FlexiForce sensors provide a stable normal force sensing capability and are designed for a variety of purposes, including medical applications. For many of the studies performed throughout this research project, the 1lb variant of the B201 sensor was used. However, these sensors are only recommended for forces of up to 4.4N (using high gain read-out circuit). The main reason for this limitation is the design of the readout circuitry and the fact that the sensors behave more linearly within that range when, in reality, these sensors can record forces as high as 111N if provided with the appropriate readout circuitry. A new sensor board was developed with the goal of expanding the dynamic range of the sensors (Figure 19). The board utilized a simple voltage divider circuit with a 10K resistor, a selection that would allow accurate sensor readings of up to 15N. The newly developed sensor board also allowed up to 12 simultaneous sensors to be connected to the system.

The sensor board utilized an Atmel SAM3X8E ARM Cortex M3 MCU (as part of the Arduino Due dev kit) for data processing and transmission to the computer. The MCU was programmed to transmit packets to the computer at 35Hz using the packet format described in Figure 18.

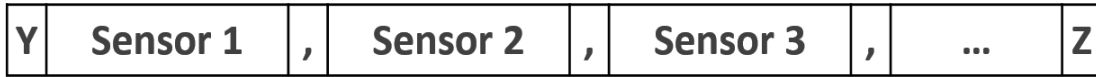


Figure 18: Sensor Board Packet Format

In this packet format, “Y” marks the beginning of the packet and “Z” marks the end. Sensor values are separated using “,”. This allows the number of sensors and the number of bits/sensor to change, without requiring any changes to the software that reads data from the sensor board. Calibration of the sensors (Figure 20) was performed using Mark-10 Series 3 force gauge (Figure 29).

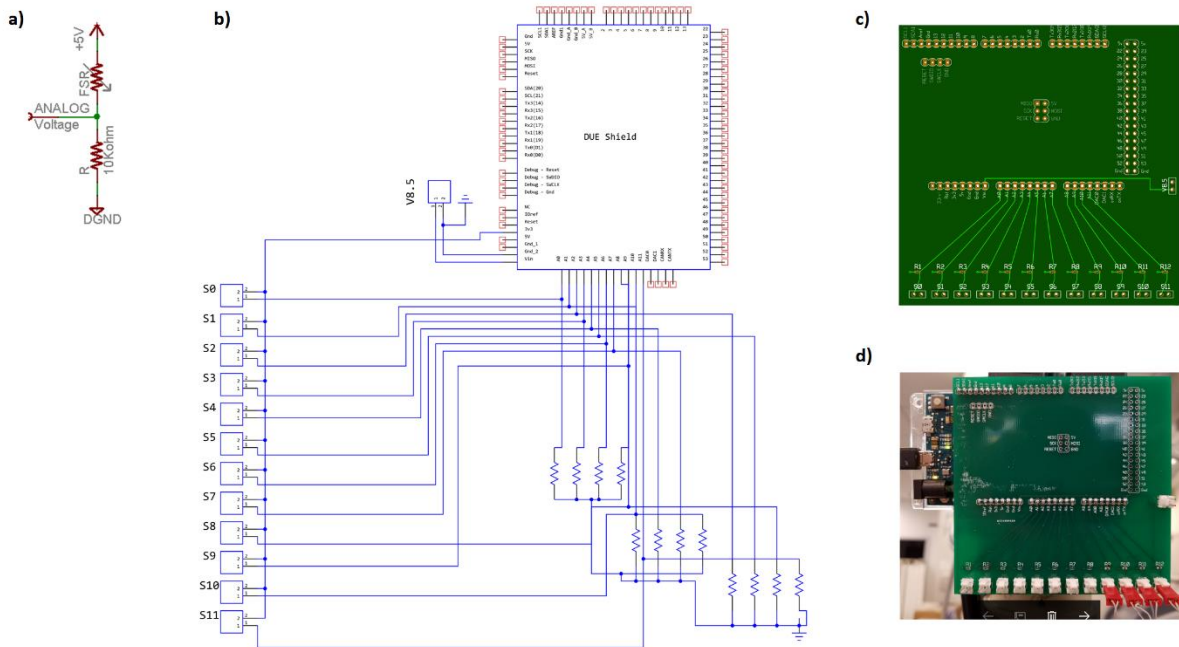


Figure 19: Newly Designed Sensor Board

(a) Voltage Divider Circuit for Reading from FlexiForce Sensors (b & c) Sensor Board Schematic (d) Sensor Board Connected to Atmel SAM3X8E ARM Cortex M3 MCU

The design of the sensor board and readout circuitry is highly dependent on the target application. The aforementioned design was utilized because it provided the right combination of resolution and dynamic range.

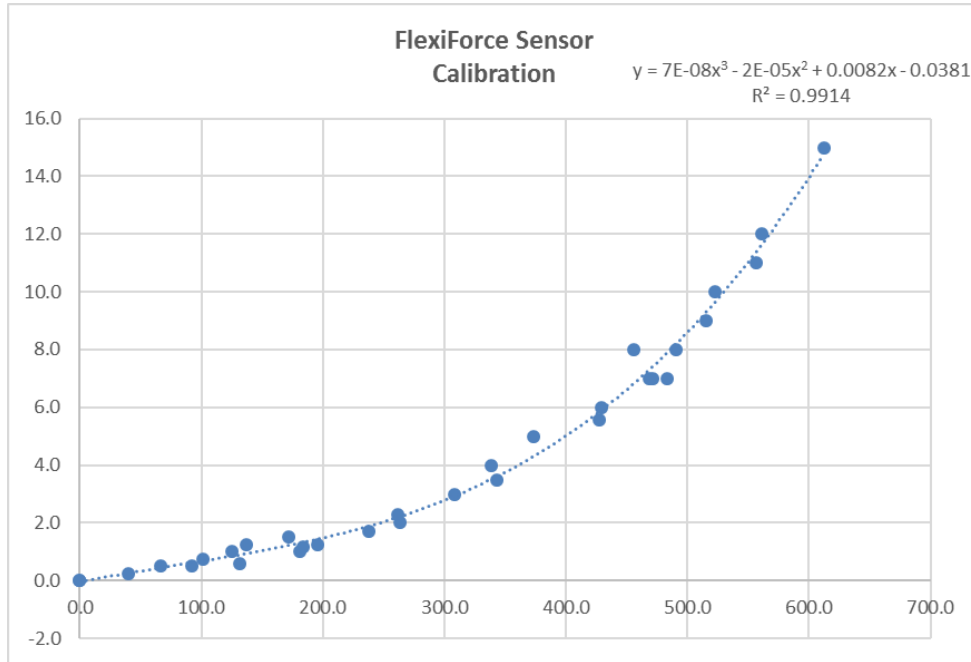


Figure 20: Calibration of Tekscan FlexiForce 11b Sensor

5.2 TASK B: IMPROVING THE PNEUMATIC NORMAL FORCE FEEDBACK ACTUATORS

5.2.1 DESIGN OF DEPRESSED-MEMBRANE PNEUMATIC ACTUATORS

The silicon-based pneumatic actuators that have been used in CASIT's tactile feedback system were fabricated by first creating a thin PDMS membrane and then bonding it to a base consisting of six small air chambers. The base was also made of PDMS by using a custom design mold²⁰. The result was an actuator with six small balloons capable of deforming up to 2-3mm.

These actuators, however, suffered from a number of issues. The first was the manufacturing mechanism which had low yield and high failure due to the bonding procedure. In many cases, the membrane detached from the base at high pressures. The second problem was that the manufacturing process limited the complexity of the design. This was because the mold had to be created in such a way that the base component could be removed after the PDMS had cured. More complex designs would, therefore, require complex, multi-part molds which may not have led to a functional actuator due to the small size of the device.

Finally, the flat design of these actuators could potentially make them susceptible to sensory desensitization. This effect could in turn dampen the impact of feedback for long running tasks and cause subjects to not notice the changes in the pressure.

In order to resolve these problems, a new actuator was designed. With the advent of 3D printing and the possibilities that rapid prototyping technologies provided, a new depressed-membrane design was engineered (Figure 21).

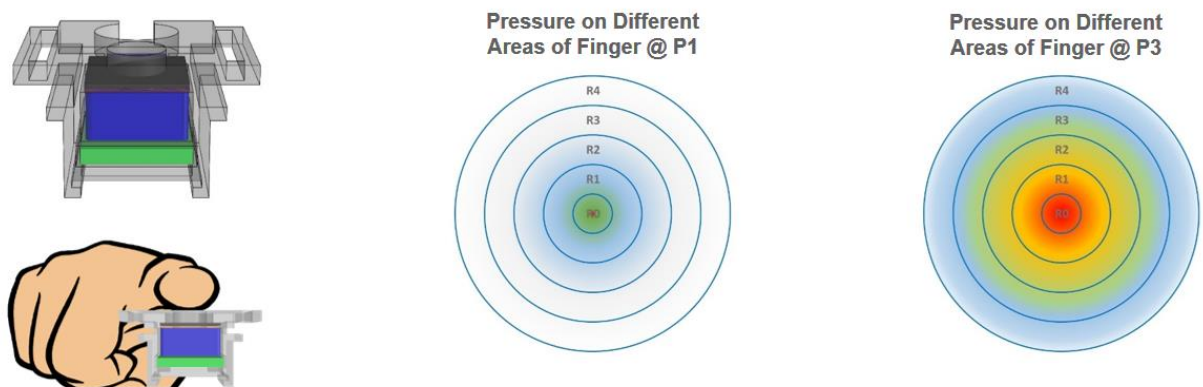


Figure 21: Depressed Membrane Actuator Design Concept

The depressed-membrane actuator attempted to simulate real world conditions by depressing the balloon membrane relative to the surface of the actuators. This, in turn, would result in the center

of the fingertip to not have any contact with the membrane under normal, non-inflated conditions. When the actuator was activated to Pressure Level 1 (P1), the membrane would deform just enough that it would make light contact with the surface of the skin. This simulated the sensation of light touch that normally takes place during the initial phases of contact (e.g. when grasping an object). In order to achieve this behavior, a series of benchtop tests helped identify the appropriate depth for the depressed membrane. As the surface of the skin on the fingertips itself has some curvature, the depth of the membrane relative to the surface of the actuator must be large enough to allow the fingertip to sit comfortably on top of the actuator without making contact with the surface of the skin. The first pressure level was then adjusted such that a subject would just barely feel the presence of the membrane once it was inflated (6.5). As the actuator pressure level is increased, the contact area between balloon and the skin would thus increase, therefore retrieving new light touch mechanoreceptors while simultaneously increasing the pressure on the mechanoreceptors that were previously activated (Figure 21). This behavior allowed migration from light touch to deep pressure and thus supplementing the behavior of the original silicon-based actuators used for feedback.

It is worth noting that there is some variation in the curvature of the fingers of different subjects. While the pressure levels were configured based on an average of a small number of subjects, it did not reflect the ideal pressure for any one individual. This issue can be resolved by implementing an adaptable feedback system that can maintain user profiles and pressure levels specific to each subject.

Engineering a depressed-membrane actuator faced a number of challenges. The first difficulty was in allowing large deformations in the pneumatic balloon without causing failure, such as slippage and rupture. This eliminated any method that relied upon bonding for the attachment of a

membrane to the actuator body. The second problem was that 3D printed models suffered from limited resolution, creating roughness on surfaces, making it difficult to maintain airtightness at high pressures (0 – 20PSI).

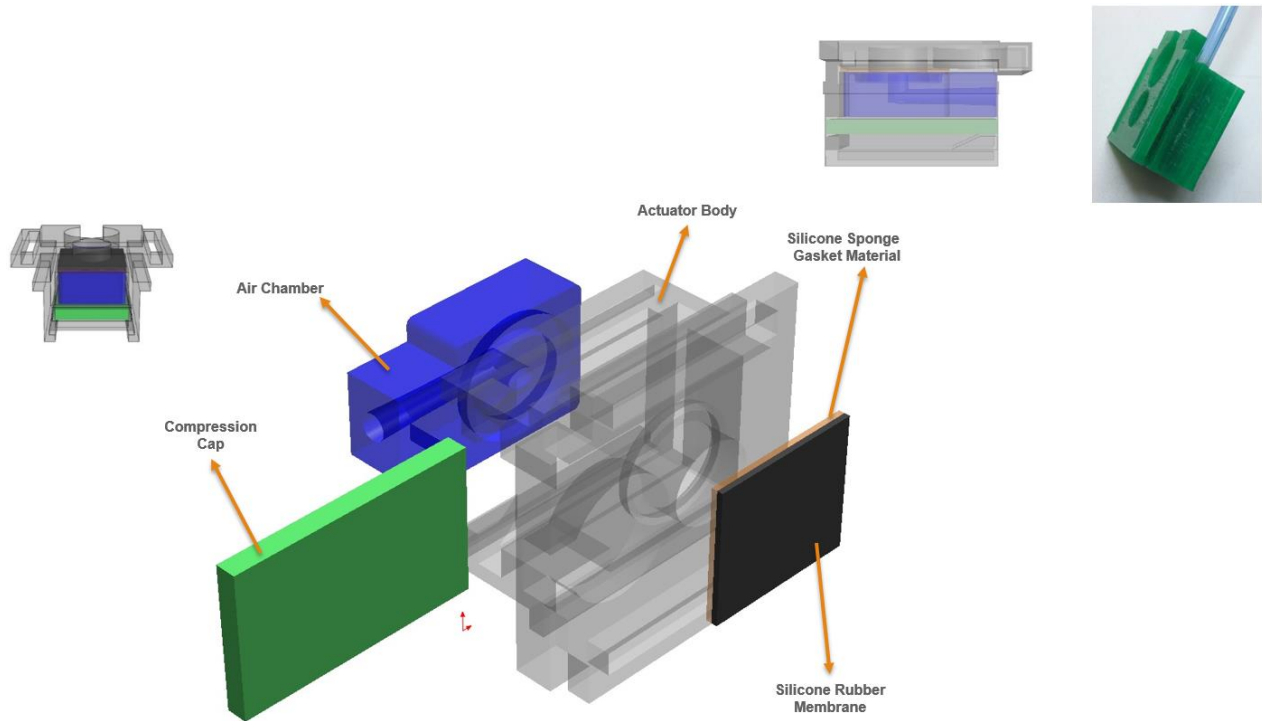


Figure 22: Design of 3D-Printed Depressed-Membrane Actuators

Utilizing a multi-part design (Figure 22), a functional actuator was developed that would remain airtight for pressures of up to 20PSI. This design, which does not utilize any type of bonding material in any of its components, is easily manufacturable. More importantly, the actuator can be taken apart and put back together in case there is a failure in any one component.

The design utilized multiple three 3D printed components in which an air chamber guided the flow of air towards the back of the membrane. To achieve airtightness, two membranes were used. The first was a Silicone Sponge Rubber gasket material which is extremely flexible and is punctured in the center to avoid any impact on the deformation of the primary Silicone Rubber membrane. The Silicone Sponge Rubber (medium density) membrane is 0.813 mm thick and the primary

Silicone Rubber Membrane is a 20 Shore A, 0.51 mm thick membrane. Both membranes are commercially available and are not custom made. The membranes are compressed between the Actuator Body and the Air Chamber. Compression force is maintained by sliding a Compression Cap into the Actuator Body right behind the Air Chamber.

5.2.2 EVALUATION OF DEPRESSED-MEMBRANE PNEUMATIC ACTUATORS

A study was designed to compare the performance of the newly developed actuator against the original flat silicon-based actuators (Figure 23). The goal of this study was twofold: (1) determine whether the newly developed actuators are effective in reducing grip-force, and (2) determine whether sensory desensitization plays any role in reducing the effectiveness of pneumatic actuators and whether the newly developed actuators can eliminate sensory desensitization.

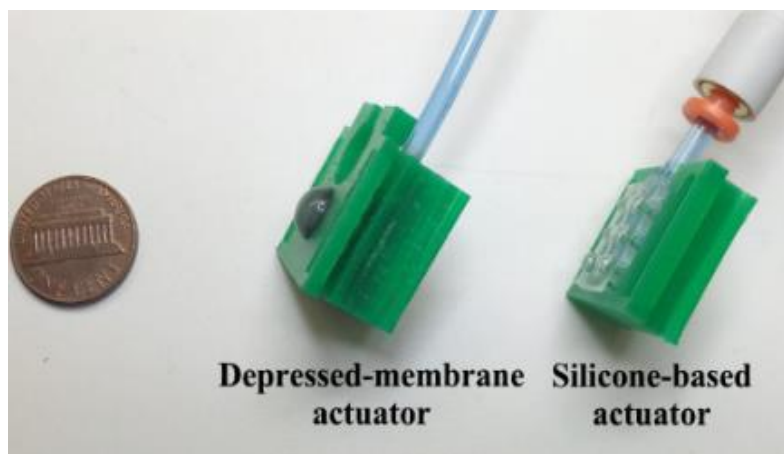


Figure 23: Side-by-side view of depressed-membrane actuator and silicone-based actuator

5.2.2.1 Methods

In order to study the impact of sensory desensitization, the experiment must have involved a task that would allow the mechanoreceptors in the skin to desensitize to the existence of the actuators. With this in mind, subjects were asked to perform a double handed peg transfer task in which each

subject performed ten transfers in total. The large number of transfers led to a longer trial period, therefore allowing the effects of sensory adaptation to be visible. The task was performed using an Intuitive Surgical da Vinci Si system. Tekscan's FlexiForce B201 piezoresistive force sensors were utilized for this study and installed on da Vinci Prograsp instruments (Figure 24).



Figure 24: FlexiForce Sensors Installed on Da Vinci Prograsp Forceps

The study was designed as a repeated measure experiment with 8 subjects. Subjects were specifically selected from a population of users that had some experience with the da Vinci system and could comfortably perform peg transfers. This enrollment requirement was used to avoid confounding variables that could be introduced from very novice subjects that have difficulty operating the da Vinci system.

The PDMS pneumatic actuator was installed on one hand and the depressed-membrane actuator was installed on the other. To prevent any bias from either hand, half of the subjects performed the task with the PDMS actuator on the right hand and half with the PDMS actuator on the left hand.

For data analysis, (1) the average grip force throughout the trial, (2) the number of faults/peg-drops of each hand, and (3) the change in force (i.e. Force Slope) were measured. The average grip force was identified by treating all forces above 7% of the minimum force value, as gripped data points. This approach allowed identification of the times when the peg was being held by the grasper (as opposed to a free-floating grasper) with the threshold determined to be just above the sensor baseline force plus any present noise.

The force slope was identified by using a linear fit on the gripped data points. This allowed for the observation of any trend in the force values throughout the trial to determine whether the applied force is increasing or decreasing as the subject spent more time on the system. Analysis of the data was performed using Student's t-test for normally distributed data and Wilcoxon Signed Rank test for non-normal data.

5.2.2.2 Results

The results of the study showed (Figure 25) a significant difference between the actuators for both average applied force ($p = 0.032$) and the change in force ($p = 0.0156$). While change-in-force (i.e. force-slope) is valuable for observing the significant change between the two groups, it is not a good indication of the actual forces involved. The actual force values are valuable because they can better be correlated to tissue damage (Figure 4). Therefore, the peak force for the last and first peg transfers in each trial was also compared. The results showed that on average, for the flat, PDMS-based actuators, the peak force in the last peg-transfer was 4.32N higher than the first peg-transfer. On the other hand, for the new depressed-membrane actuator, this value was -3.02N, indicating that the peak force for the last peg-transfer was lower than the first peg-transfer. With regards to the number of times a subject dropped the peg, no significant difference was observed.

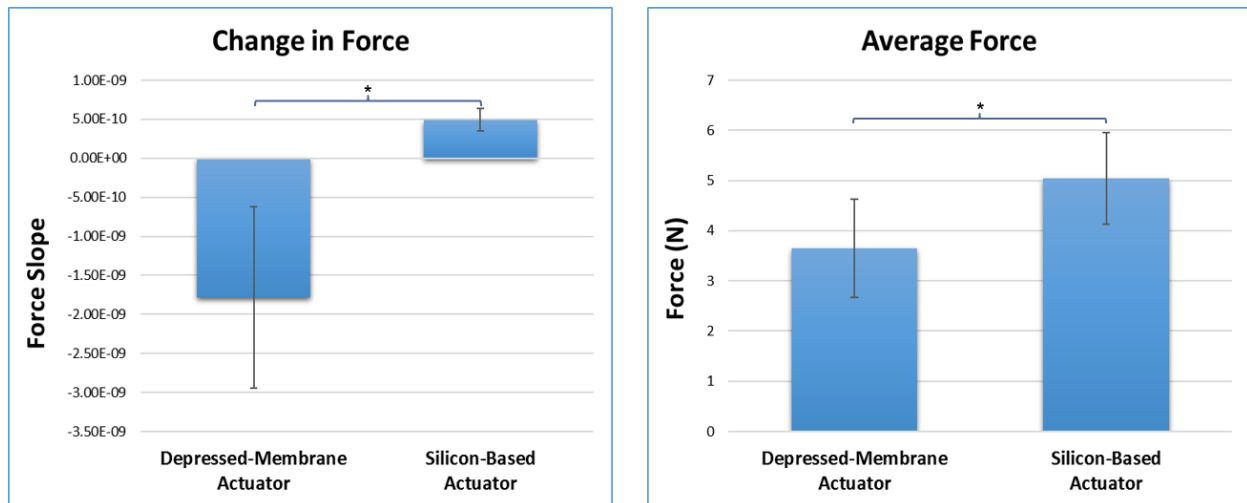


Figure 25: Results of Actuator Comparison Study

5.2.2.3 Discussion

The depressed-membrane actuators appear to outperform the traditional silicon based actuators in every way. Not only is the new actuator more effective in reducing grip force, but it also helps in reduction of sensory adaptation. The negative force slope of the depressed-membrane actuators indicate that the subjects applied lower force as they approached the end of the trial. This improvement is most likely caused by a learning effect. On the other hand, the positive force slope observed for the silicon-based actuator confirmed the original hypothesis that the flat design of the actuators caused users to become desensitized to the feedback as the trial progressed.

5.3 TASK C: IMPROVING THE NORMAL FORCE SENSING MECHANISM

The detection of normal forces in the current HFS is achieved using Tekscan FlexiForce B201 piezoresistive force sensors. The detection area of these sensors is 9.52mm in diameter. An additional 4.47mm is taken up by transparent polyester (i.e. Mylar) which makes the sensors waterproof. Previous work has relied upon a 10-step process that involves trimming down the sensors and then performing waterproofing steps in order to make the sensors installable on da

Vinci instruments such as the Cadiere forceps (Figure 26a)²⁰. There are two reasons for trimming down the sensors: (1) the total diameter of 14mm is too large to go through the trocar (2) the sensors must be installed on the solid backing of the Cadiere forceps which are only 5mm in width. This approach has served as a functional sensing solution for much of the studies previously completed on the CASIT tactile feedback system. Unfortunately, this method has also faced numerous problems and has led to many sensing component failures during experiments. The first issue involves the length of the waterproofing process which has very limited yield. Many of the sensors prepared in this way are damaged during the parylene and Silithane 803 coating process. Even after the waterproofing process is completed, there is less than ideal variability in sensor readings from the coating process. Furthermore, the attachment of the sensors to the graspers are less than ideal. Large shear forces from handling the tissue with the graspers causes the sensors to move around. This movement changes the position of the solid surface of the forceps relative to the sensor, thereby adding some variability in sensor readings. The sensors, having been weakened from the process of being trimmed down, also often completely tear during an experiment due to the excessive shear forces applied. Finally, the previous sensor readout circuitry and feedback system control software was developed using a PIC microcontroller unit. These components were hard-coded with support for the Tekscan B201 sensors and would not easily permit utilization of additional sensors without reprogramming. This further limited the scope of application of haptic feedback as different applications often require different sensor types with varying resolution and dynamic range.

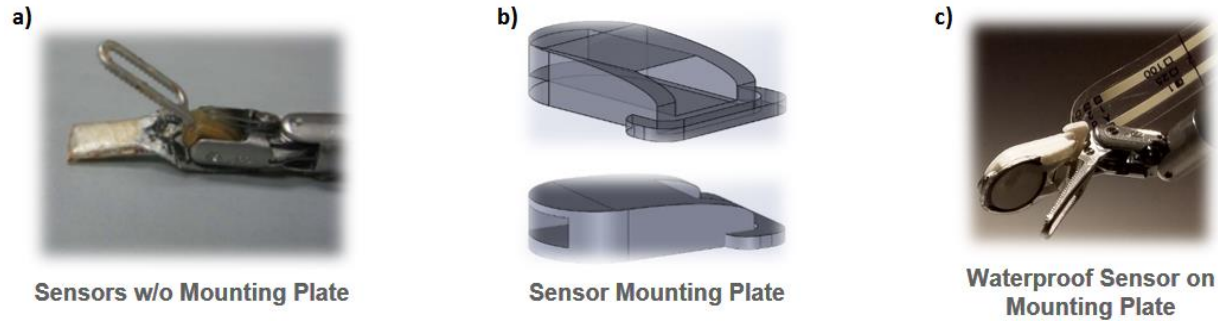


Figure 26: Traditional Sensor Mounting Mechanism vs. Sensor Installed on 3D Printed Mounting Plate

In order to address the aforementioned limitations, a 3D-printed sensor mounting component was designed with a width of 10mm (Figure 26b). This mounting plate provides a stable surface that covers the entire sensing area of the B201 sensor. The sensor is attached to the mounting plate using a 0.1mm acrylic adhesive which maintains a strong bond between the sensor and the mounting plate without any impact on sensor readings. The sensors are trimmed down from 14mm to 11mm in diameter, maintaining the bonding on the outer shell of the sensing area and therefore upholding the integrity of the sensor and preserving its waterproof seal. The resulting sensing component fits easily through the 12mm trocar, is easy to manufacture, and produces consistent readings even exposed to large normal and shear forces during tissue manipulation. Support for multiple sensor types on the other hand is a limitation that must be addressed through redesign of some of the primary components of the tactile feedback system. To this end, these changes were implemented as part of system architecture changes discussed in Aim II (6) of this research project.

5.4 TASK D: DEVELOPMENT OF SHEAR SENSORS

5.4.1 DESIGN OF SHEAR SENSORS

In addition to normal forces, shear forces can also play an important role in certain applications of robotic minimally invasive surgery, such as suturing. In order to allow research on this topic, grasper mounted shear sensors were designed to detect shear forces on the end effectors of the da Vinci surgical system. These shear sensors were designed primarily for installation on the Cadere forceps; however, they could be easily modified to fit other instruments as well.

The primary goal of this research task was the development of proof-of-concept shear sensors to allow investigation into the benefits of haptic feedback for knot tying tasks (Section 7.1.1). To this end, the sensors were designed with the following criteria: (a) size must be sufficiently small to fit on Cadere graspers and not interfere with the ability to hold on to sutures (b) sensors must allow detection of shear forces in at least one direction/axis, (c) device must provide high dynamic range and resolution to be effective in applications for surgical robotics. To this end, a shear sensing mechanism was developed by utilizing two commercially available Tekscan A101 piezoresistive sensors.

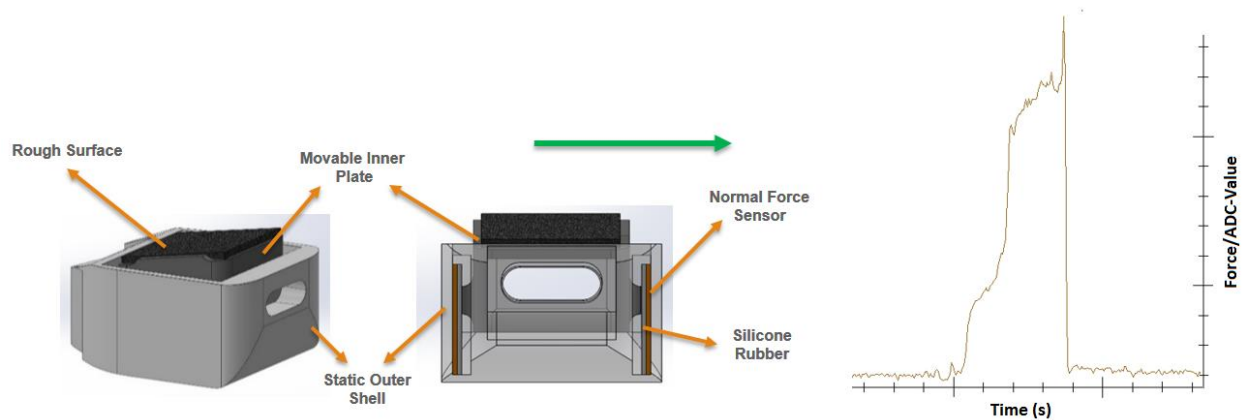


Figure 27: Uni-axial Shear Sensor Design

The A101 sensor is one of the smallest commercially available piezoresistive sensors with a dynamic range of 0-44N. The sensing area is 3.8mm in diameter with the total sensor width of 7.6mm which, for this application, was trimmed down to 6mm (while maintaining water-tightness).

The sensing concept relied on two components, a static Outer Shell and an inner Movable Plate (Figure 27). The outer shell was kept from moving by tightly fitting the Cadiere grasper. The inner plate also had an opening in the center to allow the Cadiere grasper to freely pass through its center. This approach allowed the outer shell to remain static while the inner shell could move slightly from side to side.

On each side of the inner component, an A101 sensor was sandwiched between the outer shell and an extruded area of the inner plate. A 20 shore A silicone rubber membrane with 0.5mm thickness was placed between the sensor and the inner movable plate. The elasticity of this material allowed the inner plate to move back to the original center position after shear forces have been removed. The inner movable plate was also designed to be taller than the outer shell, insuring that contact would only be made with this inner component. Applying shear to the top surface of the inner plate pushes the inner component against the A101 sensor, leading to an increase in the force values reported by the sensor.

It is worth noting that while the inner component is referred to as a Movable Plate, in reality, the size of the inner movable plate and the outer shell are adjusted such that no movement/sliding of the inner plate can take place. This is necessary to avoid any shifts from static to dynamic friction and hence sudden changes in the forces detected by the A101 force sensors.

The surface of the inner component was developed with an angle to account for the tilt that exists on the surface of a Cadere grasper. This was necessary to ensure that the two surfaces become completely aligned when the grasper is closed (Figure 28).

Since the ultimate application of these shear sensors involved manipulating sutures, a problem that arose in benchtop tests was that the finer sutures (5-0, 4-0 and 3-0) would slip when placed in between the claws of the grasper. The original da Vinci Cadere graspers and, more importantly, the Large Needle Driver instrument that is primarily used during suturing both have teeth-like structures that hold onto the sutures. On the other hand, the 3D printed inner component, which is made of Polylactide (PLA), has a relatively smooth surface. While applying a sufficiently high normal force creates enough friction to hold onto the suture on this smooth surface, the Cadere graspers are only capable of applying up to 5N of normal force. This is not sufficient to securely hold many commonly used sutures (such as Silk 3-0). To resolve this problem, a thin sheet of metal with a Corundum coated surface was cut and glued onto the surface of the inner component. A number of sheets were tested out and the selection was made such that the failure load of a suture using this surface would be similar to that of a da Vinci Large Needle Driver (~ 9N for Silk 3-0 suture).

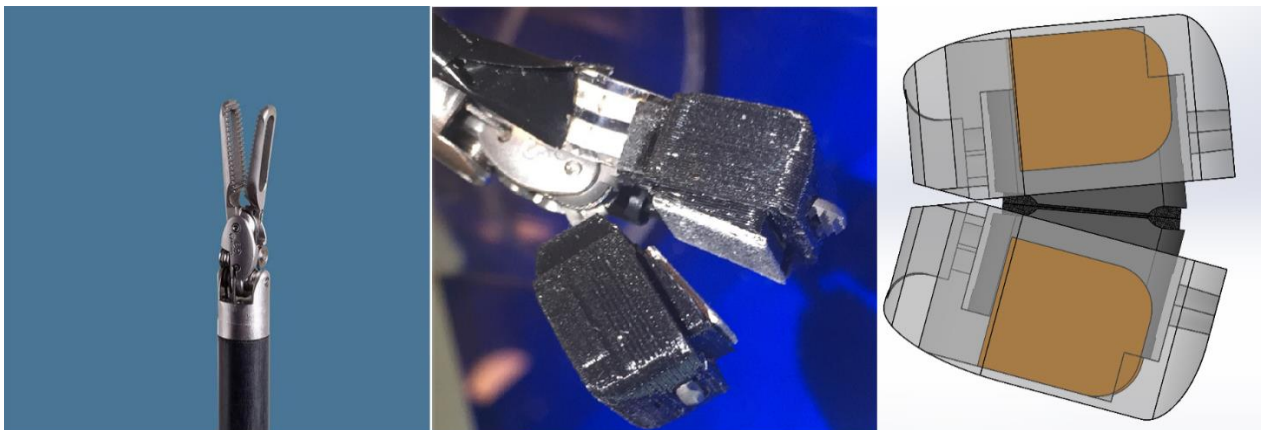


Figure 28: Shear Sensors Installed on Cadere Graspers

The total size of this sensing component was 14.3mm x 10mm which was large enough to prevent movement through the trocar. The size was intentionally excluded from the design criteria as the goal of this sensing component was to perform preliminary studies to evaluate the effectiveness of HFS in a new RMIS application. Ultimately, bi-axial and tri-axial optimized variations of this sensor can be developed that are much smaller and can easily fit through a trocar for pre-clinical testing.

5.4.2 CALIBRATION OF SHEAR SENSORS

Calibration of the shear sensors was necessary to allow a mapping between the digital values reported by the ADC and actual force values in newtons. A readout circuit for the FlexiForce A101 sensors was used based on a simple voltage divider circuit and 10K resistors (Figure 19).

While the theoretical dynamic range of the sensors was 0 – 44N, the calibration was performed for forces below 10N. The reason for this experimental design choice was that the sensors behave linearly at forces below 15N. Since these sensors are designed primarily for use with finer sutures in which failure loads are below 15N, this design choice was justifiable within the scope of this investigation.



Figure 29: Mark-10 Series 3 Digital Force Gauge

Force measurements were performed using a Mark-10 Series 3 force gauge (Figure 29). A Silk 3-0 suture was tied to a hook on the force gauge. The other end of the suture was placed between the claws of the grasper. To prevent any minor suture slippage from impacting the data, a small knot was added to the end of the suture and positioned such that it would prevent any slipping after the claws were closed. The force gauge was then used to pull the suture and the corresponding force and ADC values were recorded (Figure 30).

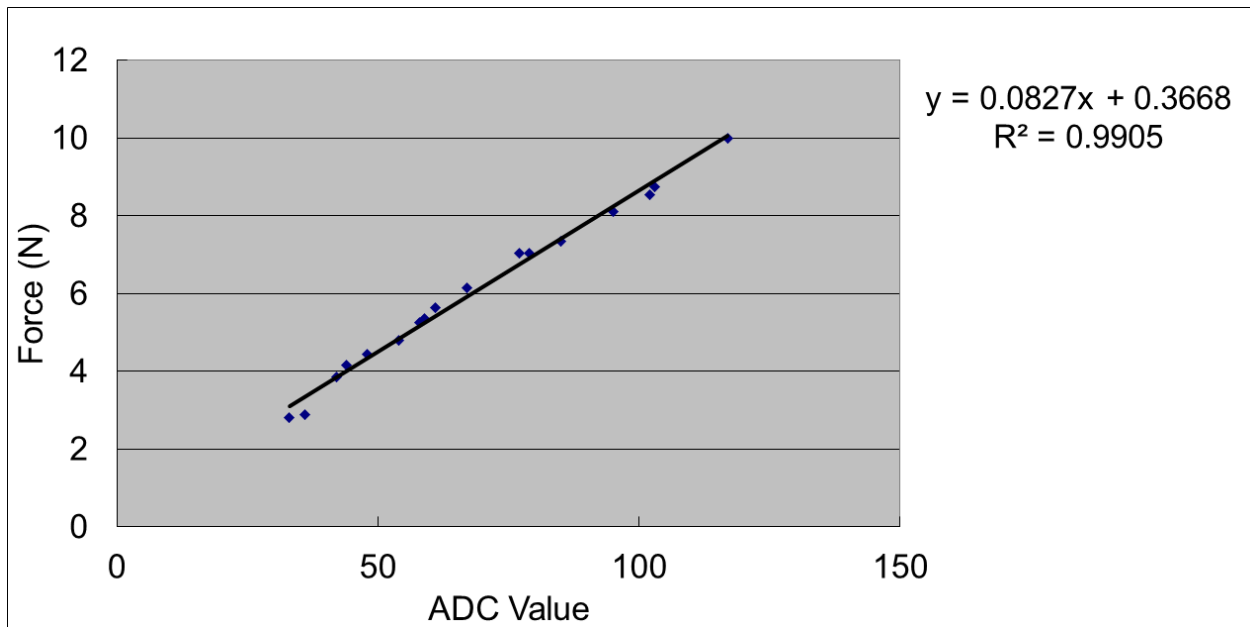


Figure 30: Shear Sensor Calibration

5.5 SUMMARY OF TACTILE FEEDBACK SYSTEM IMPROVEMENT

The purpose of this research aim was to improve upon the CASIT tactile feedback system and eliminate some of the drawbacks of sensing and actuation components. To this end, new depressed-membrane actuators were developed that were more effective at conveying grip forces and in reducing sensory desensitization. The sensing mechanism was also improved with the development of a new sensor board and accompanying communication protocol. The new sensor

board supports reading data from up to 12 sensors simultaneously and with varying dynamic range and resolution for each sensor. In addition, it also supports a larger dynamic range from the Tekscan B201 sensor, increasing its read range from 0 – 4.4N to 0 – 15N. The sensor mounting mechanism was also improved, increasing the reliability of sensor readings and the lifespan of the sensors. Finally, new shear sensors were developed, tested, and calibrated. These shear sensors will play a critical role in expanding the use of haptics in robotic surgery applications, such as suturing and knot tying.

6 DEVELOPING A MULTI-MODAL HAPTIC FEEDBACK SYSTEM

The sense of touch in humans involves the activation of two sets of mechanoreceptors, those in the skin and those in the muscles. The activation of mechanoreceptors in the muscle contribute to the sense of kinesthesia. Consciously, an individual perceives this as an object resisting a motion. The mechanoreceptors in the skin, on the other hand, contribute to perception of vibration, deep pressure, light touch and other more complex senses through integration with higher cognitive processes in the brain. The goal of this research aim was to develop a haptic feedback system capable of conveying information using multiple modalities of haptic feedback. Most specifically, the three primary modes of feedback being investigated as Kinesthetic Force Feedback, Vibration Feedback, and Tactile Normal Force Feedback (Figure 31).

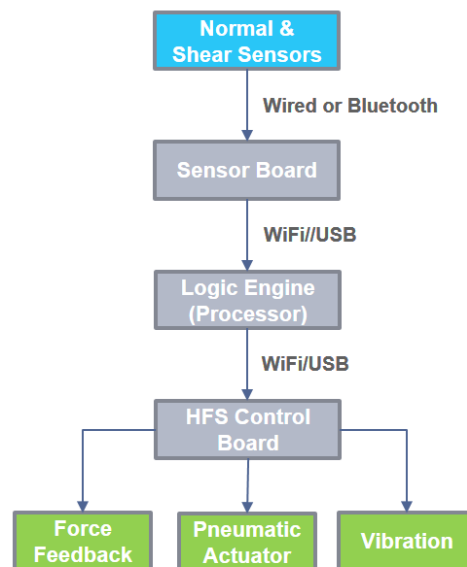


Figure 31: Abstract View of Multi-Modal HFS Architecture

Tactile normal force feedback technology has been investigated for many years through the development of CASIT's tactile feedback system and also through enhancements discussed in Chapter 5. Therefore, this research aim focused on two tasks: (a) developing a system architecture

capable of activating multiple modalities of feedback,(b) engineering technologies for providing vibration feedback, and (c) engineering technologies for providing kinesthetic force feedback.

6.1 MULTI-MODAL HFS DESIGN CRITERIA

The development of the multi-modal HFS architecture relies on four primary design criteria:

1. Low Latency Communication & Support HFS Over Internet
2. Low Latency Processing
3. Support for Multiple Sensor Types
4. Support for Multi-Modal Feedback

Low latency communication and processing are one of the most important criteria in the design of a multi-modal HFS. The primary reason for the importance of these features is the additional latency that is introduced by implementing additional modalities of feedback. Many actuation systems, including those which will be introduced later in this chapter as part of the kinesthetic force feedback, require significantly more time to operate. Therefore, enhancements in communication and processing latency are necessary in order to make sure that overall system response time remain low. Research has shown that latencies beyond 200ms can be easily noticed by the surgeon and lead to performance deficits^{104,105}.

6.2 LOW LATENCY WIRELESS COMMUNICATION

One of the advantages of robotic surgical systems is their teleoperation capabilities. In addition, even when surgery is not being performed remotely, the robot and the master control can often be many meters apart. The original CASIT tactile feedback system utilized a commercial, off-the-shelf, pass-through serial-to-Bluetooth dongle to transmit data from the sensor board to the haptic control board. This approach is less than ideal due to limitations of range and latency.

Alternatively, all components of the haptic feedback system can be directly connected to the internet. This design choice would provide remote site teleoperation capabilities and potentially reduce latency.

6.2.1 PROGRAMMING OF ESP8266 WiFi MODULE



Figure 32: ESP8266 Module

An ESP8266 was utilized to implement a pass-through WiFi-to-UART module (Figure 32). ESP8266 is a self-contained System-on-Chip (SOC) with an integrated antenna and microcontroller unit. Utilizing available TCP/IP protocol stack, a TCP server was implemented and programmed onto the ESP8266 module. The custom pass-through interface was programmed to support the following capabilities:

1. Write any data from the ESP8266 Serial Rx to all connected TCP clients
2. Write any data received from connected TCP clients to the ESP8266 Serial Tx
3. Accept commands from the connected serial device (through the ES8266 Serial Rx) in the following format:

<	Command Type	,	Argument 1	,	Argument 2	,	...	>
---	---------------------	---	-------------------	---	-------------------	---	-----	---

Support for the following set of commands was implemented:

- ConnectSSID (<ConnectSSID,SSIDNAME,SSIDKEY>): allows the attached serial device to request connection to any available WiFi hotspot.
 - GetSSIDs (<GetSSIDs>): provides a list of all visible WiFi hotspots to the attached serial device.
4. Write status information about the current WiFi connection to the attached serial device (through the ESP8266 Serial Tx)

<	Status Info Type	,	Value 1	,	Value 2	,	...	>
---	-------------------------	---	----------------	---	----------------	---	-----	---

Support for the following set of status information were implemented:

- IP (<IP,192.168.1.2>): Reports the local IP address
- SSIDs (<SSID,Hotspot1,Key1>): Reports list of all available SSIDs
- Error (<Error,Message>): Reports any errors that may occur
- Disconnected (<Disconnected,Client,1>): Reports that a client was disconnected followed by the number of remaining connected clients
- Connected (<Connected,Client,1>): Reports when a new client is connected and followed by the total number of connected clients.

Another issue that arose when testing the newly developed WiFi module was related to dropped TCP connections. In some routers and firewalls TCP connections that remain idle beyond a certain period of time are closed. In most cases this is not a problem because a new TCP connection can easily be reestablished. The issue, however, is that creating a new TCP connection is far more time consuming than sending data over an already open connection. Therefore, dropped TCP connections can be costly in a haptic feedback system that attempts to minimize latency. To resolve

this issue, a callback function was implemented on the ESP8266 server code. In other words, the ESP8266 would response to an incoming “~” character from a TCP client with a “~” ACK character. On the TCP client side, a heartbeat function was implemented such that a “~” character would be sent to the server in instances when the connection was idle for long periods of time. This approach maintains the TCP connection’s open status, thereby eliminating unnecessary connection delay.

6.2.2 EVALUATION OF WiFi MODULE RESPONSE TIME

In order to test the response time of the ESP8266 module, two methods were used. The first was an Internet Control Message Protocol (ICMP) ping request to the module. This was repeated 100 times over the local WiFi network and the average response time was measured. All 100 requested pings returned in less than 1ms. As a second method and a way to test how much time the ESP8266 would spend processing the data, a TCP client software was developed in C# which would utilize the callback function on the ESP8266 as a way to test its response time. The software would send a packet to the ESP8266 and wait for the “~” response character, at which time the next packet would be sent. Three separate tests were performed using 1000, 10,000 and 100,000 iterations. In all cases, the average delay per packet was <1ms.

6.3 SYSTEM ARCHITECTURE

The traditional approach used by many feedback systems, including the CASIT tactile feedback system, is to create a direct mapping between sensor data and actuator feedback levels. These mappings are often hard-coded on a microcontroller unit and serve as the control center of the

system. This approach, however, creates significant limitations with regards to system adaptability and application in different surgical tasks.

The multi-modal haptic feedback system architecture was designed to allow significant flexibility in the way sensor data could be mapped to activation of feedback actuators. The goal was to allow investigation of the benefits of haptic feedback for various tasks in robotic surgery without requiring any reprogramming or redesign of the sensor boards and/or control boards of the HFS. To this end, all decision making and logic would be performed on a separate computer within the accessible network. An overview of this system architecture can be seen in Figure 33.

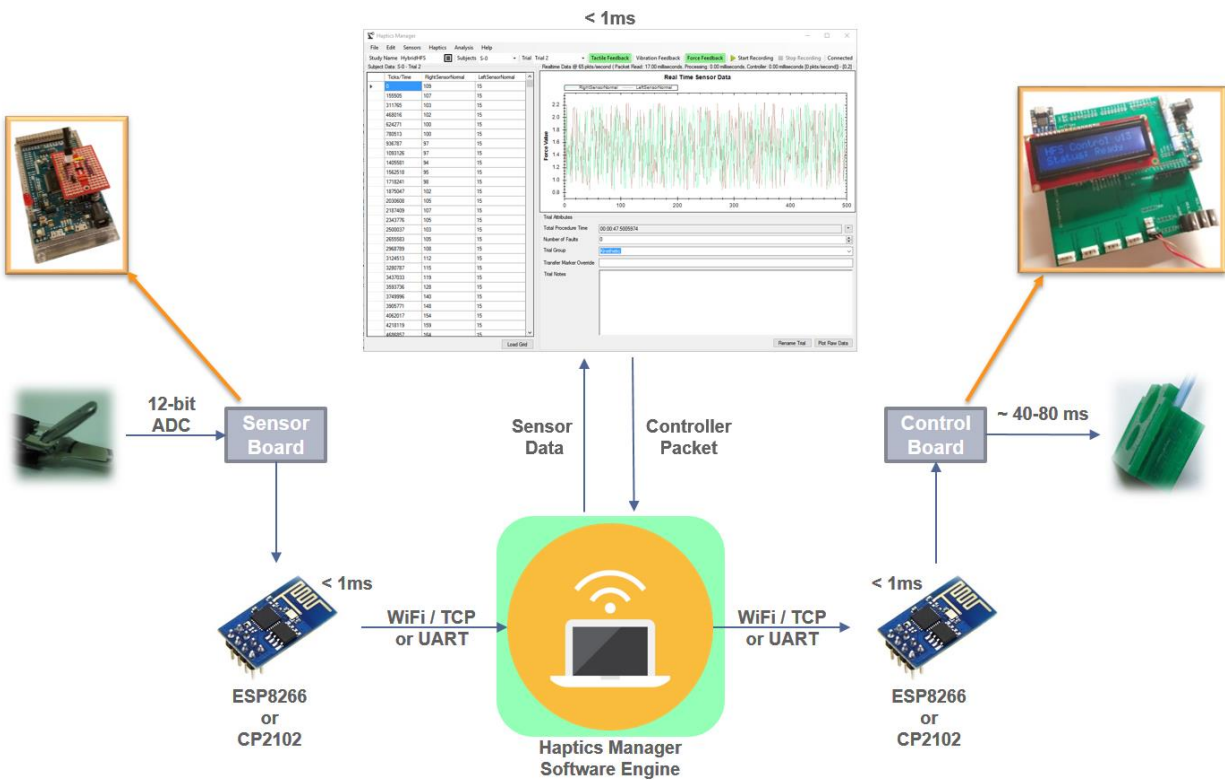


Figure 33: Multi-Modal HFS System Architecture

In this design, a software engine (i.e. Haptics Manager) is developed using C# and the .Net framework and used as the central processing unit for the multi-modal HFS. The sensor board and the control board functionalities are thereby simplified. The sensor board (Section 5.1) would thus

be only responsible for transmitting data of the connected sensors to the Haptics Manager software, using the previously developed ESP8266 WiFi module or a USB wired connection which relies on a CP2102 controller for Serial-to-USB data transmission. The control board also relies on the same two communication modalities for receiving control packets from the Haptics Manager software. All logic and control decisions are made in the Haptic Manager software. The software will handle filtering of sensor data, deciding what actuation modality and level setting should be invoked in response to the current sensor values. A control packet is then created with the target actuation levels and sent to the control board which will activate the appropriate feedback modality (Figure 33).

6.4 HAPTICS MANAGER SOFTWARE

The Haptic Manager software serves as the primary filter and control component of the multi-modal haptic feedback system. The software is a C# application developed using Microsoft's .Net framework. In the most abstract way, the software is designed to receive sensor data in a particular packet format and generate a controller packet in response.

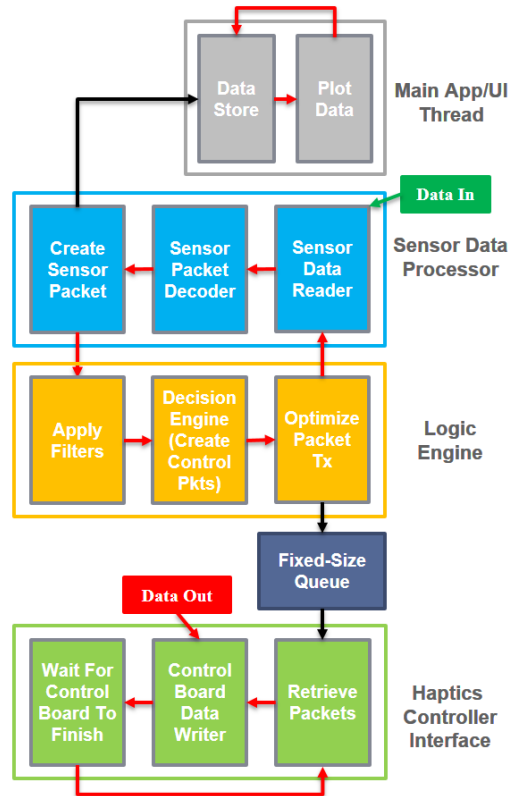


Figure 34: Haptics Manager Software Architecture Using WiFi for Sensor and Control Board Communication

Figure 34 illustrated the Haptics Manager software architecture. The Haptics Manager provides five major functions:

1. Process & Filter Sensor Data (Sensor Data Processor)
2. Generate Control Board Packets (Logic Engine)
3. Transmit Data to Control Board (Haptics Controller Interface)
4. Plot Data and Store Sensor Data in Real-Time (Main UI)
5. Perform Statistical Analysis of Recorded Data

The Haptics Manager software architecture was designed with data processing latency in mind. While most haptic feedback systems are designed based on a single-threaded, pipelined approach, this solution is inefficient for more complex multi-modal feedback systems. In a single-threaded

approach, the data processing is synchronous, starting with sensor packets being generated, then filtered and processed. This is followed by control packets being generated and sent out to the control board. Additional functions such as storing the data and plotting the data in real-time add additional steps to the pipeline. The pipelined design is, therefore, extremely costly for the overall system latency as each sub-process adds some delay, lengthening the processing time. Most importantly, a pipelined approach makes the system highly susceptible to failures. Particularly in a system with many wireless components, unexpected delays can be introduced, even under the best of conditions. If any component of the system faces delays (ex. the control board or the WiFi connection to the control board), then a buildup of packets can arise, leading to build up of packets further up the processing chain and hence additional unnecessary delays.

To resolve these issues, an asynchronous, multi-threaded architecture with fixed-size processing queues was used in the design of Haptics Manager software architecture. In Figure 34, transition of data between processing units within the same thread can be seen in red, while cross-thread operations can be observed in black. The Haptics Manager software relies on three primary processing threads. The first is one that receives data from the sensor board, performs decoding, filter, processing and controller packet generation. This thread then writes the data in a thread-safe fixed size queue. The second thread constantly retrieves data from the queue and transmits data to the control board. The third thread is responsible for data storage and user interface updates, both of which are extremely slow processes and therefore critical to keep out of the main processing loop. The purpose of the fixed-size queue is to ensure that any slowdowns in handling the controller packets, whether it'd be related to communication or mechanical delays in the actuators, would have no impact on data processing. Under such conditions, the queue can become full and then begin to lose older items as new items are inserted. When the controller thread begins

responding again, a few packets may have been skipped, but the system quickly begins to respond to the most recent data, rather than spending time processing previous requests that may no longer be relevant. This approach allows the system to quickly recover from any unexpected delays within any component. The same benefits also apply to the data storage and user interface updates which suffer slowdowns particularly when the computer's hard disk or graphics card are busy with another task.

6.4.1 SENSOR DATA PROCESSOR

The Sensor Data Processor is a sub-component of the Haptics Manager software that is responsible for retrieving data packets from the sensor board and decoding the sensor data into a packet format that can be easily processed by the Haptics Manager software.

The Sensor Data Read is a sub-component of the Sensor Data Processor that is responsible for retrieving data from the sensor board. This component can either connect to an ESP8266 module (Section 6.2) through the Haptics Manager's telnet client or read data directly from a COM port which represents a direct USB connection to the sensor board. Communication through the COM port is configured to occur at a baud rate of 115200 bps.

6.4.2 LOGIC ENGINE

The Logic Engine is a sub-component of the Haptics Manager software responsible for applying filters to the incoming sensor data, applying packet transmission optimization and most importantly creating the controller packets based on the engine configuration (Figure 35).

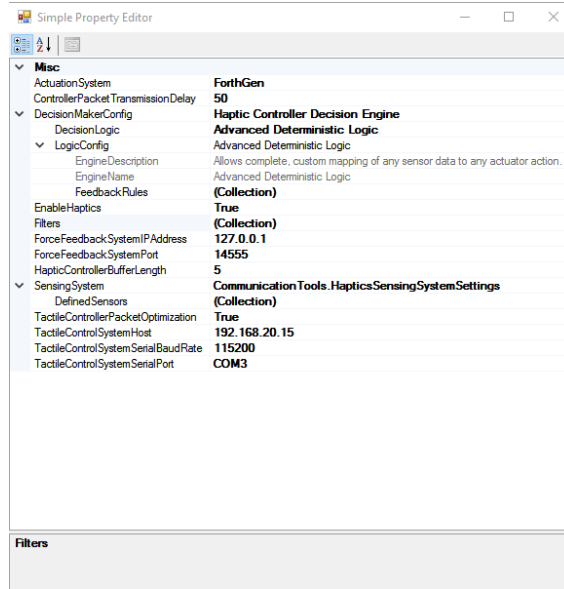


Figure 35: Logic Engine Configuration Page

6.4.2.1 Sensor Data Filters

Two different data filter types were developed and tested during the development of the multi-modal HFS. The Haptics Manager software allows multiple filters to be applied to the incoming sensor data to reduce sensor noise and reduce unnecessary processing of data packets (Figure 36).

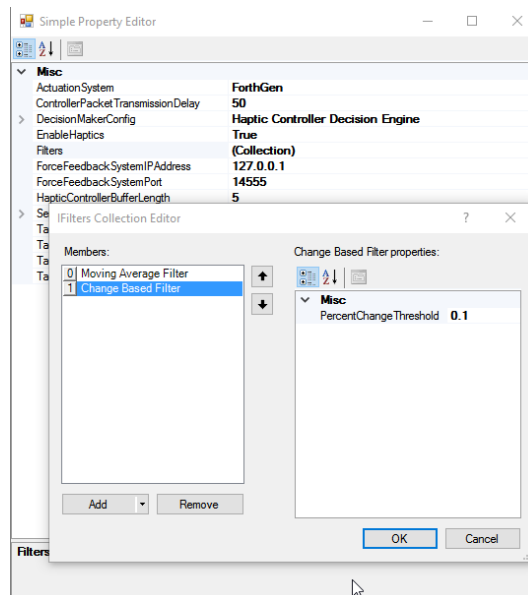


Figure 36: Data Filter Collection Configuration Page

The following filters were developed:

- **Moving Average Filter:** A low pass, finite impulse response filter that allows for smoothing of the sensor data curve.
- **Change Based Filter:** Eliminates sensor values that are less than or greater than some percentage (ex. 10%) of the previous sensor data. If the sensor is within the range to be eliminated, the last sensor value is reported in its place. This type of sensor eliminates noise by eliminating changes that are not significant enough to result in a change in any of the actuator feedback levels. This filtering method can be a better alternative to the moving average filter because it does not introduce any additional delay to the packet processing.

6.4.2.2 Sensor Definitions

In order to support multiple data sensors, the Haptics Manager software allows the definition of an unlimited number of sensors in software. The data from the sensor board is mapped to these sensor definitions based on the index of the value in the sensor packet (Figure 18).

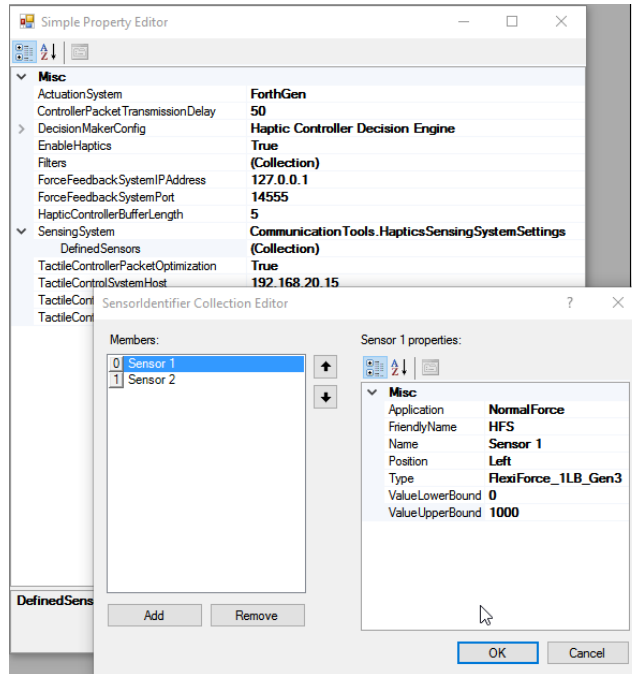


Figure 37: Sensor Definition in Haptics Manager Software

Each sensor is defined using the following set of parameters:

- Name: Unique sensor name
- Friendly Name: Allows reporting data for a specific sensor using a friendly sensor name during data analysis.
- Type: Defines the type of the sensor. This information is used as a unique identifier (i.e. Make/Model of the sensor). The following sensor types have been used throughout the various haptic feedback studies and therefore have been programmed into Haptics Manager:
 - *FlexiForce_1LB_Gen1*: This represents the FlexiForce B201 sensor when used with the sensor board from the original CASIT Tactile Feedback System²⁰.

- *FlexiForce_1LB_Gen2*: This represents the FlexiForce B201 sensor when used with a 2nd generation sensor board which utilized 47K resistor instead of the 10K resistor described in Section 5.1.
- *FlexiForce_1LB_Gen3*: This represents the FlexiForce B201 sensor when used with the 3rd generation (most recent) sensor board described in Section 5.1.
- *FlexiForce_10LB*: This represents the FlexiForce A101 sensor which was used for the development of shear sensors described in Section 5.4.
- Application: The sensor application type is used to identify the type of data that the sensor is providing. This field, in combination with the sensor type, are used to identify the calibration equation that is used to convert ADC values from the sensor board to actual force values in Newtons. The following sensor types are supported: *Generic, Normal, Shear X, Shear Y*
- Value Lower Bound/Value Upper Bound: These values define the minimum and maximum ADC values that can be recorded by this sensor. These values are used during data analysis when calculating gripped-threshold (see Section 4.1.1).
- Position: Defines whether the sensor is installed on the Right or Left arm of the robot.

6.4.2.3 Decision Engine: Controller Packet Generation & Feedback Rules

The most important sub-component of the Haptics Manager Logic Engine is the Decision Engine. Sensor packets which have been filtered out are sent to this component at which point the Decision Engine configuration is used to generate a control packet in response to each sensor packet (Figure 38).

Haptics Manager supports multiple types of decision engines. In fact, throughout this research project, seven different decision engines were created, each generation with some additional capabilities compared to the last. The final and most flexible decision engine is the “Advanced Deterministic Logic Engine” which allows the definition of a series of rules that are ultimately used to map any sensor value to activation of any actuator within the multi-modal haptic feedback system.

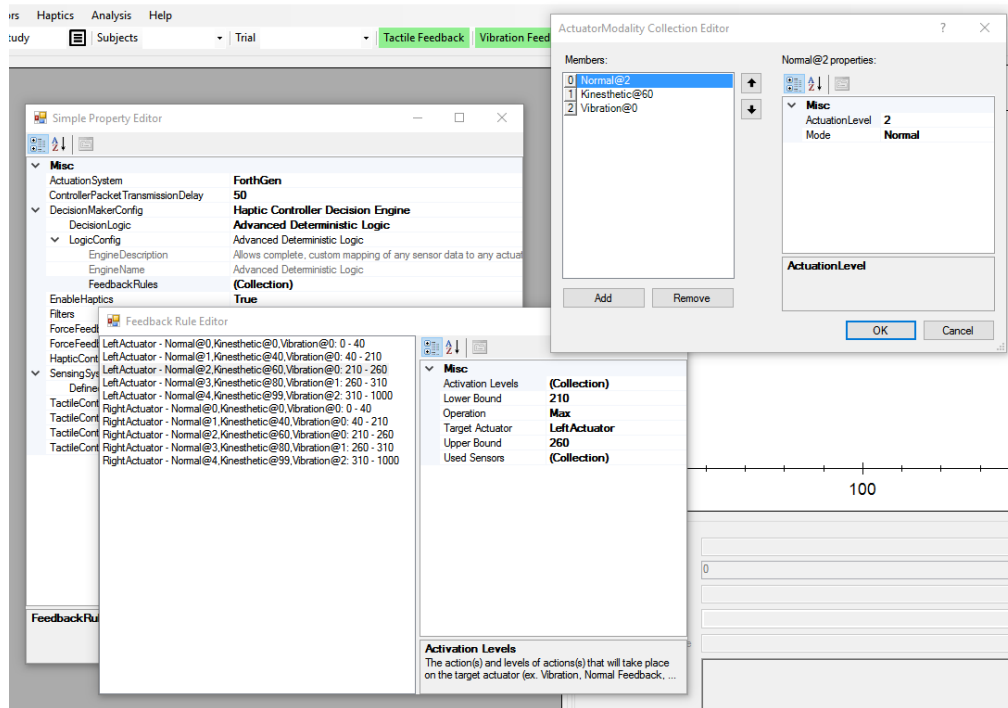


Figure 38: Configuration of Advanced Deterministic Logic Engine (Generation 7 Decision Engine Used in Haptics Manager)

Each Feedback Rule is defined using a series of parameters which help the engine determine when and how to apply the rule to an incoming sensor packet and generate a new Controller Packet.

The following feedback rule parameters are implemented:

- **Target Actuator:** specifies which actuator (right or left arm) is targeted by this rule. It is worth noting that this is not defining the actuation mode, but only whether the actuators on the right or left arm of the subject are being targeted.

- **Used Sensors:** defines the list of all sensors that are used by this rule. In the most basic HFS, one sensor is associated with one rule (Figure 39). For example, a normal force sensor on the right arm of the robot may be used to provide data for actuation on the right hand of the surgeon. In more complex, multi-modal HFS applications, however, (ex. tissue palpation) it is possible that the data from multiple sensors is necessary for providing the appropriate feedback level. For example, a sensor array may be used with a series of reference and data sensors all contributing to the feedback operation.
- **Operation:** defines the operation that is performed on the values from all the “Used Sensors”. The operation will lead to a single double-precision value which will be used as the single value representing the values of all the Used Sensors combined. Three operations are supported:
 - **Max:** the maximum value of all the sensor values is used
 - **Add:** all the sensor values are added together to produce one value
 - **Subtract:** all sensor values are subtracted from the maximum sensor value. This operation is most often used in sensor arrays with reference sensors used to eliminate noise.
- **Actuation Levels:** used to create the control board packet. This parameter contains a list of Actuator Activation levels. This list basically defines which actuator and to what level it should be activated. An example of an Actuator Activation list can be seen in Figure 38.
- **Lower Bound/Upper Bound:** used to determine whether the current feedback rule should be used in response to a specific sensor packet. After having applied the “Operation” on the “Used Sensor” values from an incoming sensor packet, if the resulting double-precision value is between this lower and upper bound, then the current feedback rule is applied to

the incoming sensor packet and a new control board packet is generated using the Actuation Levels parameter.

Ultimately, the combined effect of all of the configured Feedback Rules leads to creation of a complete Controller Board packet which can be sent to the control board to provide feedback.

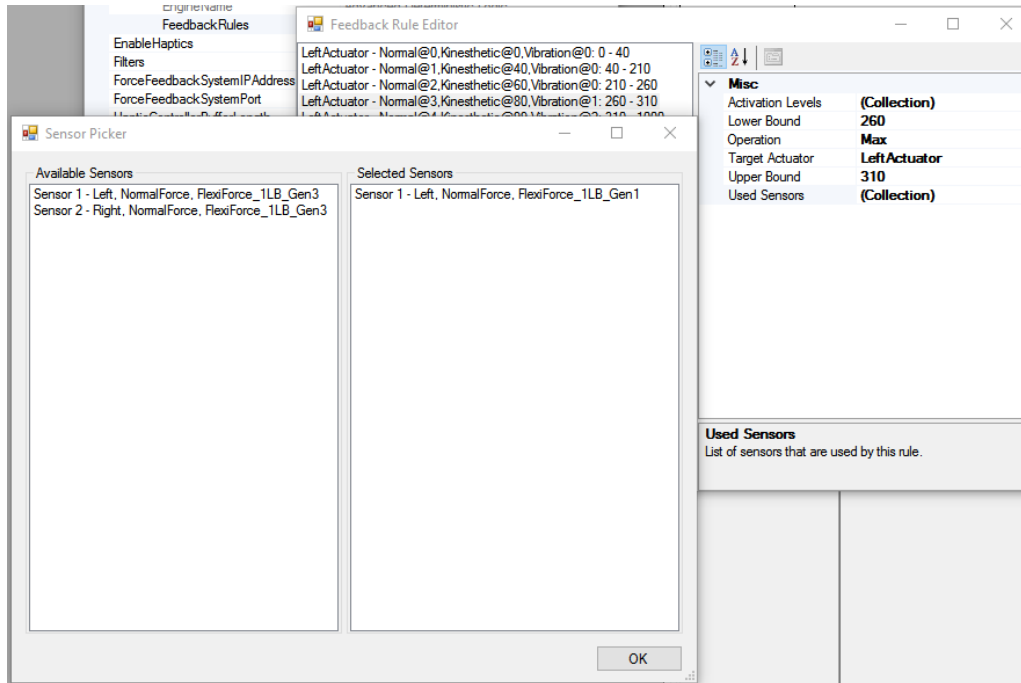
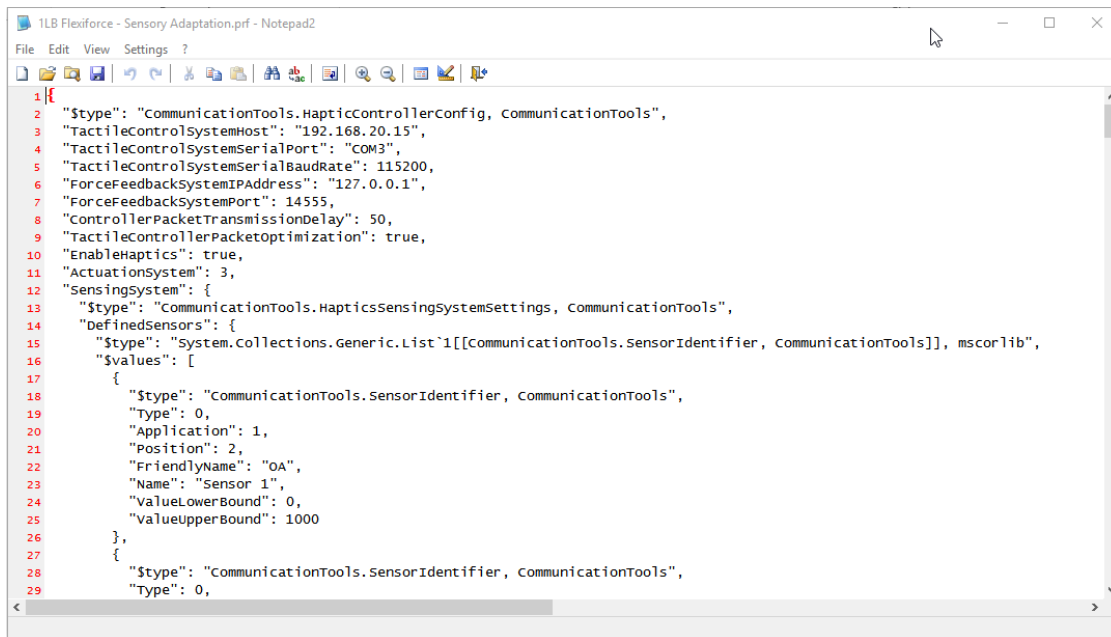


Figure 39: Used Sensor Selection During Feedback Rule Configuration

Haptics Manager also allows the importing and exporting of Logic Engine configuration to an HFS Profile file (*.prf). The file is stored in Json format and contains all configuration of the Logic Engine (Figure 40). This file also contains control board settings such as the IP address and/or COM port name for communication with the HFS control board hardware. This ability to import and export engine settings is critical to the study of multi-modal HFS for various robotic surgical tasks. The ability to easily reconfigure the entire behavior of the haptic feedback system makes the structure adaptable, allowing it to be easily changed for applications in different surgical tasks. For

example, while one profile may be configured to allow the multi-modal HFS to provide artificial palpation for surgeons in robotic surgery, a different profile may use a completely different set of sensors and actuators to help reduce suture breakage in robotic surgery.

Furthermore, ultimately, as part of future investigations, this design allows engine profiles to be automatically updated and saved for each individual user, leading to completely customized user-specific feedback profiles.



```
1 {
2   "$type": "CommunicationTools.HapticControllerConfig, CommunicationTools",
3   "TactileControlSystemHost": "192.168.20.15",
4   "TactileControlSystemSerialPort": "COM3",
5   "TactileControlSystemSerialBaudRate": 115200,
6   "ForceFeedbackSystemIPAddress": "127.0.0.1",
7   "ForceFeedbackSystemPort": 14555,
8   "ControllerPacketTransmissionDelay": 50,
9   "TactileControllerPacketOptimization": true,
10  "EnableHaptics": true,
11  "ActuationSystem": 3,
12  "SensingSystem": {
13    "$type": "CommunicationTools.HapticsSensingSystemSettings, CommunicationTools",
14    "DefinedSensors": {
15      "$type": "System.Collections.Generic.List`1[[CommunicationTools.SensorIdentifier, CommunicationTools]], mscorlib",
16      "$values": [
17        {
18          "$type": "CommunicationTools.SensorIdentifier, CommunicationTools",
19          "Type": 0,
20          "Application": 1,
21          "Position": 2,
22          "FriendlyName": "OA",
23          "Name": "Sensor 1",
24          "ValueLowerBound": 0,
25          "ValueUpperBound": 1000
26        },
27        {
28          "$type": "CommunicationTools.SensorIdentifier, CommunicationTools",
29          "Type": 0,
```

Figure 40: Feedback Profiles File Stored in Json Format

6.4.2.4 Packet Transmission Optimization

In the developed multi-modal haptic feedback system, the components with the slowest response are the feedback actuators. In fact, the rest of the system components, including sensing, processing and communication have response times that average <1ms each. Sending every packet that is received and processed in the Haptics Manager to the controller board can in fact reduce the average system response time. The main reason for this is that two packets may arrive back to back but the first may lead to no change in feedback levels (no change in actuation) while the

second may contain a relevant change that requires actuator response. If the first packet had been sent to the control board for actuation to take place, the control board may still be busy processing the first packet when the second packet arrives. By holding on to the last haptic controller packet that has been generated and sent out to the control board, it is possible to throw out any identical packet that arrives. Using this approach, in combination with the fixed-size queue (Figure 33), it is possible to utilize a much higher sensor board sampling rate, even if the control board response time is significantly slower.

6.4.2.5 Data Storage & Real-Time Sensor Data Plotting

The Haptics Manager software plots all incoming sensor data in real-time (Figure 41). Basic statistics such as the number of packets received per second, processing latency, control board response delay, and maximum sensor values are also reported in real-time. These real-time data and statistics are critical for debugging purposes in case of a failure somewhere in the system.

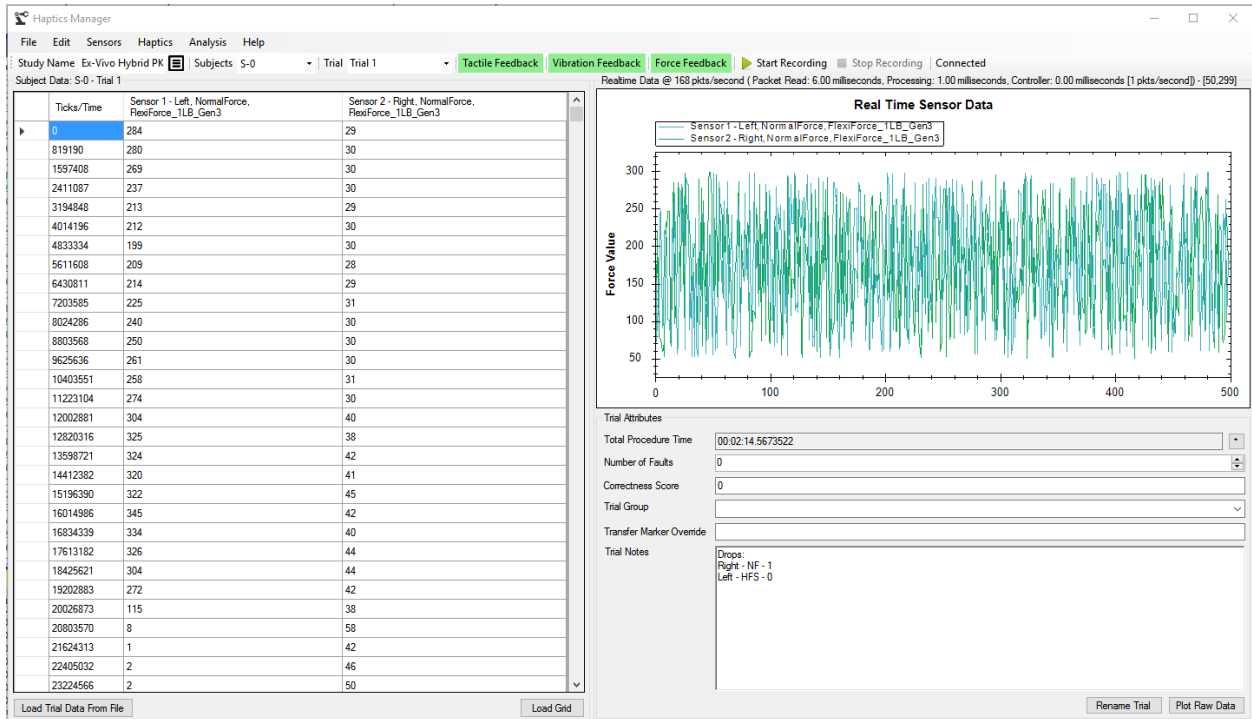


Figure 41: Haptics Manager Main Interface

The Haptics Manager software is also responsible for storing experimental data. All data is stored using a hierarchical data structure (Figure 42) and saved in a Study Data (*.sd) file.

- Study Data
 - Study Name: name of the study
 - Study Notes: a description of the study and experimental protocols
 - Study Start Date: the date on which the first experiment took place
 - Study Groups: the list of all study groups (ex. No Feedback, Tactile Feedback, etc.)
 - Subjects
 - Subject 1
 - Subject Name: name of subject (can be randomly generated to protect subject identity)
 - Trials
 - Trial 1
 - All Sensor Data: all sensor packets received (including sensor type information)
 - Time to Completion: total amount of time for the trial
 - Group: what study group does this trial belong to
 - Number of Faults: the number of mistakes or errors during the trial
 - Correctness Score: a generic field which can be associated with any study variables (ex. Correct detections, etc.)
 - Trial 1
 - Trial 2
 - .
 - .
 - .
 - Trial t
 - Subject 2
 - .
 - .
 - Subject n

Figure 42: Hierarchical Data Structure for Storing HFS Experimental Data

6.4.3 STATISTICAL ANALYSIS

The decision to utilize the Haptics Manager software as a means of performing all statistical analysis for investigations performed under this research project was based on the fact that the experimental data stores (*.sd files) could be more easily parsed and analyzed. This approach would also shorten the time needed for performing data analysis on experimental data because some HFS experiments utilized a similar protocol and could use the same data analysis techniques as a previous study.

The Haptics Manager software itself does not implement any statistical methods. Instead it relies on Accord.Statistics mathematical libraries¹⁰⁶ and R.Net¹⁰⁷. R.Net acts as a communication interface with a local R-Statistics software package¹⁰⁸. Most statistical analysis were, therefore, performed using R-statistics packages and commands. The Study Analyzer function of the Haptics Manager software is designed to prepare and organize the study data in a format that could be understood by R, and then execute the appropriate commands depending on the selected analysis methods. The following statistical analyses were implemented using R statistical libraries:

- Two Sample Comparison
 - Paired T-Test: paired version of student's t-test for studies performed using repeated measures design. This analysis is performed using Accord.Statistics package.
 - Two Sample T-Test (Equal Variance): student's t-test performed using Accord.Statistics package. This test assumes that the samples have equal variances.

- Two Sample T-Test (Unequal Variance): student's t-test performed using `Accord.Statistics` package. This test is used when the samples do not have equal variances.
- Wilcoxon Rank Sum Test: this test is an alternative to student's t-test for data that is not normally distributed. This nonparametric test is performed using `wilcox.test` function in R statistics.
- Wilcoxon Signed Rank Test: this test is a paired variant of the Wilcoxon Rank Sum test, performed for repeated measures studies. This nonparametric test is performed using `wilcox.test` function in R statistics.
- Multiple Sample Comparison
 - One-way ANOVA (Equal Variance): analysis of variance for comparison of group means for more than two groups. This test assumes that the variance of all groups is equal and is performed using `oneway.test` function in the R statistics package.
 - One-way ANOVA (Unequal Variance): analysis of variance for comparison of group means for more than two groups. This test does not assume equal variance between groups and is performed using `oneway.test` function in the R statistics package.
 - Kruskal-Wallis One-way ANOVA (Nonparametric, Equal Variance): a non-parametric variant of one-way ANOVA for cases when normality assumption is not met. This test is performed using the `Kruskal.test` function in R statistics.

- Repeated Measures ANOVA: a variant of ANOVA test used for repeated measures studies. This method uses the Linear Mixed Effects (*lme*) and *anova* functions of R statistics¹⁰⁹.
- Friedman's Test (Nonparametric Repeated Measures ANOVA): this test is a nonparametric alternative to one-way ANOVA with repeated measures. Friedman's test can be used when assumption of normality cannot be met¹¹⁰. This test utilizes functions in the *coin* and *multcomp* packages of R statistics. Friedman's test however is not always the right choice because it ignores the relative size of the differences between participants¹¹¹. Therefore, the utilization of this test should be avoided when other alternatives exist.
- Rank Transformed Repeated Measures ANOVA: this test relies on rank sum transformation to allow repeated measures variant of one-way ANOVA to be used when normality assumption cannot be met¹¹¹. This test performs the transformation using the *rank* function in R statistics, followed by utilization of Linear Mixed Effects (*lme*) and *anova* functions in R.
- Ordinal Repeated Measures ANOVA: this test is a one-way repeated ordinal regression analysis using the *clmm* function of R statistics¹¹². This analysis is an alternative to one-way ANOVA for repeated measures experiments with ordinal data.

For ANOVA tests, when the p-value was < 0.05 , post-hoc analyses were performed for pair-wise group comparisons. Post-hoc tests using Tukey, Bonferroni, Holm, Hommel, and Hochberg corrections were implemented. It is worth mentioning that Holm and Tukey tests were used as the preferred methods for p-value adjustment in most experiments.

Other tests such as Shapiro-Wilk normality test and various methods for comparing variance of two samples were also implemented (Figure 43).

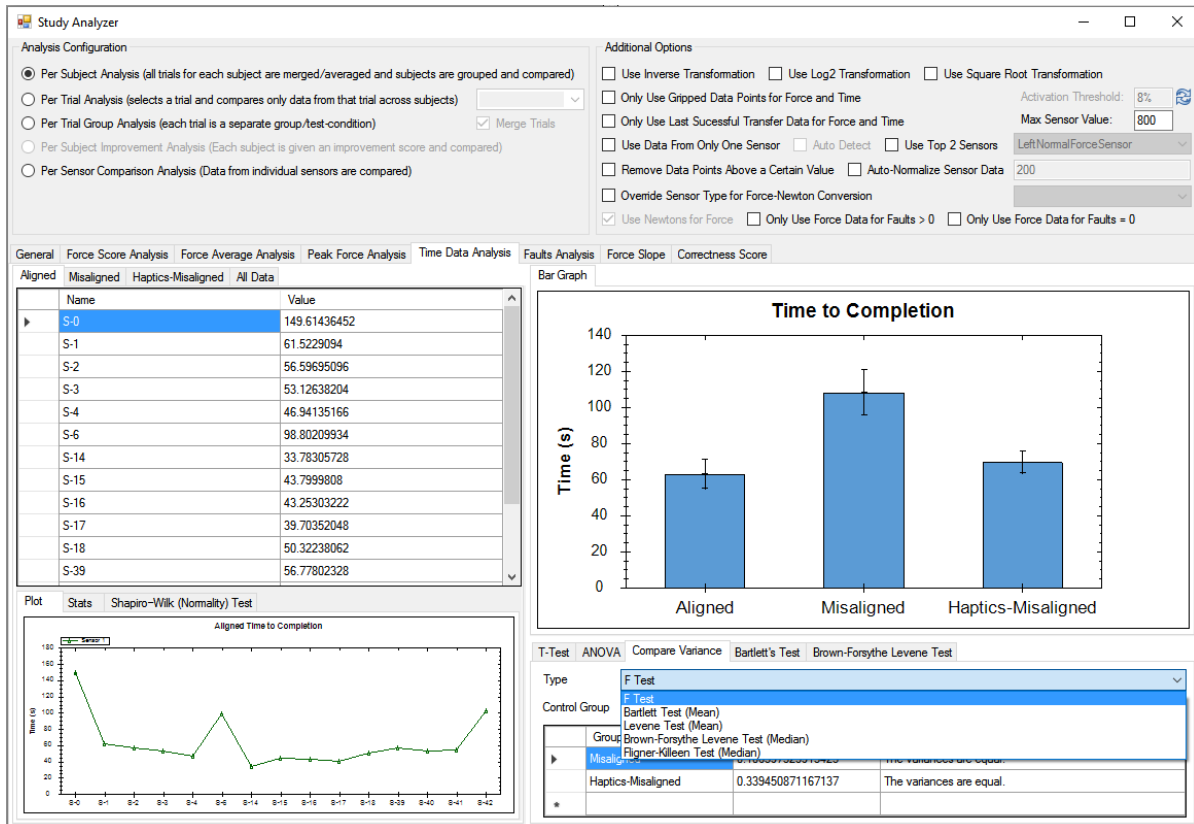


Figure 43: Haptics Manager Study Analyzer Main Interface

Figure 43 shows a view of the main interface of the Haptic Manager’s Study Analyzer. Study Analyzer supports four major analysis methods:

1. **Per Subject Analysis:** this analysis method is used for experiments where each subject falls into a separate study group. Under this analysis method, the data for all the trials (if more than one) for a single subject are averaged together.
2. **Per Trial Analysis:** this type of analysis allows one trial of each subject to be compared against the same trial for all other subjects

3. Per Trial Group Analysis: this type of analysis is used for repeated measures studies where each trial belongs to a different study group
4. Per Sensor Comparison Analysis: this type of analysis is also used for repeated measures studies with the difference that data from each sensor belongs to a separate study group. In this type of analysis, the sensor's FriendlyName parameter (Section 6.4.2.2) is used as the name of the study group.

Study Analyzer also supports built-in functions for Log2, Square Root and Inverse transformations which can be used in some cases when data is not normally distributed.

Finally, for calculating grip forces, Study Analyzer uses a threshold-based method to identify the sensor data corresponding to the times when the subject was holding onto the tissue. Calculating grip times is very important in analyzing the average grip-force. Without eliminating sensor values from instances when the robotic forceps are not gripping the tissue, the average grip-force values will not be correct. The threshold-based method works by identifying any sensor value beyond a specific threshold as gripped data points. The Activation Threshold must be selected such that it sits above the sensor baseline noise level, but also not be high enough that it eliminates data points representing a tissue grasped with a very light grip. This threshold value is often entered as a percentage value (though absolute values are also supported). When entered as a percentage, the absolute gripped-threshold for each trial is calculated using the following equation:

$$Threshold = [(Sensor_{Max} - Recorded_{Min}) \times Threshold_{percent}] + Recorded_{Min}$$

The $Sensor_{Max}$ is the maximum possible sensor value, defined as part of the sensor definition (Section 6.4.2.2). $Recorded_{Min}$ is the minimum recorded sensor value during the entire duration of the trial. $Threshold_{percent}$ is the threshold percentage value that is entered in Study Analyzer. For

most sensors, the threshold percentage is between 5-10%. For all data analysis, the correctness of the selected threshold is validated manually by looking at the raw sensor data plots and ensuring that the calculated threshold values fall correctly above the baseline noise level for the sensor.

6.5 PNEUMATIC TACTILE FEEDBACK

The pneumatic tactile feedback was provided using a multiplexed, 5-level solenoid valve array. This is the same technology that was used in the original CASIT tactile feedback system²⁰. In this case, however, since the system was utilizing the depressed-membrane actuators (Section 5.2), the pressure for each level was reconfigured (Table 1). The first pressure level was then adjusted such that a subject would just barely feel the presence of the membrane once it was inflated. The other pressure levels were adjusted such that the difference between the different levels was noticeable. The last pressure level was configured such that it didn't cause discomfort due to high deformation of the skin.

Pneumatic Level 0	0 PSI
Pneumatic Level 1	9 PSI
Pneumatic Level 2	11 PSI
Pneumatic Level 3	14 PSI
Pneumatic Level 4	20 PSI

Table 1: Pneumatic Tactile Feedback Pressure Levels

6.6 VIBRATION FEEDBACK

Vibration as a feedback modality is implemented through the use of vibration motors installed directly on the fingertips of the surgeon. The 3D printed pneumatic actuators were modified to allow installation of flat, 10mm x 2mm vibration motors (Figure 44).

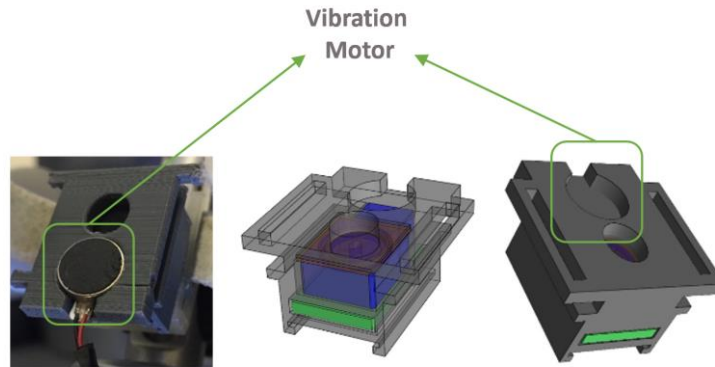


Figure 44: Vibration Motors Installed on 3D Printed Pneumatic Actuators

Each vibration motor is activated initially at voltages as low as 1.5V and will provide stronger feedback at voltages up to 5V. The vibration motors were controlled using Pulse Width Modulation (PWM) from a digital output pin on the Atmel ARM core of the HFS control board (6.8). However, due to power consumptions and the lower output voltage of the Atmel MCU's digital output pin (3.3V), it is not possible to effectively drive the vibration motors directly. To resolve this issue, analog switch ICs (Analog Devices ADG451) with high response times ($< 90\text{ns}$) were used to provide power directly from a 5V power supply. The analog switch IC's logic pins were then controlled using the Atmel MCU's digital pins. In this way, a 5V PWM signal with sufficient power could be used to drive the vibration motors.

A series of benchtop tests were performed to identify the resolution that vibration could provide as a feedback modality. The goal was to determine how many different levels of vibration could be easily recognizable for the average user. These tests led to the result that between 3-4 different

levels of vibration could be uniquely recognized if the changes were made in a step-wise manner. In other words, gradually increasing the vibration intensity was more difficult to perceive than sudden changes. This behavior is expected since vibration is often used by the somatosensory system as a way to draw attention of the brain to a specific event⁶⁸.

Due to variations that existed between different tests and the fact that higher vibration intensities resulted in discomfort for the user, it was decided that vibration would be used with at most two feedback intensities. Level 0 would correspond to no feedback, Level 1 would be vibration at 25% of maximum vibration intensity and Level 2 was set at 50%.

6.7 KINESTHETIC FORCE FEEDBACK

Kinesthetic Force Feedback is designed to trigger activation of mechanoreceptors in the muscles, particularly the Golgi tendon organ (GTO). The GTO is responsible for measuring tension in the muscles. The integration of this sensory information in the brain helps create a sense of resistance when applying force and deforming an object. In the context for grip-force during robotic surgical tasks, the kinesthetic force feedback helps provide information particularly as the magnitude of force becomes larger. This is in contrast to the normal force tactile feedback, which is highly involved in light touch. The combination of kinesthetic force feedback and normal force tactile feedback can, therefore, create a more natural sense of touch for grasping in RMIS.

The most common method for providing kinesthetic force feedback is through utilization of motors installed on the joints of the robotic console. Many systems already provide this type of feedback in the larger muscle groups in the arms, but have not implemented this same feedback at the fingertips for application in grasping tasks in RMIS. Utilizing a similar approach, this research

project implemented Kinesthetic Force Feedback using motors installed on the grasper controls of the RAVEN II surgical system's master console.

Despite its effectiveness in providing feedback for the larger muscle groups in the arms, investigation into the aforementioned feedback mechanism indicated a series of unforeseen problems (Section 7.3.1.3). For this reason, an alternative method for providing Kinesthetic Force Feedback for grasping was developed. This Pneumatic Kinesthetic Force Feedback solution aimed to provide a more natural sense of kinesthesia than the traditional motor-dependent technique.

6.7.1 KINESTHETIC FORCE FEEDBACK USING RAVEN II CONSOLE

The Raven II surgical system (Figure 45), originally developed at the University of Washington, is an open platform for research and collaboration in the field of surgical robotics⁹⁷.

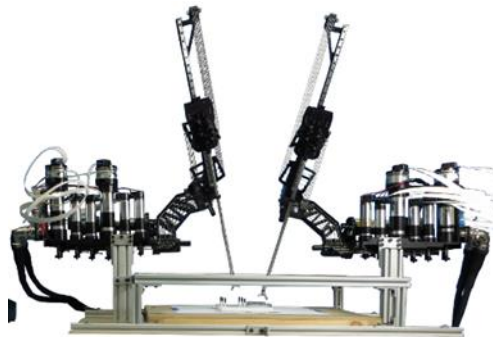


Figure 45: RAVEN II Surgical Robot

A newer variant of the Raven surgical system, originally developed at UC Santa Cruz, consists of a four-arm robotic system and a surgical console. The Raven was selected as the target surgical system instead of Intuitive Surgical's da Vinci due to the lack of any motors at the hinge of the surgical console's graspers. On the other hand, the Raven surgical console was already fitted with a motor at the hinge of the grasper controls (Figure 46).

In collaboration with the Bionics lab, now located in UCLA, a kinesthetic force feedback system was developed by utilizing motors installed on the graspers of the surgical master console (Figure 46).

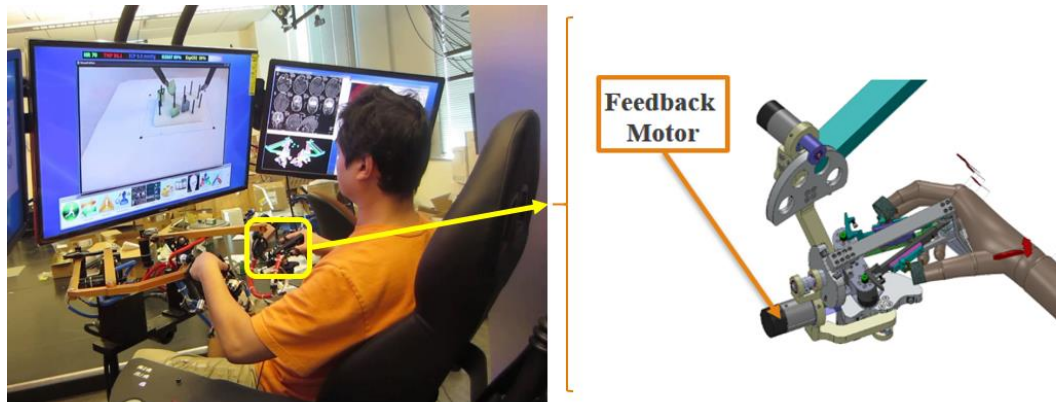


Figure 46: Feedback Motor on the Raven Surgical Console¹¹³

A UDP server was installed on the RAVEN console's control software which received a value between 0-99, indicating the amount of power that would be provided to the feedback motor. This would in turn control the resistance the motor would provide when the user attempted to close the grasper. A UDP client was also built into the Haptics Manager software which would allow the Logic Engine to send kinesthetic feedback levels to the RAVEN console. This approach allowed the haptic feedback system to provide kinesthetic feedback in response to increasing grip forces detected by the sensors installed on the graspers of the RAVEN surgical system.

6.7.2 PNEUMATIC KINESTHETIC FORCE FEEDBACK

The implementation of kinesthetic force feedback for grip force reduction using the motors at the hinge of the master console's graspers failed to provide effective feedback (see studies in Section 7.3.1.3). A pneumatic kinesthetic force feedback system was developed as an alternative, aiming

to provide a more natural sense of kinesthesia. This solution relied on the placement of a pneumatic tube between the graspers of the master console.

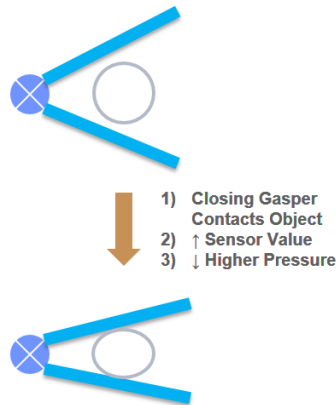


Figure 47: Placement of Pneumatic Tube Between the Console Graspers to Provide Feedback During Grasping

The increase in air pressure (0 – 19 PSI) inside the tube would lead to constriction of the grasper’s ability to close, hence resisting the grasping action. The higher the pressure inside the tube, the more the grasper would resist being closed, indicating stronger kinesthetic feedback.

One of the disadvantages of the motor-based kinesthetic feedback design was its dependency on modifications to the robotic console. The pneumatic feedback was instead designed as an add-on solution with compatibility in mind. The 3D printed pneumatic actuators, which already supported vibration feedback, were modified even further, thus allowing installation of the kinesthetic feedback system directly on the same actuator (Figure 48).

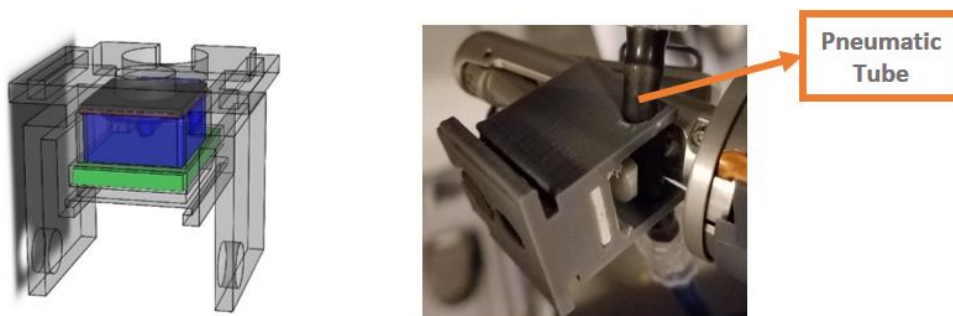


Figure 48: Modified 3D Printed Actuators with Pneumatic Tube Installed for Providing Kinesthetic Force Feedback

In order to control the air pressure for this kinesthetic feedback system, it was necessary to investigate an alternative pressure regulation system compared to the one in use for the normal force tactile feedback. The reason for this change from the quantized levels of the original CASIT tactile feedback system was the lack of scalability. With the utilization of the multiplexed solenoid valve array, each additional pressure level, for each actuator, required one additional solenoid valve. For this reason, providing a pressure control system that would simulate continuous pressure regulation would require an extremely large number of solenoid valves, a design which, due to cost and complexity of the system, would not be practical. A more compact pressure regulation system with a high number of pressure levels (i.e. simulating continuous pressure regulation), was critical for two reasons: (1) large pressure changes can reduce user performance, particularly in a kinesthetic feedback where sudden changes in feedback can result in the user dropping the peg, and (2) a user-based, adaptive feedback requires pressure levels to be variable and changeable electronically.

Previous research had investigated the possibility of utilizing electro-pneumatic pressure regulators; however, these systems generally have slow response times and produce significant vibration during pressure changes²⁰. To resolve these issues, a dual-valve continuous pressure regulation system was developed that would provide continuous pressure regulation with low latency.

The dual-valve pressure regulation technology relied on a Asco Sentronic D electro-pneumatic valve placed in series with a SMC solenoid valve. The Sentronic D utilizes a direct acting proportional coil to control output pressure. The benefits of this type of electro-pneumatic valve is the stable pressure output that it can provide. The stable response, however, comes at the expense of system response times. System response time can be reduced, but reducing the response time

comes at the expense of large pressure overshoots when pressure levels are being changed (Figure 49). The Sentronic D’s output pressure is controlled by providing a voltage of 0 – 10V to its analog control pin.

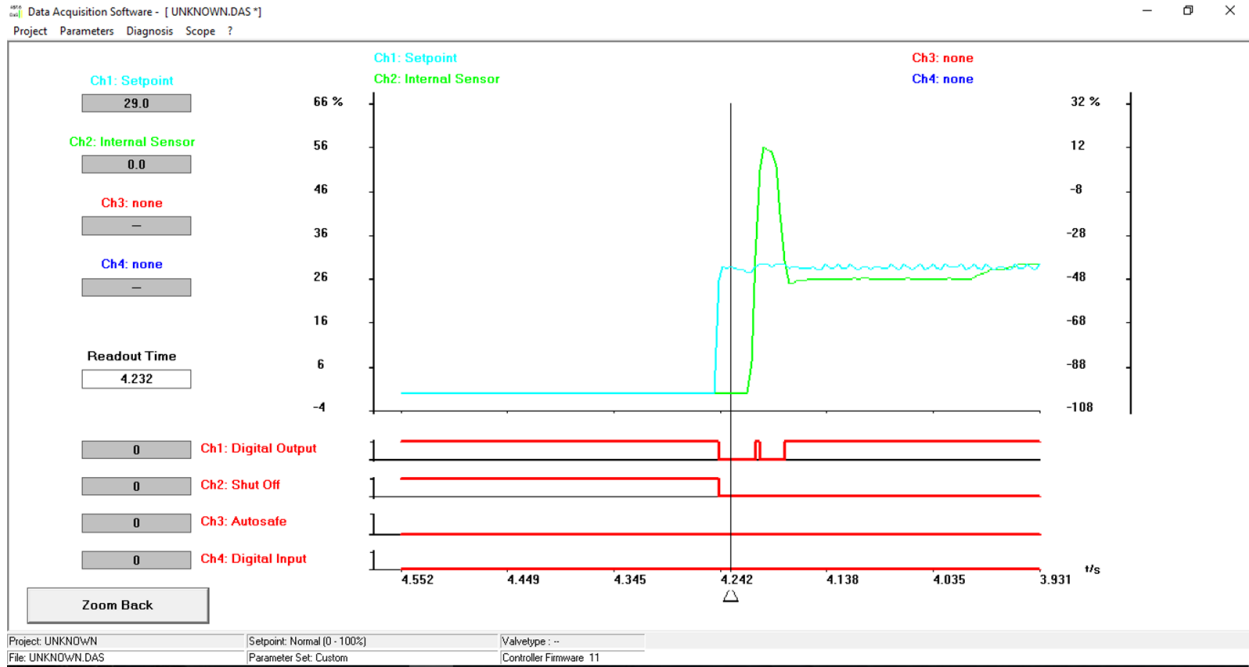


Figure 49: Pressure Overshoot in Sentronic D Valve Seen in Green. Plot Shown in Asco’s Data Acquisition Software.

This large pressure overshoot could not be allowed to reach the pneumatic tubing. To resolve this issue, a dual-input solenoid valve was placed in series after the Sentronic D valve (Figure 50). The solenoid valve, when in the off position, would allow air flow from the first input to its output. When turned on, the solenoid valve would allow air flow from the second input to its output. The haptic feedback controller (6.8) was then programmed to change the solenoid valve to its on position right before changing the pressure of the Sentronic D valve. By feeding the output of the solenoid valve back to its second input port, the system would maintain the output pressure until the Sentronic D’s output pressure had stabilized. At that time, the solenoid valve would be turned off, and the new pressure would flow to the actuators.

The Sentronic D valve has a built-in controller which can be programmed using Asco's data acquisition software (Figure 49). By modifying various control parameters of the valve, a stable pressure output was achieved while also reducing the total response time of the dual-value system to < 70ms (Average: 65ms, Std. Dev.: 7.5ms, Max: 67ms, Min: 50ms).

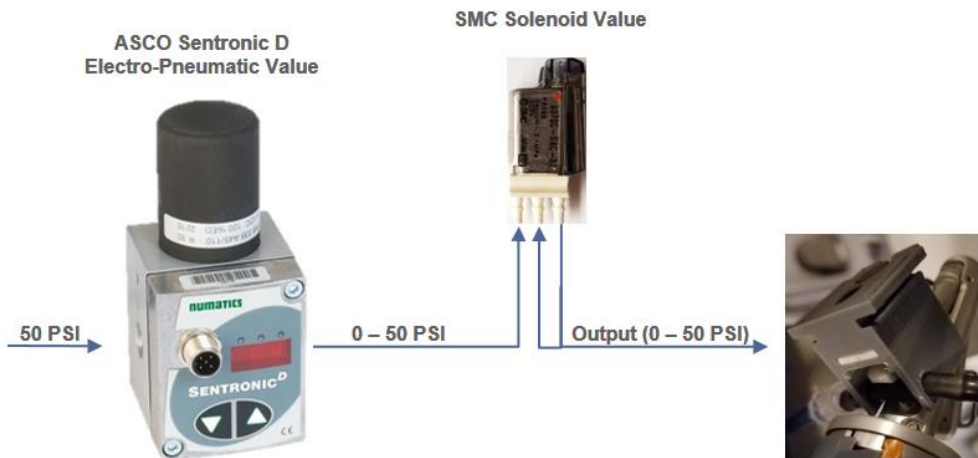


Figure 50: Dual-Valve Pressure Regulation System

It is worth mentioning that while this pressure regulation technique was used only in the kinesthetic force feedback system, it's application has the potential to expand to the tactile feedback modality as well.

6.8 MULTI-MODAL HFS CONTROL HARDWARE

The hardware control system for the Multi-Modal HFS consists of a custom circuit board that is driven by an Atmel SAM3X8E ARM core, and accompanying pneumatic control system (Figure 51). The entire HFS control architecture was designed to be highly portable to allow the system for use in various research labs around the UCLA campus and the Ronald Reagan Hospital.

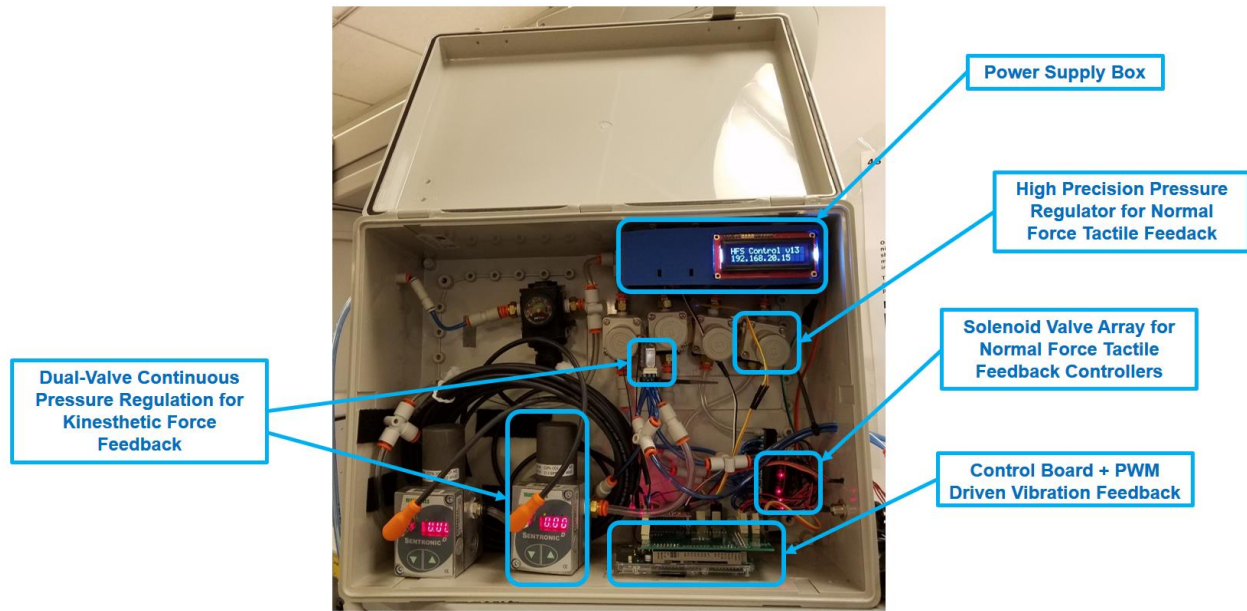


Figure 51: Multi-Modal HFS Control Hardware

In order to provide flexibility in the type of power supply that could drive the haptic feedback system, a power supply box was added that would allow any external 9-24V power supply (50 Watts minimum) to turn on the system. Each solenoid valve in the haptic feedback system required 5V power supply and drew 0.6 – 1A of current when activated. In order to provide sufficient power for simultaneous activation of all solenoid valves and to also power the HFS Control Board and vibration motors, the power supply box consisted of one 8A step down voltage regulator. The Sentronic D valve required a 24V supply in order to turn on. For this reason, the power supply box contained a 3-35V, 3A DC step up voltage regulator as well.

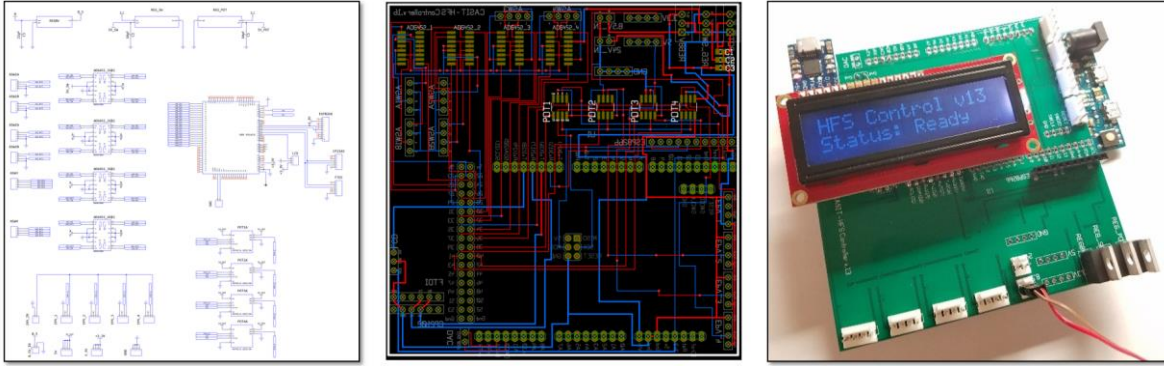


Figure 52: Schematic of the Multi-Modal HFS Control Board

The HFS Control Board (Figure 52) was designed to control up to four dual-valve continuous pressure regulation systems, four vibration actuators and eight solenoid valves. This was achieved by utilizing four, quad-channel ADG451 analog switch ICs coupled with four SPI controlled potentiometers. The control board also used the three TTL ports of the SAM3X MCU to communicate with a ESP8266 and CP2102 modules as well as an external LCD for providing information such as status information, error code and control board IP address. The ESP8266 was used when the control board was wirelessly connected to the Haptics Manager software and the CP2102 provided a wired, USB interface when WiFi was not available.

The control board was built with no decision-making capabilities. Control packets contained all the feedback levels for all the connected actuators in the following format (Figure 53):

Y	Tactile Normal Actuator 1	,	Tactile Normal Actuator 1	,	Vibro Actuator 1	,	Vibro Actuator 2	,	Kinesthetic Actuator 1	,	Kinesthetic Actuator 2	>
---	---------------------------	---	---------------------------	---	------------------	---	------------------	---	------------------------	---	------------------------	---

Figure 53: Haptics Control Board Packet Format

In this packet format, “Y” marks the beginning of the packet and “Z” marks the end. The control board utilized these markers and the “,” characters to validate the packet and eliminate corrupted or incomplete packets. This type of packets only occurred during system boot up and turn off times

and were not a common occurrence, particularly since TCP protocol has mechanisms that deal with packet corruptions directly on the protocol stack.

6.9 SYSTEM DELAY MEASUREMENTS

Throughout this chapter, the response of various components of the Multi-Modal Haptic Feedback System have been reported. This section discusses the methods used for measuring these delays.

6.9.1 SENSOR BOARD DELAY

This delay was measured as the amount of time taken for a sensor data packet to be sent from the sensor board to the Haptics Manager software and decoded. Initial tests were performed using a wired USB connection, through the use of a CP2102 controller which acted as a UART-to-USB interface. To measure the delay, an LED was installed on the sensor board and configured to turn on when the sensor board was sending a packet with a sensor value larger than 200. In Haptics Manager, a sensor testing functionality was developed, where the same threshold value would result in a marker to appear on the software screen (Figure 54). A FlexiForce sensor was connected to the sensor board and compressed while a camera was used to record the LED and the computer screen at 60 frames per second (fps). The delay was, therefore, measured as the amount of time between the sensor board LED activating and the red marker appearing on the status bar in the Haptics Manager software. Measurements performed using the wired and WiFi connection (6.2) showed both the LED and the software marker appearing at the same time, indicating the delay was less than the 16.67ms error from the 60fps camera.

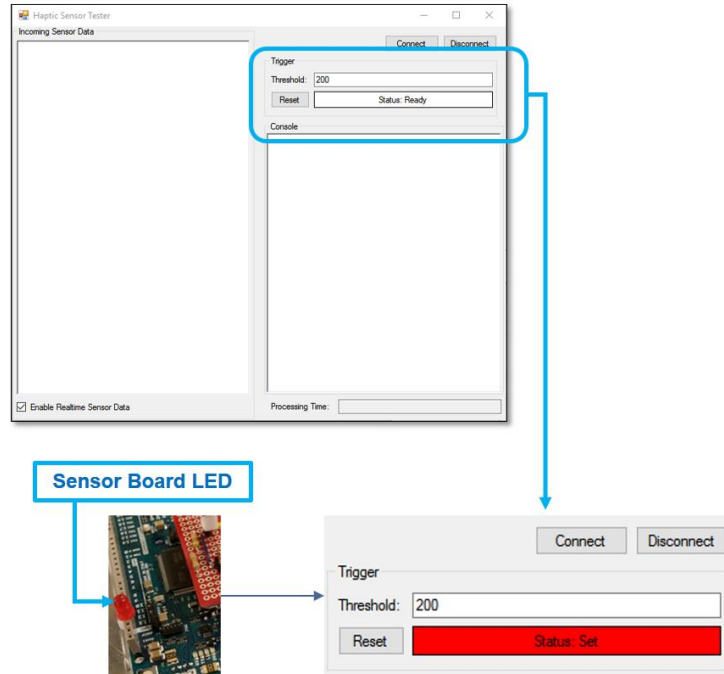


Figure 54: Measurements of Sensor Board-Haptics Manager Software Communication Delay

6.9.2 TOTAL SYSTEM DELAY

The total system delay was measured as the time from when the sensor board LED would turn on, indicating that a sensor packet above a certain threshold was about to be sent out, to the time when the HFS Control Board activated the actuators. The activation of actuators on the Control Board was measured using an LED installed on the Control Board which would turn on after the actuators were activated.

Furthermore, while vibration motors have high response time, pneumatic actuators are much slower. More specifically, the slowest component of the entire HFS was the dual-valve continuous pressure regulators which used a Sentronic D valve and a SMC solenoid valve in series. To also be able to measure the time it took for the actuator to respond and the pressures to change, a pressure regulator was connected to the output of the regulator to observe the change. A 60fps camera was used to record the events.

For these measurements, the sensor board was connected to the laptop and the Haptics Manager through a USB connection while the Control Board was wirelessly connected through the local WiFi network. This was the most common setup for HFS studies because the proctor and the laptop were often located right next to the robotic arms and, therefore, the sensors during an experiment (consequently, there was no need for the sensor board to be wireless connected to the laptop).

Measurements made using this method showed the LED of the sensor board and the Control Board activating either with 0 or 1 frame delay, corresponding to an average delay of less than 16.67ms (considering that there is a 16.67ms error when recording using the 60fps camera). The delay from the sensor board to the moment the air pressure changed was measured to be 65.6ms on average (Section 6.7.2).

6.9.3 HAPTICS MANAGER SOFTWARE PROCESSING TIME DELAY

Measuring the delays within the Haptics Manager software relied on a series of performance benchmarking features built into the software. This benchmarking information was important during the engineering and optimization phases of the Haptics Manager software development as they helped in improving the overall software performance. However, by the time the system was optimized, these delays were usually small enough (<1ms on average) that they were negligible compared to the delays within the rest of the system.

Measurements were performed by recording the system time at different stages during the packet decoding, processing and transmission stages. The values were reported in the Haptics Manager software above the real-time sensor plot (Figure 55).

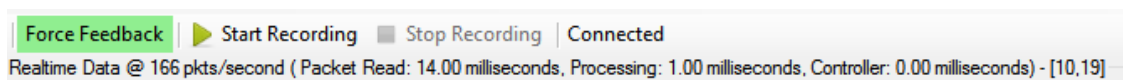


Figure 55: Haptics Manager Benchmarking Information Displayed Above the Real-Time Sensor Plot.

Delays of zero milliseconds indicate values smaller than the system 1/1000 of a millisecond.

Packet Read delay is defined as the amount of time between the reception of each new packet and is dependent on the scanning frequency of the Sensor Board. Processing delay is the amount of time it takes for the packet to be decoded, filtered and added to the Fixed-Size Queue. Controller Delay is the amount of time from the moment the Haptics Manager received the packet to the time when a response was sent to the Control Board. It is worth noting that Controller Delay includes Processing Delay time as well.

6.10 MULTI-MODAL HFS SUMMARY

The developed Multi-Modal Haptic Feedback System has resulted in major changes to the original CASIT tactile feedback solution (Table 2). The adaptive and configurable nature of this newly developed HFS will not only help in the investigation of the benefits of HFS for several different robotic surgical applications, but also help speed up further research in the field by reducing the time necessary to integrate a variety of sensors and feedback actuators.

	CASIT HFS (2013)	CASIT Multi-Modal HFS
Communication	<ul style="list-style-type: none"> • Bluetooth • Wired 	<ul style="list-style-type: none"> • WiFi • Wired
Processing	<ul style="list-style-type: none"> • Hard-Coded on MCU (51ms) 	<ul style="list-style-type: none"> • Adaptive Engine in C# (< 1ms)
Sensing	<ul style="list-style-type: none"> • Normal Force (4.4 N) 	<ul style="list-style-type: none"> • Normal (4.4N, 20N, 40N) • Shear
Actuators	<ul style="list-style-type: none"> • PDMS-Based Pneumatic Actuation 	<ul style="list-style-type: none"> • 3D Printed, Depressed-Membrane Actuators
Feedback Types		<ul style="list-style-type: none"> • Tactile Normal Force • Kinesthetic Normal Force • Vibration
Other Features		<ul style="list-style-type: none"> • User Feedback Profiles • Multiple Simultaneous Sensor Types • Real-time Filters • Packet Transmission Optimization

Table 2: Comparison of 2013 Variant of CASIT's Tactile Feedback System and the Newly Developed Multi-Modal HFS

7 EVALUATION OF MULTI-MODAL HFS

A series of studies were conducted using the developed Multi-Modal HFS to evaluate effectiveness of each feedback modality in several applications for robotic minimally invasive surgery. Furthermore, these studies also aimed to better understand the benefits of a multi-modal haptic feedback system over the simpler, unimodal design. More specifically, these experiments were conducted as part of four major research investigations:

1. Investigation of the benefits and drawbacks of vibration as a feedback modality (Section 7.1)
2. Investigation of clinical application of a hybrid vibro-tactile HFS for tissue palpation (Section 7.2)
3. Investigation of the benefits of a complete, kinesthetic-tactile feedback system for grip-force reduction in RMIS (Section 7.3)
4. Investigation of the impact of vibration as an additional feedback modality for reduction of peak grip-forces in RMIS (7.4)

7.1 A SUTURE BREAKAGE WARNING SYSTEM

This investigation focuses on the potential benefits of vibrotactile feedback as a warning mechanism in robotic surgical applications. Previous research has pointed out the potential benefits of vibration as a feedback modality in tasks where the user's attention must be directed toward a critical event^{114,115}. This research task focused on utilization of vibrotactile feedback in improving outcomes in suturing and knot tying tasks in RMIS. More specifically, HFS was used to develop a Suture Breakage Warning System that aimed to reduce suture breakage in knot tying tasks where the lack of force feedback and excessive shear forces lead to intraoperative suture failure.

7.1.1 SUTURE FAILURE LOADS IN ROBOTIC SURGERY

To be able to prevent intraoperative suture breakage in robotic surgery, it is first necessary measure and characterize failure loads and tensile strengths for the most commonly used sutures. Suture failure loads depends on several factors, including material properties, strain conditions and the type of robotic instrument handling the suture. A series of experiments were therefore conducted to both quantify suture failure loads and to better understand the conditions that impact suture breakage.

7.1.1.1 Methods

The experiments performed under this investigation focused on evaluating Prolene, Polydioxane (PDS), Silk and Vicryl because of their ubiquity in gastrointestinal robotic surgeries. Sutures of gauges 5-0 to 1-0 USP (United States Pharmacopeia), corresponding to diameters of 0.4mm to 0.1mm, were studied.

Absolute suture tensile strength and failure loads were measured by pulling the sutures to failure/breakage using a high precision Tytron system (Tytron, MTS Systems Corporation, Eden Prairie, MN, USA). The mounting mechanism of the suture was designed to be similar to the robotic instrument that is used for suturing tasks in RMIS. The only difference was that the initial set of experiments used a smooth surface for gripping the suture avoid tearing into the suture (Figure 56). This experimental design choice was made to serve two goals. The first was to find the best possible suture failure load. The second was that unlike the da Vinci Microneedle driver which has a rough surface that digs into the suture to hold it, some other instruments such as the Cadiere forceps cause less structure damage. Therefore, a measure of the absolute suture failure load was critical to the characterization of the sutures.

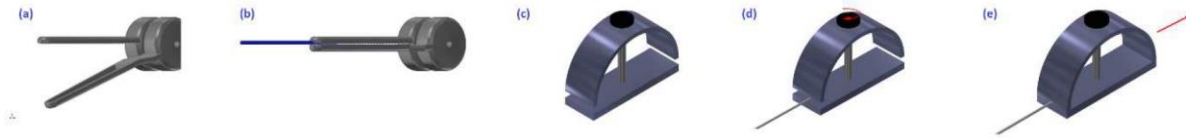


Figure 56: Comparison of Suture Mounting Mechanism on da Vinci Forceps vs. Tytron System

- (a) CAD depiction of robotic forceps
- (b) Robotic forceps holding on to a suture, collapsing the cylindrical structure of the suture
- (c) Mounting bracket for holding on to a suture using MTS Tytron
- (d) Suture held in place such that it mimics surgical forceps
- (e) Suture being pulled by MTS system

Sutures were positioned and held in place such that no slipping would occur when the Tytron system pulled the suture. Suture slippage was observable using the force-time plot provided by the Tytron system. In the rare case that slippage occurred, the experiment was repeated. In this study, sutures were pulled at a constant rate of 50 mm/min until failure occurred (parameters adopted from Fraunhofer et al., 1985)¹¹⁶. For each suture/gauge combination, three trials were performed and the results were reported as mean and standard deviation.

Since in real clinical conditions, sutures may be pulled at varying rates depending on how the surgeon operates and moves the robotic arms, it was also necessary to understand the impact of rate on the failure load of the sutures. In order to observe any patterns that may arise from changes in pull rate, sutures of gauges 2-0 and 3-0 were pulled using the Tytron system at 200 mm/min and 400 mm/min. All other conditions were identical to the initial experiment, with samples being tested three times. Statistical analysis was performed using Analysis of Variance (ANOVA). A p-value < 0.05 was found to be statistically significant.

In addition to the potential impact of pull rate, the type of surgical instrument that holds the suture can also have a major impact on the failure load of a suture. Some instruments such as the Fenestrated Bipolar or Cadiere forceps have large teeth-like structures while others such as the

Micro-Needle Driver have a higher density, more fine set of grooves. It is therefore possible for the suture's structure to be weakened when held by such instruments.

Due to the size and mobility limitations of the Tytron system, it was not possible to use it for performing failure tests with the da Vinci robot. For this reason, a USSC Sutures Force Gauge (Figure 57) was used in place of the Tytron system.



Figure 57: USSC Suture Force Gauge

Since the original failure load measurements were performed using the high precision Tytron system, it was necessary to compare the USSC Sutures force gauge with the Tytron system. To do this, Vicryl sutures of gauges 5-0 to 1-0 were pulled to breakage using the USSC force gauge. To simulate the same suture mounting conditions as the original experimental setup, 3D printed components were designed and manufactured such that the suture could be held between two smooth metal surfaces (Figure 58). As before, experiments were performed in triplicates.



Figure 58: USSC Force Gauge Modified Using 3D Printed Components

During robotic surgical procedures, sutures are often pulled in different ways and using several different instruments. Results from previous studies show that instruments with grooves such as

the Microneedle driver can impact the breaking force¹¹⁷. Since the ultimate goal of this study is to help in the programming of a suture-breakage warning system, it is necessary to determine the worst possible suture failure load. For this reason, sutures were pulled under three different conditions: (1) Unlooped: pull suture directly parallel to the plane of the table, 2) Looped: turn the grasper to wrap the suture thread around the tip of the grasper once, then pull suture directly parallel to the table and (3) Needle: pull suture by holding on to the needle at the end of the suture. For these experiments, a da Vinci IS1200 system was used. The USSC force gauge was mounted on a table, with one end of the suture being held between two smooth metal washers (similar to the original smooth metal surfaces that held the suture on the Tytron system). To determine any variations that might exist between suture materials when placed under stress by the microneedle driver, 3-0 sutures of all four material types were tested. All tests were performed in triplicates and data was reported as mean and standard deviation.

7.1.1.2 Results

Table 2 shows the failure load and tensile strength for Vicryl, PDS, Prolene and Silk sutures when pulled using the Tytron system at 50 mm/min. Vicryl and PDS sutures show the highest mechanical strength while Silk has the lowest ($p < 0.05$). Sutures with larger diameters can withstand higher loads. Interestingly however, tensile strength and gauge appear to be indirectly related. Considering that tensile strength is a material property, it is indeed interesting to observe that sutures of smaller diameters can handle higher force per unit area. Direct comparison of this data with previous work from 1985¹¹⁶ indicates that there is a 27-50% improvement in tensile strength, possibly due to changes in manufacturing technologies.

Material	Gauge	Failure Load (kg)	Failure Load (N)	Tensile Strength (kg/cm ²)	Tensile Strength (kN/cm ²)
Polydioxane (PDS)	0	6.18 (0.55)	60.61 (5.39)	6423 (573)	62.990 (5.619)
	2-0	3.40 (0.27)	33.34 (2.65)	4811 (383)	47.181 (3.756)
	3-0	3.39 (0.16)	33.25 (1.57)	10786 (524)	105.778 (5.138)
	4-0	2.03 (0.22)	19.91 (2.16)	11472 (1267)	112.505 (12.425)
	5-0	1.3 (0.12)	12.75 (1.18)	16588 (1514)	162.678 (14.847)
Silk	0	3.79 (0.24)	37.17 (2.35)	4126 (247)	40.463 (2.422)
	2-0	3.39 (0.07)	33.25 (0.69)	4791 (93)	46.985 (0.912)
	3-0	1.81 (0.13)	17.75 (1.27)	5759 (425)	56.478 (4.167)
	4-0	1.36 (0.03)	13.34 (0.29)	7712 (162)	75.631 (1.588)
	5-0	0.86 (0.01)	8.43 (0.10)	10897 (159)	106.866 (1.559)
Vicryl (Braided)	0	5.97 (0.39)	58.55 (3.82)	6200 (409)	60.803 (4.011)
	2-0	4.61 (0.02)	45.21 (0.20)	6525 (30)	63.990 (0.294)
	3-0	3.15 (0.08)	30.89 (0.78)	10015 (258)	98.217 (2.530)
	4-0	2.21 (0.26)	21.67 (2.55)	12519 (1474)	122.773 (14.455)
	5-0	1.43 (0.18)	14.02 (1.77)	18268 (2302)	179.154 (22.575)
Prolene	0	4.40 (0.05)	42.94 (0.52)	4573 (55)	44.669 (0.541)
	2-0	3.45 (0.26)	33.73 (2.54)	4885 (368)	47.724 (3.597)
	3-0	2.51 (0.11)	24.53 (1.06)	7993 (344)	78.078 (3.360)
	4-0	1.84 (0.06)	17.93 (0.62)	10387 (359)	101.469 (3.512)
	5-0	1.14 (0.05)	11.14 (0.47)	14515 (610)	141.795 (5.966)

Table 3: Suture Failure Load and Tensile Strength Measurements Using Tytron System. Data is reported as Mean (Std. Dev.)

For most cases, the failure loads of sutures were not significantly different ($p > 0.05$) when pulled at different rates, at least not within the range of rates relevant to robotic surgical procedures. This data is presented in Table 4. It is worth mentioning that small variations can be observed but no obvious patterns appear to be present (Figure 59).

Material	Gauge	Failure Load (N) 50 mm/min	Failure Load (N) 200 mm/min	Failure Load (N) 400 mm/min
Polydioxane (PDS)	2-0	33.34 (2.65)	33.61 (1.21)	36.21 (1.04)
	3-0	33.25 (1.57)	29.75 (2.91)	29.54 (1.67)
Silk	2-0	33.25 (0.69)	33.88 (5.45)	35.84 (2.99)
	3-0	17.75 (1.27)	21.21 (2.56)	21.58 (1.96)
Vicryl (Braided)	2-0	45.21 (0.20)	41.92 (0.73)	44.82 (3.44)
	3-0	30.89 (0.78)	33.64 (3.10)	31.69 (3.71)
Prolene	2-0	33.73 (2.54)	32.76 (1.24)	34.63 (1.79)
	3-0	24.53 (1.06)	22.87 (2.78)	25.23 (0.48)

Table 4: Comparison of Failure Loads when Sutures are Pulled at Different Rates. Data is reported as Mean (Std. Dev.)

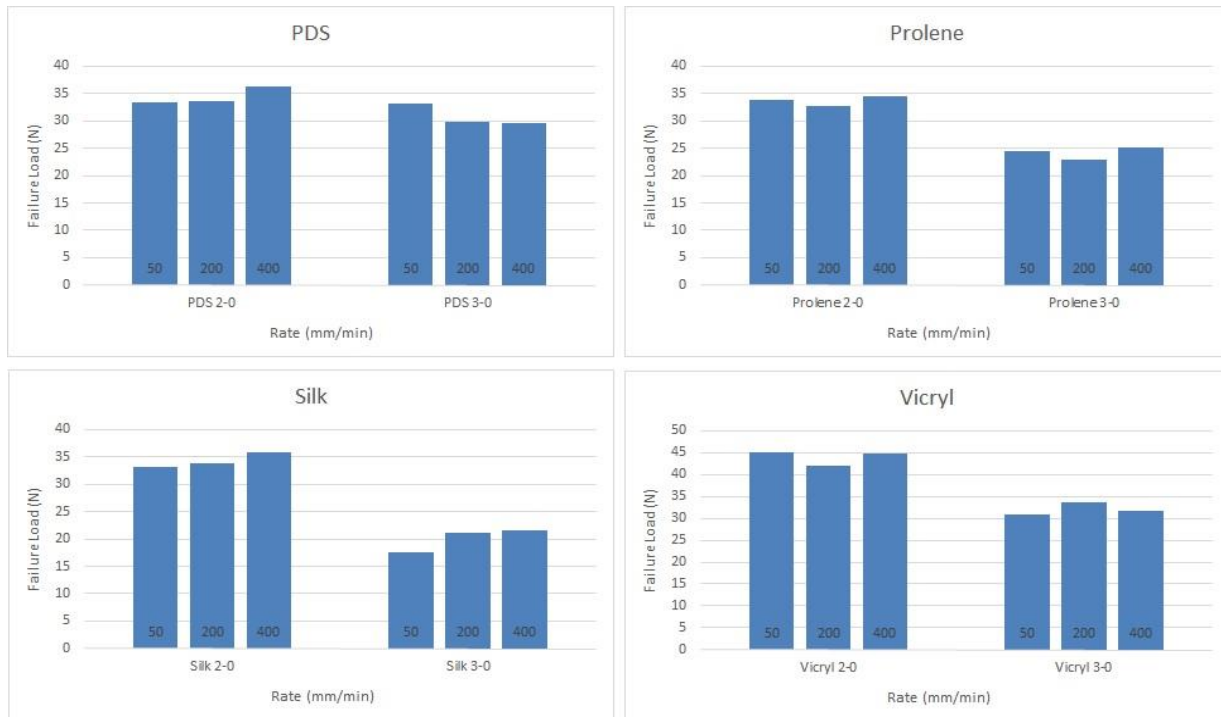


Figure 59: Failure Load of Sutures when Pulled at Different Rates Using the Tytron System

The comparison of the Tytron system and the USSC Sutures force gauge is presented in Table 5. Treating the high precision Tytron system’s measurements as true failure loads, the USSC system reports data with errors ranging from 2.45% - 7.67%.

	Failure Load (Kg) Tytron	Std. Dev. Tytron	Failure Load (Kg) USSC	Std. Dev. USSC	% Error
0	5.97	0.39	6.07	0.61	2.45%
2-0	4.61	0.02	4.29	0.21	6.73%
3-0	3.15	0.08	2.92	0.04	7.00%
4-0	2.21	0.26	2.04	0.15	7.67%
5-0	1.43	0.18	1.37	0.19	4.78%

Table 5: Comparison of Mean Suture Failure Loads Recorded Using Tytron System and USSC Sutures Force Gauge

The results from tests performed using the da Vinci system and the micro-needle driver, indicate that suture failure loads can change significantly with utilization of the robotic instrument. In general, pulling the suture thread with a micro-needle driver, directly parallel to the plane of the table, resulted in lower failure loads (Table 6), comparing to data recorded using the Tytron system.

This reduction in failure load ranges from 45% to 62% of the original values (Table 2). Alternatively, if the suture is wrapped around the micro-needle driver's end effector before pulling, then the failure load is improved. It is worth mentioning that in nearly all cases when the suture thread was being held by the micro-needle driver, the breaking point was closest (or directly at) the point of contact with the instrument.

When the suture is pulled by holding on to the needle, some variability is observed in the failure loads. Vicryl appears to show a higher failure load under this condition compared to holding on to the un-looped condition. All other three materials show that the worst possible failure load values are observed when the suture is pulled with the needle. In all cases, the suture failed at the swaged end (i.e. connection point with the needle).

Material	Suture Thread - Unlooped	Suture Thread - Looped	Suture Needle
PDS 3-0	20.46 (1.18)	22.46 (4.58)	14.06 (3.15)
Prolene 3-0	13.47 (1.84)	15.53 (3.88)	12.81 (3.11)
Vicryl 3-0	13.86 (0.49)	19.81 (1.95)	15.56 (4.03)
Silk 3-0	9.77 (0.54)	17.33 (0.60)	4.87 (2.03)

Table 6: Comparison of Suture Failure Loads Recorded Using USSC Force Gauge when Pulled Under Different Conditions with da Vinci Micro-Needle Driver. Data is reported as Mean (Std. Dev.)

7.1.1.3 Discussion

The results of the aforementioned experiments which was published in Surgical Endoscopy¹¹⁸, provide the necessary data for programming a suture breakage warning system. The data recorded using the Tytron system attempts to simulate the way sutures are held by robotic graspers. However, this mounting mechanism does not precisely mirror the conditions that occur during surgery. Under normal surgical conditions, the suture is held on one end by a robotic instrument while the other end is usually sutured into the tissue or tied in a knot. Despite this difference, these measurements provided best case suture failure loads as well as identify patterns when using

different suture materials and gauges. This dataset clearly showed that Vicryl and PDS sutures demonstrate the highest tensile strength. Silk was consistently weaker than the other materials.

The data also demonstrated that sutures with smaller diameters can withstand higher force per unit area. Considering that tensile strength is a material property, one expects that tensile strength should remain constant across all gauges. The observed difference could potentially result from alterations in the manufacturing processes. Alternatively, it is possible that the way the suture is pressed between the two metal plates creates microfractures in the material¹¹⁷, which may grow at a reduced rate in sutures with smaller diameters due to the structure of the suture mounting mechanism.

The data from pulling sutures at different rates does not indicate the presence of any patterns. In other words, there is no impact on the failure load of sutures even if the suture is pulled at a higher rate. This result significantly simplifies the development of a suture breakage warning system, because such a system would not need to monitor the rate of the increase in shear forces in order to estimate the correct failure load.

Measurement performed using the da Vinci system and the micro-needle driver provide critical data for the design of a suture breakage warning system. The fact that sutures consistently break close to the edge of the micro-needle driver (< 5mm away from the edge) indicates that the rough surface of the instrument is the primary cause for the large reduction in failure load. Previous research also supports this observation¹¹⁷, hence leading to the conclusion that any effective suture breakage warning system must be programmed with instrument-dependent suture failure loads.

7.1.2 EVALUATION OF A SUTURE BREAKAGE WARNING SYSTEM

In robotic minimally invasive surgery, suturing tasks can be significantly more challenging than open surgery. The lack of haptic feedback further intensifies the difficulty of the tasks by eliminating tactile information that help the surgeon quantify the tension on the suture. This information can be particularly valuable in knot tying tasks where the excessive force, easily produced by large displacements of the robotic arms can lead to suture breakage and knot failure. Furthermore, even when the suture does not break, the possibility of post-operative knot slippage exists, potentially resulting in additional complications for the patient. The goal of this investigation was therefore to determine the impact of haptic feedback on improving the outcomes of knot tying tasks.

7.1.2.1 Methods

Utilizing the previously developed uniaxial shear sensors (Section 5.4), forces applied to the suture could be detected, compared to the previously acquired failure load data (Section 7.1.1), and used to provide feedback when shear forces were nearing the breaking force of the suture. Figure 60 shows the configuration of the multi-modal haptic feedback system for this study.

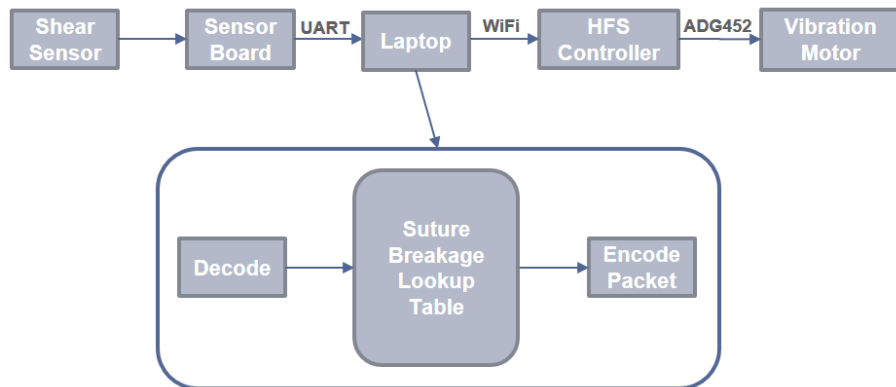


Figure 60: Control System of the Suture Breakage Warning System

The uniaxial shear sensor was installed on one side of the da Vinci Cadiere grasper. A similar component to the uniaxial shear sensor but without the piezoresistive sensing component was installed on the other side of the grasper (Figure 61). This structure is extremely important for ensuring that the shear sensors are able to detect the forces applied to the sutures. If the other side of the grasper was not mounted with a sensor-like component with a movable inner plate, no shear forces could be detected. This behavior is because a solid, non-movable component applying normal force to one side of a suture would prevent the suture from moving in either direction (assuming there was sufficient friction to prevent the suture from slipping). If the suture does not move, then shear forces cannot be detected by the shear sensor on the other side of the grasper. By placing two movable plates on the grasper, when the suture is pulled, both sides of the grasper shift, allowing the sensors to detect the applied force.



Figure 61: Uniaxial Shear Sensor Installed on the Right Side of the Grasper and A Similar Mechanism Without the Sensing Component Installed on the Left Side of the Grasper

The multi-modal HFS was configured to provide vibration feedback at two levels of intensity. The first level was activated at 40% below the failure load of the suture while the second level, with a higher vibration intensity, was activated at 10% below the suture's failure load. For this study, Silk 3-0 sutures were used with failure loads of 9.77 N (Table 6).

A total of 15 novice subjects were asked to tighten a knot by pulling on both free ends of the suture (Figure 62). Each subject was provided with a setup containing four knots, two of which were tightened while HFS was enabled and two of which were tightened without any feedback. The number of suture breakages was measured with each trial having at maximum two possible breakages, one on each arm. In addition, the knots were specifically made around a smooth, solid cylindrical object to allow the knots to easily slide out after the completion of the trial (Figure 62). Removal of the knots was necessary for testing of the knot quality, which was measured as the amount of knot slippage (in mm) that occurred when pulling on both end of the knot after having removed it from the solid cylinder. Applied shear forces were also recorded throughout the trial. HFS was enabled in an alternating fashion with the order of the trials being randomized to avoid any bias toward HFS or no feedback trials. Furthermore, the knot that the subject was asked to tighten was the third knot, with the first two knots already having been made by the proctor to maintain consistency of tightness around the solid cylinder. The data for each of the two trials in the same condition (i.e. HFS vs. No Feedback) were averaged and statistical analysis was performed using Wilcoxon Signed Rank Test.



Figure 62: Experimental Set-up for the Suture Breakage Warning System Study Including Four Loose Knots that were Tightened by the Subject

7.1.2.2 Results

The study included a total of 60 trials, 30 of which utilized vibrotactile feedback and 30 of which received no feedback. A total of 9 instances of suture breakage occurred during the HFS trials, while without HFS, there were 22 instances of failure. Comparing the peak force for trials with and without suture breakage (Figure 63), it can be clearly seen that peak forces are significantly higher for trials with suture failure ($p = 0.017$). Therefore, as expected, the data confirms that the primary cause of suture breakage was excessive force.

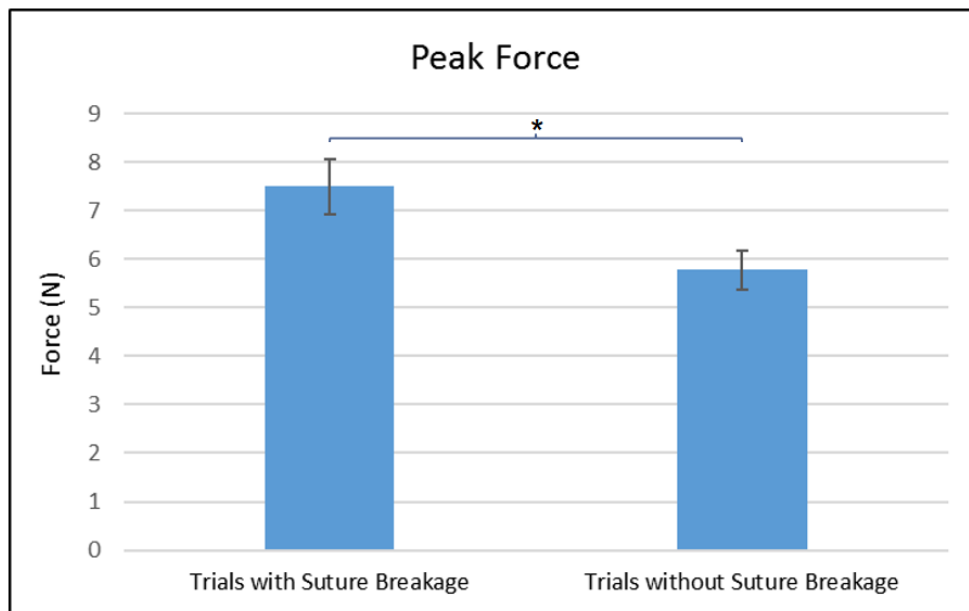


Figure 63: Peak Shear Force of Trials with and without Suture Breakage Compared

The average number of suture failure and the amount of knot slippage per subject is shown in Figure 64. The average number of suture failure per subject is significantly higher when haptic feedback is not present ($p = 0.0078$). More interestingly, the amount of knot slippage (in millimeters) is also significantly higher when haptic feedback is not present ($p = 0.010$).

It's worth mentioning that all sutures failed at the point of contact with the grasper. This is consistent with observations made in previous experiments conducted with the da Vinci micro-needle driver (Section 7.1.1.2).

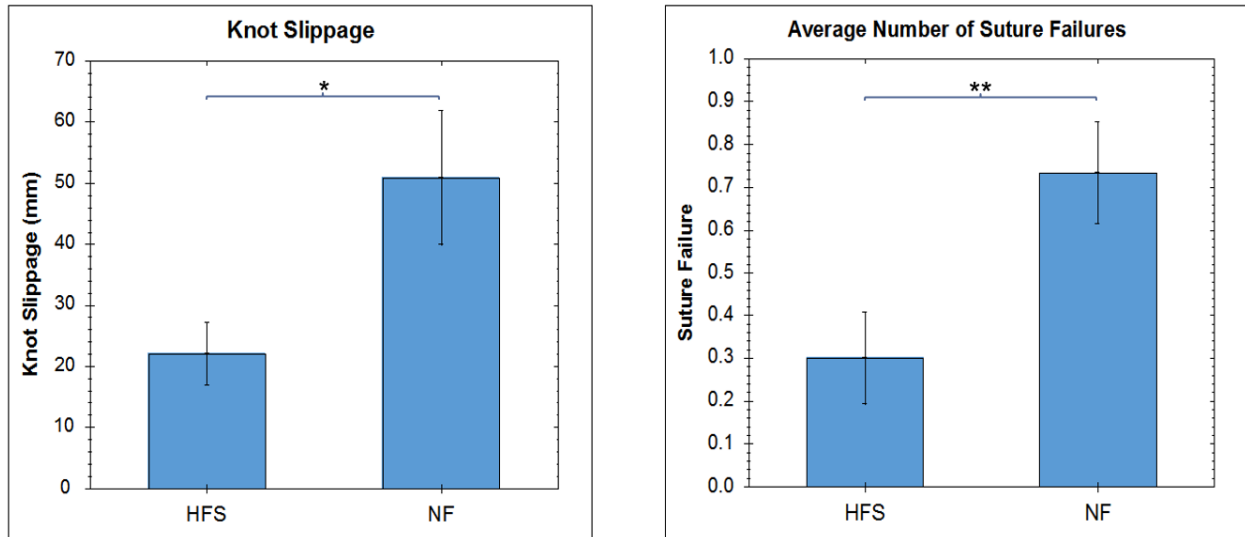


Figure 64: The Average Number of Suture Failures/Faults and Knot Slippage (in millimeters) Per Subject

7.1.2.3 Discussion

The results of the suture breakage experiments provide valuable insight into the benefits of haptic feedback for RMIS applications involving suturing. Knot tying is one of the more challenging tasks in robotic surgery not solely because of the complexity of forming a knot but also because the surgeon needs to determine how hard to pull a suture before the knot is just tight enough. Forming a quality knot can mean the difference between a quick recovery for the patient or post-operative suture failure and serious complications.

In these experiments, vibration feedback is provided prior to shear forces approaching the suture's failure load. While a significant reduction in the number of suture breakages can be seen when haptic feedback is present, the question does arise as to why any breakages occurred at all. The reason for this behavior may lie in the way novice subjects pull the sutures. Many subjects pulled

the sutures so rapidly that even though feedback was provided as soon as the subject approached the suture's failure load, he/she did not have sufficient time to respond to the feedback, thereby resulting in suture failure. There are two possible solutions to this problem. The first is to train a subject such that the rate at which the suture is pulled is reduced. The second is to build a more intelligent and adaptive feedback system which takes into consideration the rate at which shear force is increasing and provide feedback earlier (i.e. lower threshold).

In addition to the benefits related to suture breakage, another valuable result of this study is the indication that haptic feedback also improved the quality of a knot. The reduction in knot slippage indicates that providing feedback also helped produce knots that were more secure. This outcome can potentially have significant clinical benefits as it may reduce the occurrence of post-operative complications. Having said that, an interesting question does arise. Considering that the lack of feedback resulted in the subject pulling harder and hence breaking the suture, one may expect that a knot produced without any HFS should be more secure than one created with HFS. Yet, the results indicate otherwise. The underlying reason for this observation may lie in the way the structure of the suture fails under load. The excessive forces applied to the suture may be resulting in crack formation and mechanical failures within the suture material, hence weakening the entire structure of the knot. In fact, the results of these studies indicate that there may be an ideal tension for producing the best possible knot, one that does not result in structural changes to the suture, but creates a tight enough knot that does not slip. In such a case, a vibrotactile feedback system can inform the surgeon as soon as he/she achieves ideal tension, therefore producing the ideal knot each and every time.

7.2 A HYBRID VIBRO-TACTILE HFS FOR TISSUE PALPATION

The lack of haptic feedback in robotic surgery has created significant diagnostic limitations. Whereas in traditional open surgery, a surgeon can use palpation to identify various structures in soft tissue such as vessels, lymph nodes, nerves, and ureter, in robotic surgery, the surgeon is forced to rely solely on visual feedback. This makes detection of tissue hardness/softness and such non-compressible structures extremely difficult, if not impossible. In procedures involving removal of small tumors, this same problem can lead to difficulty in localization of the unwanted structures, making the procedure more challenging and time consuming, particularly in larger patients.

The goal of this investigation is to determine whether multi-modal haptic feedback systems can be effective in providing surgeons with a method for detection of non-compressible structures in soft tissue.

7.2.1 VIBRO-TACTILE HYBRID HFS

A hybrid feedback system was developed by configuring the previously designed multi-modal HFS to provide a combination of tactile normal force feedback and vibration feedback. In such a system, the pneumatic tactile feedback was meant to provide graded normal force feedback to assist in identifying hard structures in soft tissue. The vibration feedback was meant to act as a computer-assisted detection and feedback modality. The concept of an assisted detection method relied on the fact that applying pressure to soft tissue would result in lower forces than applying pressure to non-compressible structures such as blood vessels and lymph nodes. When scanning a large area, these changes may be difficult to detect with a graded pneumatic feedback. On the other hand, vibration which was previously shown as an effective mechanism for directing the operator's

attention to a critical event, could help in rapid identification of such structures. The user could then utilize the pneumatic normal force to confirm the presence, and identify the margins, of the non-compressible structure. The goal of this study was therefore to determine whether the aforementioned bi-modal HFS, and the synergistic utilization of pneumatic tactile feedback and vibration, could improve the performance of the surgeon in robotic tasks involving palpation.

7.2.1.1 Methods

The control system for the bi-modal vibro-tactile HFS was implemented by configuring the logic engine of the Haptics Manager software with two sets of rules (Figure 65). The first ruleset controlled the behavior of the pneumatic normal force feedback actuators (Section 6.5) while the second was a threshold based activation of vibration motors (Section 6.6). For these preliminary studies, the vibration threshold was configured as the same threshold for level 4 pneumatic feedback activation.

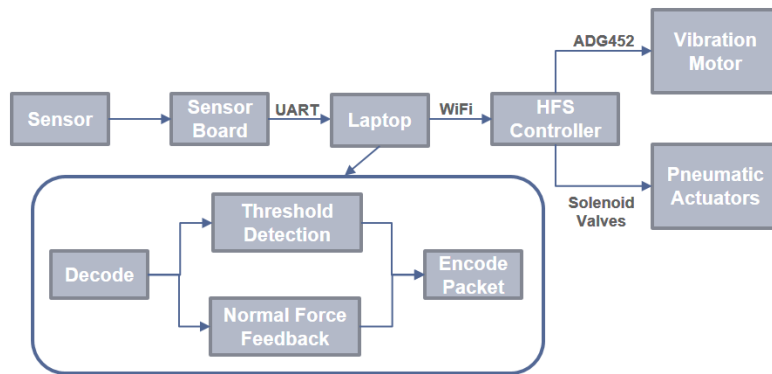


Figure 65: Control System of the Hybrid Vibro-Tactile HFS

The sensing mechanism was a single FlexiForce B201 sensor installed on a 3D-printed support and mounted at the end of da Vinci Fenestrated Bipolar forceps (Figure 66).



Figure 66: Normal Force Sensor Installed on da Vinci Fenestrated Bipolar Forceps

To simulate the presence of a vessel-like structure inside soft tissue, a phantom was created by placing a semi-compressible, silicone-based tube, inside a soft Eva foam material (Figure 67) and then covering it up with a soft, but thick, patterned cloth (Figure 66). The cloth made purely visual localization of the tubular structure challenging.



Figure 67: Phantom Made of a Polyurethane Tube Hidden Inside a Soft EVA Foam

Utilizing a repeated measures study design, 19 subjects were asked to use a da Vinci Si system to palpate the surface of the phantom by pressing down the sensor on the surface. Subjects were asked to localize the tube. Each subject performed the same task three times, once with no feedback (visual inspection only), once with pure normal force tactile feedback and once with the hybrid vibro-tactile HFS activated. Subjects were asked to look away in between the trials so the phantom could be switched out. Subjects were also informed that a phantom may or may not contain any tubular structure and therefore the subject could report that no tubular structure was present. However, in reality, all phantoms contained a tube. Furthermore, in order to eliminate any bias from the depth of placement and positioning of the tube, the same phantom was used for all trials

of the same subject with the difference that the phantom was repositioned to ensure that the tube was no always placed in the same spot. The order of the trials was also randomized to eliminate any bias arising from subject gaining experience with the system.

Statistical analysis of the ordinal data (i.e. detections, faults) would ideally be performed using One-way Repeated Ordinal Regression¹¹², however this test would fail due to the binary nature of the data in this study. For this reason, Friedman's test which a non-parametric alternative to Repeated Measures ANOVA was used instead. For time-to-completion, Log2 transformation was used to achieve normality, followed by statistical analysis using Repeated Measures ANOVA. Follow up post-hoc analysis was performed using Tukey correction method when p-value was < 0.05.

7.2.1.2 Results

In total, there were 4 instances of false positives, 10 instances of subject not finding the tube and 5 correct detections of the tube in the no feedback group. When tactile feedback was provided, there was 3 false positives, 4 instances of subject not finding the tube and 12 correct detections. When the bi-modal vibro-tactile HFS was activated, there were no instances of false positives, 2 instances of the subject not being able to locate the tube and 17 correct detections.

For the purposes of statistical analysis, a fault/false-positive was identified at either a subject not being able to locate the tube or incorrectly identifying the location of the tube. A correct detection was defined as correct localization of the vessel-like structure (Figure 68). The hybrid vibro-tactile HFS performed significantly better than no feedback with regards to faults ($p = 0.0001$) and correct detections ($p = 0.0001$). When comparing the single modality pneumatic tactile feedback with the no feedback conditions, a significant reduction in faults ($p = 0.0457$) and correct detections ($p =$

0.0459) can also be observed. No significant difference was observed between the vibro-tactile feedback and single-modality pneumatic tactile feedback with regards to fault ($p = 0.206$) nor the correct localization of the tube ($p = 0.206$).

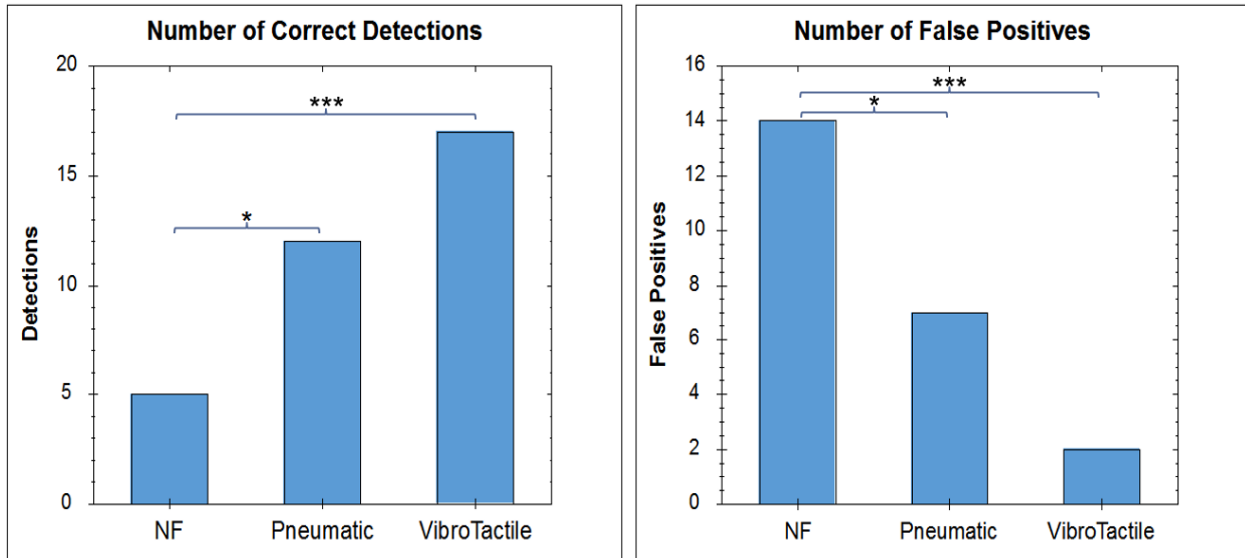


Figure 68: Comparison of Correctness Score (Number of Correct Detections) and Number of Faults (False Positives and Not Detected) in Detecting Non-Compressible Structure in Soft Tissue, Under Different Feedback Conditions

With regards to the time-to-completion of the tasks (Figure 69), the bi-modal HFS performed significantly better than both the no feedback ($p = 0.0033$) and the pneumatic tactile feedback ($p = 0.029$) conditions. No significant difference was present between the time-to-completion time between the no feedback and unimodal pneumatic feedback condition ($p = 0.762$).

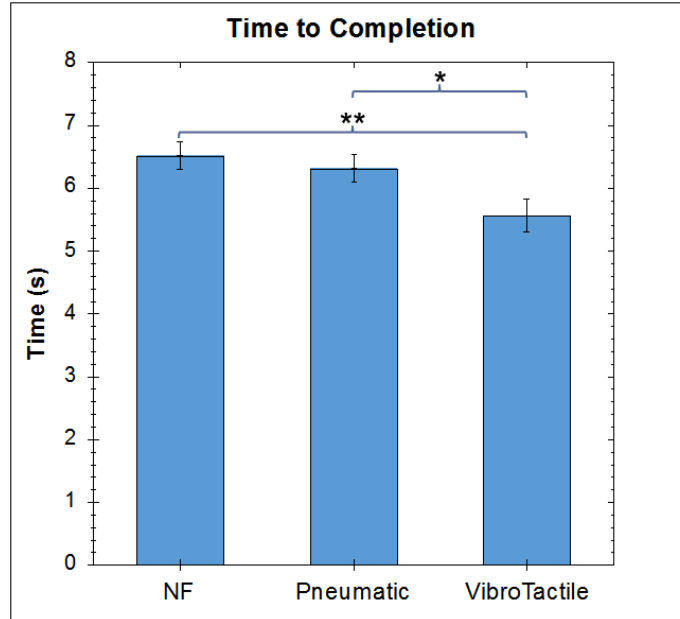


Figure 69: Comparison of Time-to-Completion for Localization of Non-Compressible Tubular Structure Under Different Feedback Conditions

7.2.1.3 Discussion

The lack of haptic feedback in robotic surgery has introduced a major diagnostic limitation, nearly eliminating any possibility of palpation during RMIS procedures. Surgeons are forced to rely solely on visual cues which, when not clearly present, can risk accidental injury to valuable tissues such as nerves and vessels. The results of this investigation show the benefits that multi-modal haptic feedback systems can have in improving the operator’s ability to detect vessel-like structures in soft tissue. Furthermore, the results also clearly show how overall performance including reduction of false positives and time-to-completion can also be improved.

The bi-modal vibro-tactile system investigated in this study was representative of only a naïve implementation of a multi-modal HFS. Despite this, it clearly shows the benefits of a multi-modal haptic feedback system over single-modality solutions. The synergistic relationship between the two feedback modalities presented in this vibro-tactile system resembles how fast adapting

mechanoreceptors in the skin work together with slow adapting pressure sensors to allow rapid scanning of an area and identification of various structures not visible to the naked eye.

7.2.2 VIBRO-TACTILE HYBRID HFS USING NORMAL FORCE SENSING ARRAY

The previous investigation of the vibro-tactile HFS focused largely on the potential benefits of a multi-modal feedback over unimodal feedback mechanisms. While the results of the study showed significant benefits of multi-modal HFS in palpation tasks, the naïve threshold-based activation of vibration feedback may not translate well to clinical settings. The non-homogenous nature of soft tissue can lead to either excessive false positives, or lack of any detections at all, hence reducing the effectiveness of such a haptic feedback system.

The problem with the original system design lies primarily in the sensing mechanism. Utilizing only one sensor does not provide sufficient information to the HFS software engine to properly detect non-compressible structures in a variety of different tissue types. Part of the reason that human hands are so effective in detecting such structures is that the skin contains thousands of mechanoreceptors, allowing differences between the sensing information in two nearby areas to be used for detecting changes in tissue texture. Therefore, any feedback system that aims to simulate the sense of touch during robotic surgery and provide artificial palpation, must also rely, not on one sensor, but rather an array of sensors. To this end, a variation of the vibro-tactile feedback system was developed utilizing an array of FlexiForce B201 normal force sensors, mounted on a 3D-printed, finger-like support (Figure 70); one that could be used for simplifying palpation in robotic surgical tasks.



Figure 70: Normal Force Sensor Array Installed on a 3D-printed Support for Palpation in Robotic Surgery

Utilizing the two outer sensors as reference sensors and the middle sensor as the data sensor, it is possible to detect tissue texture, without pre-defining any activation threshold. This concept relies on the fact that when scanning a surface, the middle sensor can never detect higher force values than the outer two reference sensors unless the array is passing over a non-compressible structure. Such a structure would cause increased force on the data sensor, while the outer reference sensors which are in contact with the nearby soft tissue, continue reporting lower forces.

To evaluate the system, this investigation utilized the normal force sensor array as part of a bi-modal vibro-tactile feedback system. The goal was to determine whether the haptic feedback provided using this multi-modal HFS can be an effective way for improving subjects' ability to detect tumor-like structures in soft tissue.

7.2.2.1 Methods

The control system of the bi-modal HFS was developed by configuring the logic engine of the Haptics Manage software (Figure 71). More specifically, utilizing the Subtract operation in the feedback rule definition of the multi-modal HFS's control software (Section 6.4.2.3), a differential detection method was implemented.

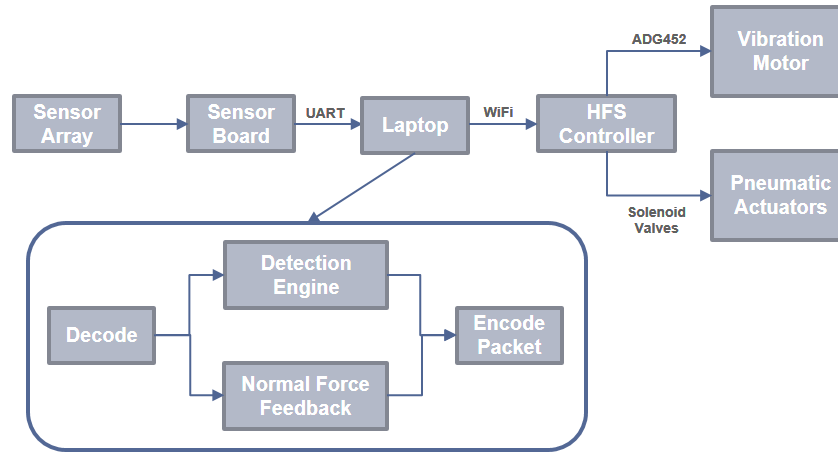


Figure 71: Control System of Vibro-Tactile Hybrid HFS using Normal Force Sensor Array

A phantom was created by injecting epoxy inside a low density soft sponge material. The developed sensor array could then be used to scan the entire surface of the rectangular phantom (Figure 72). The hardened epoxy created tumor-like, non-compressible structures which were not visually identifiable from the surface of the phantom, but could be felt by palpating the surface.

The study relied on a repeated measures design where a total of 14 subjects performed the palpation tasks three times, each time under three feedback conditions: (1) No Feedback (2) Pneumatic Normal Force Tactile Feedback (3) Hybrid Vibro-Tactile Feedback. Subjects were asked to scan the entire surface of the phantom, ensuring that the entire array remained parallel to the surface of the table where the phantom was mounted. Subjects would then point out the location of any tumors that they could find, or simply state that no tumor was present (in case none could be found). Subjects were blinded to the fact that all phantoms contained exactly four tumors.

Three phantoms were created and randomly used for three trials to eliminate any bias arising from the slight variations in the tumor size in the different phantoms. A fourth sample phantom was given to subjects prior to the study so they could use their own hands to feel for the tumor and get a better idea of what they are looking for.

Vibration was provided as a binary feedback modality when the differential detection method identified a tumor-like structure. Pneumatic normal force tactile feedback was provided based on the maximum pressure from all three sensors in the array.



Figure 72: Soft Sponge Phantom with Spherical Tumor-Like Structures Hidden Inside, Palpated Using Normal Force Sensor Array

Data analysis was performed using One-way Repeated Ordinal Regression¹¹² to help in determining the difference between each group with regards to the number of false positives and number of correct detections. In cases where p-value was < 0.05 , follow up post-hoc analysis was performed using Holm correction.

7.2.2.2 Results

The results of the experiment show (Figure 73) that the ability of the subject in detecting the tumors is significantly improved compared to the no feedback conditions, both when using pneumatic normal force feedback ($p = 8.54E-5$) and bi-modal vibro-tactile HFS ($p = 2.57E-5$). The multi-modal vibro-tactile HFS also performed better than the unimodal pneumatic tactile feedback with regards to the number of correctly detected tumors ($p = 0.019$). Looking at the total number of correctly detected tumors, the no feedback condition (i.e. visual inspection only) resulted in 3 correctly identified tumors out of a total of 56. Providing pneumatic tactile feedback increased this

number of 33/56. Finally, providing multi-modal vibro-tactile feedback resulted in 44/56 correctly identified tumors.

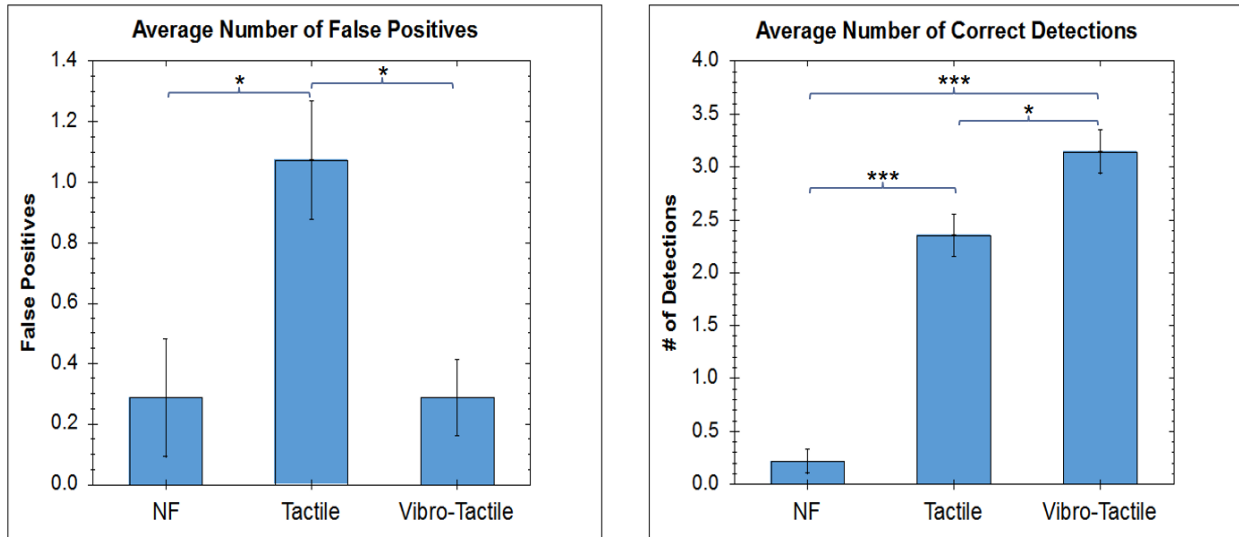


Figure 73: Comparison of the Number of Faults and Correctness Score (Number of Correct Detections) for Artificial Palpation in Robotic Surgery, Under Different Feedback Conditions

With regards to the number of faults (i.e. number of false positives), the bi-modal vibro-tactile feedback system performs significantly better than the pneumatic tactile feedback ($p = 0.025$). This corresponds to a total of false positives of 4/56, 15/56 and 4/56 for the no feedback, tactile feedback and the vibro-tactile feedback respectively.

It is worth mentioning that while there is also a significant difference between the pneumatic tactile feedback and the no feedback conditions with regards to the number of faults, in reality this value doesn't correctly present the observations of the experiment. In nearly all no feedback cases, the subject simply gave up on finding a tumor in the phantom and reported that the phantom contained no tumors at all, therefore leading to a low false positive value.

7.2.2.3 Discussion

The results of this study paint a clear image of the benefits of haptic feedback for artificial palpation applications. The experimental design of this experiment leads to a much more challenging task compared to the more straightforward detection of vessels in the previous vibrotactile HFS study. This results in only a 5% correct detection rate for the no feedback condition, demonstrating how ineffective visual inspection can be in properly localizing structures hidden in soft tissue. On the other hand, providing tactile feedback increases this number to 59% while the multi-modal feedback raises this number further to a respectable 79%. Considering that this system relies on a low-resolution array consisting of only three normal force sensors, this value is a great demonstration of how effective multi-modal haptic feedback systems can be in resolving on the most critical limitations that robotic surgical systems have faced since the beginning. Furthermore, these results also highlight the benefits of multi-modal feedback systems over traditional single modality feedback methods.

7.3 KINESTHETIC-TACTILE HYBRID HFS FOR GRIP-FORCE REDUCTION

The previous research conducted for the evaluation of CASIT's tactile feedback system was focused on reduction of grip forces and crush injuries in robotic surgeries²⁰. Even though the results of these investigations paint a promising picture for the future of haptics and its benefits for RMIS, they also emphasize how much work remains to be done. While grip forces are reduced in robotic surgical operations with the utilization of unimodal, normal force tactile feedback, the reductions and the effectiveness of HFS are not only highly variable among subjects, but also not substantial enough to eliminate all instances of tissue damage. The development of the multi-modal haptic feedback system introduced in this research project engenders the promise of a more natural and complete HFS, one that hopes to bring haptics one step closer to real touch.

The two most important feedback modalities involved in grasping are normal force tactile feedback and kinesthetic force feedback. Through the activation of the appropriate mechanoreceptors in the skin and the muscles, the human neuromuscular system is able to apply just enough force to prevent an item from slipping out of one's hand while at the same time not inducing any damage from excessive grip force. The goal of this investigation is study the impact that a bi-modal kinesthetic-tactile feedback system can have in reducing grip force for robotic surgical tasks.

7.3.1 KINESTHETIC-TACTILE HYBRID HFS

A common implementation of kinesthetic force feedback relies on motors installed on the hinge of robotic controls. The development of this kinesthetic force feedback mechanism was previously discussed in detail in Section 6.7.1. The goal of this study is to evaluate a bi-modal kinesthetic-tactile feedback system as an addition to the RAVEN Surgical Robotic System. More specifically, this study aims to compare the benefits of unimodal kinesthetic force feedback, unimodal tactile

feedback and the bi-modal hybrid HFS in reducing grip forces for RMIS tasks. Assuming that the assertion about the synergistic relationship between kinesthetic force feedback and normal force tactile feedback is correct, the bi-modal hybrid HFS would prove to be more effective than both unimodal implementations.

7.3.1.1 Methods

The control system of the hybrid kinesthetic-tactile HFS was implemented by configuring the Haptics Manager software engine to send kinesthetic force levels to an external kinesthetic feedback controller through UDP (Figure 74).

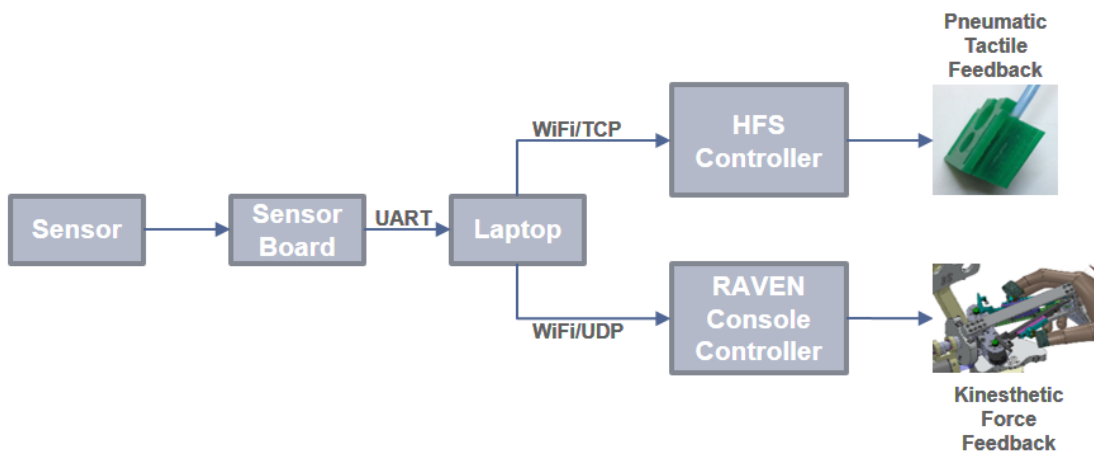


Figure 74: Control System of the Kinesthetic-Tactile Hybrid HFS Utilizing the Raven Console Motor for Kinesthetic Force Feedback

A total of 17 novice subject with limited or no experience with robotic surgery were recruited from the general population at UCLA. The study utilized a repeated measures design in which each user performed a single-handed peg transfer task, as part of seven trials under different feedback conditions: (1) No Feedback (2) Kinesthetic Force Feedback (3) Normal Force Tactile Feedback (4) Hybrid Kinesthetic-Tactile Feedback. Each trial involved two, single-handed peg transfer tasks adopted from the standard peg transfer test in the Fundamentals of Laparoscopic Surgery (FLS)

education module developed by the Society of American Gastrointestinal Endoscopic Surgeons (SAGES)¹⁰¹.

The seven trials consisted of four No Feedback trials separating three feedback trials. The three feedback trials were randomized to eliminate any training bias toward either feedback modality. The four feedback trials were also spread out in between the feedback trials to help in observing any learning effect that may be occurring over the duration of the 7 trials. Subjects were also given a 5-minute training period at the beginning to familiarize themselves with the controls of the RAVEN robotic system. During the trial, to eliminate any bias toward the position which a subject may drop the peg, if the subject dropped the peg, the proctor would quickly reset the peg's to its original position.

The sensing system relied on a FlexiForce B201 normal force sensor which was installed on the Raven instrument by modifying the original sensor mounting mechanism to also fit the Raven grasper.

During the trial, the number of faults (the number of times subject dropped the peg), time-to-completion and the applied grip force were recorded. Statistical analysis for average grip-force was later performed using Rank Transformed Repeated Measures ANOVA due to non-normality of the data. Statistical analysis for time-to-completion was performed using Repeated Measures ANOVA following a Log2 transformation to achieve normality. For analysis of the number of faults, Ordinal Repeated Measures ANOVA was used. Follow up post-hoc analysis using Tukey correction were performed when p-value was less than 0.05.

7.3.1.2 Results

The results of the study for the number of faults and time-to-completion are shown in Figure 75. This data shows that there is no significant difference between any of the groups with regards to the number of peg drops ($p = 0.534$) and the time-to-completion of the task ($p = 0.119$).

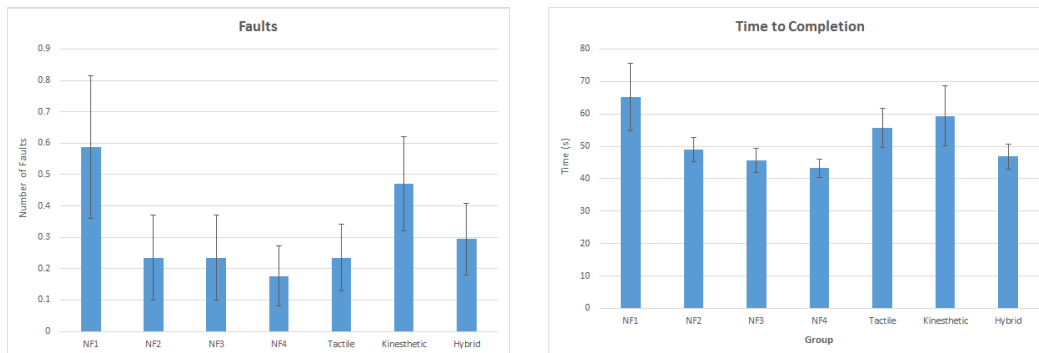


Figure 75: Comparison of Time-to-Completion and Number of Faults (Number of Peg Drops) Under Different Feedback Conditions Using the Raven Surgical System

The average grip force was significantly lower when Hybrid HFS was used compared to all No Feedback conditions ($p = 0.00069$ for Hybrid vs. NF1). The same trend was present for Tactile Feedback ($p = 0.0022$ for Tactile vs. NF1). No significant difference was observed between the kinesthetic feedback and any of the no feedback conditions. Additionally, there was no significant difference between the four no feedback conditions, indicating that there is no reduction in grip force, number of faults and time-to-completion resulting from learning behavior.

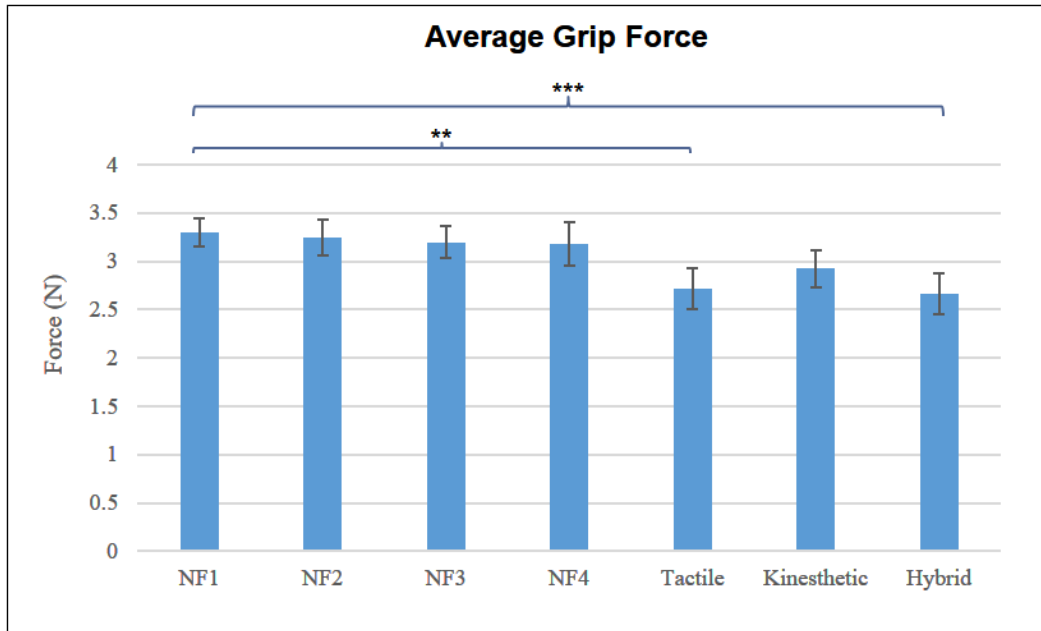


Figure 76: Comparison of Average Grip Force Under Different Feedback Conditions Using the Raven Surgical System

7.3.1.3 Discussion

As expected, normal force tactile feedback leads to reduction of grip forces compared to the no feedback conditions. This is consistent with findings of previous work in this area²⁰. However, the results of the study did not meet the original expectations of kinesthetic force feedback. In fact, there does not appear to be any benefit to the kinesthetic force feedback at all. The results also seem to point out that any benefit from the hybrid kinesthetic-tactile HFS was in fact only caused by the pneumatic normal force tactile feedback, and not the kinesthetic force feedback.

The data in Figure 76 also shows that the average grip force when kinesthetic feedback was activated, was slightly lower compared to the no feedback condition. While this difference was not significant, it may indicate that the issue causing the ineffectiveness of kinesthetic force feedback may result from a more complex underlying problem, rather than the kinesthetic feedback modality itself.

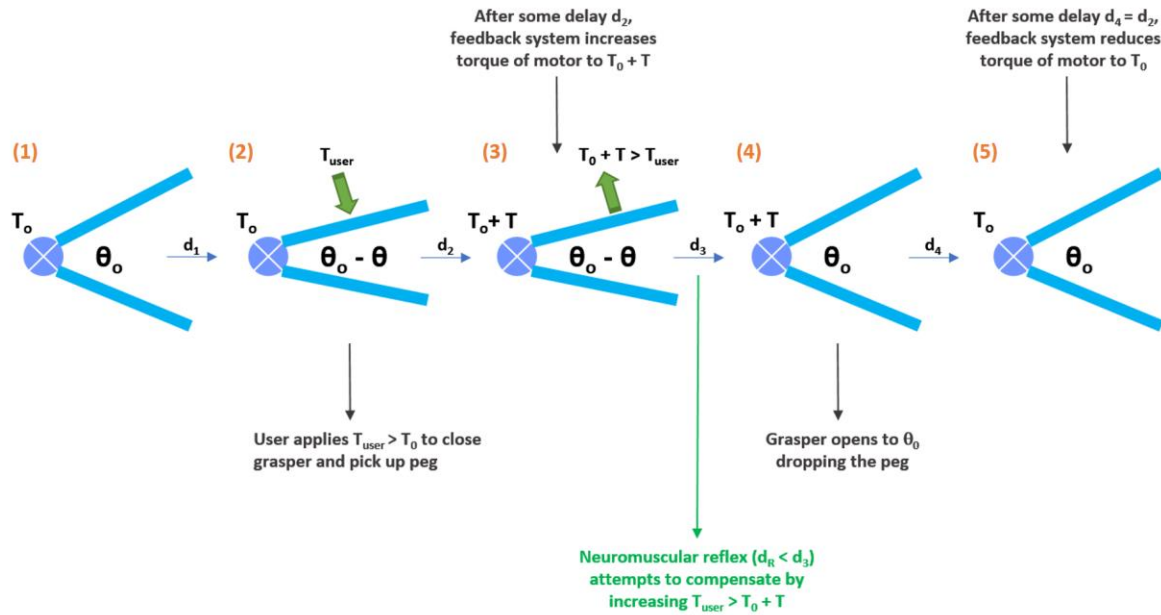


Figure 77: Series of Event Leading to Subject Dropping the Peg When Kinesthetic Feedback is Provide on the RAVEN

(1) Relaxed RAVEN Joystick/Grasper (2) User Presses and Closes the Grasper (3) Force from Motor Increases in Response to Signal from Sensors (4) Higher Forces Overcome User's Applied Muscle Force, Opening Grasper to θ_o (5) Force on the Motors is Reduced Since Sensors Aren't Detecting High Forces

Through a series of bench tests and a better understanding of human neuromuscular reflexes, the underlying problem with the kinesthetic feedback method was identified. The ineffectiveness of kinesthetic force feedback, was in fact caused by the subject's neuromuscular reflex to a series of events which would otherwise result in the subject dropping the peg. Figure 77 describes these events in five steps. At initial time, the feedback motor applies a normal force F_0 to the subject's hand for any angle larger than θ_o , where θ_o is the maximum opening angle of the grasper. This initial condition (1) is followed by (2) the user applying some addition force to the grasper to close it, after which the closed grasper comes in contact with a peg, causing the feedback system to response by (3) increasing the feedback motor power, hence applying a higher force ($F_0 + F$) to the subject's hand, after which (4) the feedback motor now overcomes the force applied by the subject's fingers and returns to its original maximum open angle of θ_o . By this time, the robotic

arms have dropped the peg, hence telling the system to (5) reduce the feedback motor power, returning the system to its initial condition. Figure 77 shows the delays between each event as d_1 through d_4 . According to events described above, the subject should drop the peg everytime he/she attempts to pick it up, because if the human neuromuscular reflexes are longer than d_3 , then there is no way the subject has enough time to increase the force applied by his/her finger in time to prevent the grasper from opening all the way to θ_0 and releasing the peg. However, the human neuromuscular response is more complicated. In fact, in some subjects, the response is faster, allowing the subject to prevent the peg drop. In other subjects, the brain quickly learns and predicts this event, thereby forcing the fingers to apply a higher initial load, one that would not be overcome by $F_0 + F$, but this extra load comes at the expense of excessive force applied to the peg.

This unexpected phenomenon arises from two fundamental problems in the kinesthetic force feedback system. The first is that the feedback delay (d_2 and d_4), that is the time it takes for values from the sensor to impact the force of the feedback motor is longer than d_3 . Let's assume that this feedback delay was zero. In such a case, as the grasper is opening during transition from (3) to (4), the applied force on the sensors would be reduced as well, hence reducing the applied feedback force, which in turn, at some point, would reach a level just low enough, that would no longer overcome the subject's muscular tension. Of course, such a system with zero delay is not feasible and reduction of delays further would not guarantee the complete resolution of this problem. The reason is that there is a second, more fundamental issue with this implementation of kinesthetic force feedback. That is, this form of kinesthetic force feedback does not mimic the behavior of real-world objects and how human hands interact with them. As opposed to the grasper which tries to force its way back to θ_0 , a real-world object does not stretch out beyond its original size and shape when it is compressed, it simply resists the compression further. Therefore, any HFS that

attempts to mimic real-world kinesthetic feedback must not rely on a spring-like response for providing feedback but rather attempt to provide a sense of resistance.

7.3.2 PNEUMATIC KINESTHETIC-TACTILE HYBRID HFS

The investigation into the pneumatic kinesthetic-tactile feedback system was based on the assertion that this bi-modal feedback solution provided a better method for simulating the sense of touch. The development of the pneumatic kinesthetic force feedback solution was previously described in 6.7.2. The goal of this investigation was to evaluate the pneumatic kinesthetic-tactile HFS in reducing grip forces during robotic surgical tasks involving tissue grasping.

The evaluation of this hybrid HFS was conducted as part of two independent studies, each designed to provide a better understanding of the impact that this multi-modal HFS would have on RMIS tasks involving tissue manipulation.

7.3.2.1 Peg Transfer Study

The goal of the peg-transfer study was to evaluate the kinesthetic-tactile HFS under the same conditions which had been used for the previous kinesthetic-tactile feedback system. More specifically this study aimed to not only evaluate the impact of the multi-modal HFS on grip forces, but also the kinesthetic force feedback as a single-modality solution.

7.3.2.1.1 Methods

The control system for the pneumatic kinesthetic-tactile hybrid HFS was implemented by configuring the logic engine of the Haptics Manager software to utilize the dual-value continuous pressure regulators as a means of changing the pressure in the pneumatic tube responsible for providing kinesthetic force feedback.

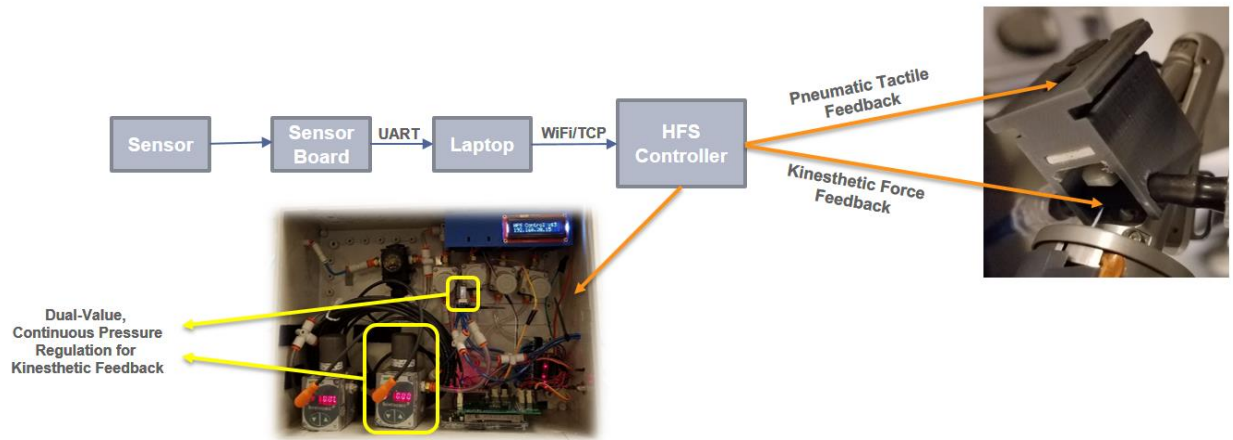


Figure 78: Control System of the Pneumatic Kinesthetic-Tactile Hybrid HFS

A total of 15 novice subjects with little to no experience with robotic surgery were recruited to perform single handed peg-transfer tasks using a da Vinci IS1200 surgical system. Subjects were given 2-minute training period prior to the start of the study to familiarize themselves with the robotic system. This training period was sufficient in most cases since the use of clutch, camera and most other complex da Vinci operations was not allowed. In order to eliminate any bias toward either hands, nearly half (7) of the subjects performed the feedback on the right hand while the remaining received feedback on the left hand (8). All subjects were right handed. Each subject was asked to perform four peg transfers during each trial. To eliminate any bias toward the position which a subject may drop the peg, if the subject dropped the peg, the proctor would quickly reset the peg to its original position.

For this study, a FlexiForce B201 sensor was installed on da Vinci Fenestrated Bipolar forceps. Each subject performed the peg transfer tasks, four separate times as part of four trials, each performed under different feedback conditions: (1) No Feedback (2) Normal Force Tactile Feedback (3) Pneumatic Kinesthetic Force Feedback (4) Hybrid Kinesthetic-Tactile Feedback.

During the trial, the number of faults (i.e. number of times the subject dropped the peg), time-to-completion and the grip force were recorded. Statistical analysis for average grip force was performed using Repeated Measures ANOVA after a Log2 transform which was used to meet the normality assumption. Repeated Measures ANOVA was also used for analysis of peak grip force. Statistical analysis for the number of faults was conducted using Ordinal Repeated Measures ANOVA (6.4.3).

7.3.2.1.2 Results

The results show (Figure 79) that the average grip force is significantly lower compared to the no feedback condition when tactile feedback ($p = 0.017$), kinesthetic feedback ($p = 1.66E-6$) or hybrid feedback ($p < 1.0E-16$) are provided. The bi-modal kinesthetic-tactile HFS also performs better than both tactile-only ($p = 5.64E-8$) and kinesthetic-only ($p = 0.0027$) feedback conditions.

With regards to the peak grip force, no significant improvement can be seen between the tactile feedback and the no feedback conditions. However, both kinesthetic ($p = 0.0008$) and hybrid HFS ($p = 0.0001$) conditions display a significant reduction in peak grip force.

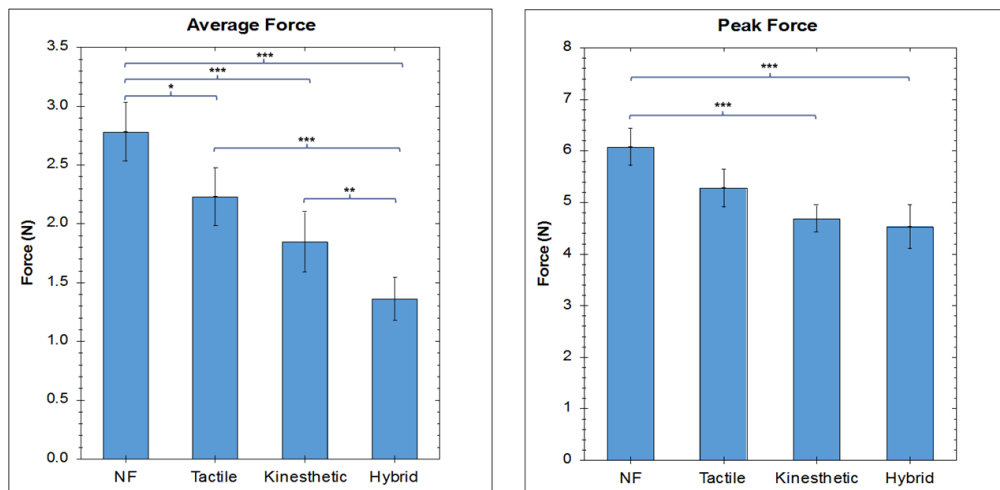


Figure 79: Comparison of Average and Peak Grip Force Under Different Feedback Conditions When Utilizing the da Vinci

The number of faults (Figure 80) appears to be significantly higher with the hybrid HFS activated, compared to the tactile feedback group ($p = 0.012$). No significant difference exists between the other conditions.

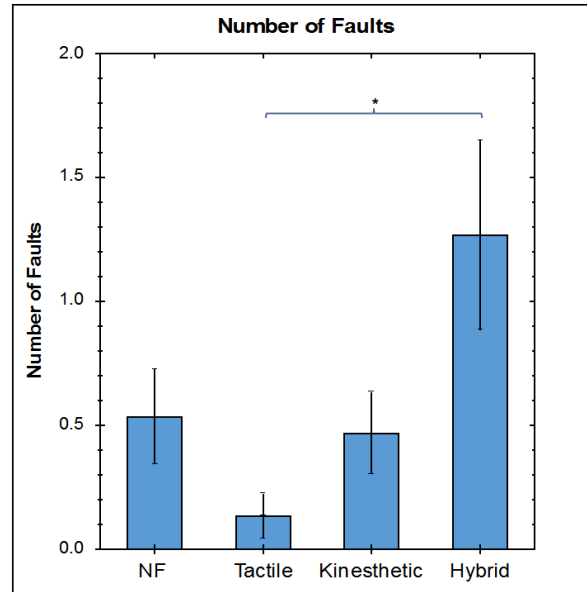


Figure 80: Comparison of Number of Faults Under Different Feedback Conditions When Utilizing the da Vinci IS1200 for Peg Transfer Tasks

7.3.2.1.3 Discussion

The results from the peg transfer study show the clear benefits of providing haptic feedback in reducing grip force. All feedback modalities performed significantly better than the no feedback condition. As expected, this new implementation of kinesthetic force feedback does not suffer from the same problem as the feedback motor-based design (Section 7.3.1). Kinesthetic feedback alone showed significant benefits in reducing the average grip force. Most importantly, there is also a clear indication that the multi-modal kinesthetic-tactile feedback system is significantly better than both single-modality feedback solutions, benefiting from the synergistic relationship from the activation of mechanoreceptors in the skin and muscle. This leads to a more natural sense

of touch, allowing the subjects utilizing the system with multi-modal HFS to apply forces nearly 50% less than when no feedback is present.

An interesting observation from the study that is worth discussing is the larger number of faults (i.e. peg drops) in the bi-modal HFS compared to the tactile-only condition ($p = 0.012$). Based on the large standard error mean, it is clear that there is also significant variation among subjects. The reason for this variation is actually the way the pneumatic kinesthetic feedback functions. The high pressures used for higher feedback levels makes compressing the grasper quite challenging due to increased resistance. When this resistance is coupled with a high tactile feedback level, it appears to result in the subject suddenly relaxing the hold on the graspers and often dropping the peg. This variation is more of a learned behavior which is most likely caused by the lack of experience with the feedback system. Even though some training with the haptic feedback system can eventually eliminate this behavior (as we observed in a series of follow up bench tests), the correct way to ultimately deal with this issue is to develop an adaptable feedback system. Such a feedback system can learn from the user's behavior and automatically lower the pressure levels to help reduce resistance and hence the number of peg drops.

7.3.3 EX-VIVO STUDIES

In order to evaluate the bi-modal kinesthetic-tactile HFS under conditions which are more representative of real-world surgical applications, an ex-vivo study was design. The original CASIT tactile feedback system was tested in an in-vivo study where subjects would run the bowel under different feedback conditions²⁰. Results of this studies showed a clear correlation between applied grip force and the number of damage sites in tissue (Figure 4). In order to be able to use these results, this study also relies on the same task for evaluation of the multi-modal HFS. Since

the correlation of applied grip force with tissue damage already exists, it is therefore possible to rely on ex-vivo experiments for evaluation of the kinesthetic-tactile HFS.

7.3.3.1.1 Methods

These experiments relied on the same control system as the previous pneumatic kinesthetic-tactile HFS (Figure 78). FlexiForce B201 sensors were installed on two da Vinci Cadiere forceps. Feedback actuators were installed on both right and left controls of the da Vinci system however only one hand received feedback throughout the trial. This experimental design choice allowed one hand to act as a control for the other. To eliminate any bias toward either hand, half of the subjects performed the task with the feedback on one hand and half with feedback on the other.

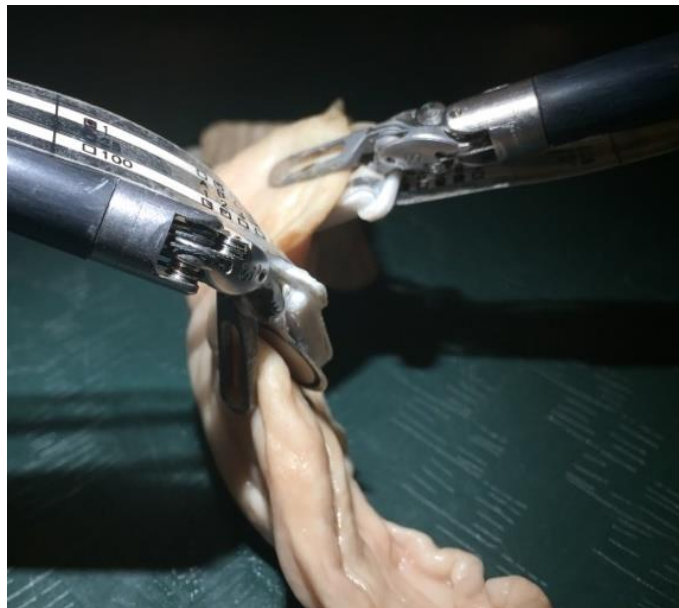


Figure 81: Ex-Vivo Porcine Large Intestine Handled Using da Vinci IS1200 Cadiere Forceps

Subjects were asked to run a porcine bowel, approximately 30 cm in length (Figure 81). Each subject performed the task only once. For this investigation, two groups of subjects were recruited. The first study was performed by recruiting 10 novice subjects with little to no experience with robotic surgery. The second group of subjects were expert robotic surgeons recruited from the

Ronald Reagan Hospital at UCLA. A total of 8 expert surgeons were recruited for participation in this study.

For all subjects, the applied grip force was recorded throughout the study. For expert subjects, the number of times the surgeon dropped the tissue with either hand was also recorded to determine any impact the hybrid HFS has on proper handling of the tissue. This parameter (number of faults) was not recorded and analyzed for novices. This experimental design choice was made because of the difficulty that many novice subjects experienced picking up and handling the bowel tissue. This lack of inexperience and the non-homogeneity of the tissue made this parameter too variable in novices to be valuable without requiring a very large number of subjects to be enrolled. For novice subjects, the study controlled for the utilization of the clutch by prohibiting subjects from using the clutch operation on the da Vinci. The proctor instead adjusted the controls such that no visual-perceptual mismatch was present and the subject could easily perform the tasks without needing access to the clutch operation.

Statistical analysis was performed using a standard student's paired t-test when normality assumption was met and a non-parametric, paired Wilcoxon Signed Rank test when the data was not normally distributed.

7.3.3.1.2 Results

The results of the study in novice subjects (Figure 82) show a significant reduction in average grip force ($p = 0.00034$) and peak grip force ($p = 0.00040$) in the hand that received feedback from the bi-modal HFS.

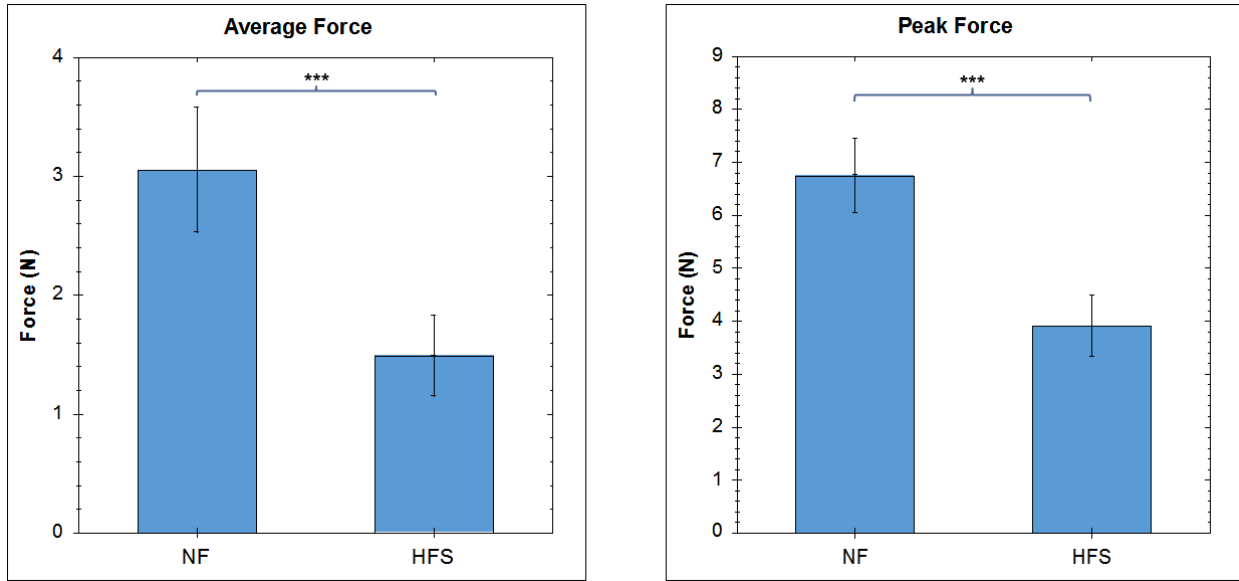


Figure 82: Comparison of Average and Peak Grip Force Between No Feedback and Kinesthetic-Tactile Feedback Condition During a Porcine Bowel Run

Looking at the inter-subject variation (Figure 83), it can clearly be seen that with regards to both average and peak grip-force, nearly all novice subjects benefited from the presence of the bi-modal kinesthetic-tactile HFS.

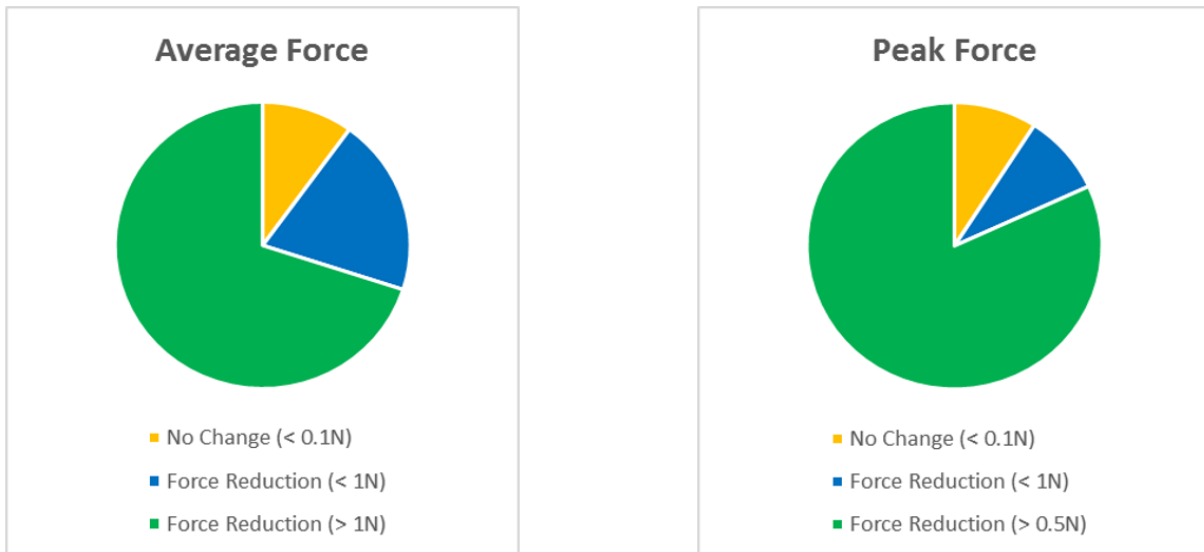


Figure 83: Variation in Effectiveness of Kinesthetic-Tactile HFS Among Novice Subjects in Ex-Vivo Porcine Bowel Run Study

In expert surgeons, the same trend followed with the hand receiving feedback showing a significant reduction in average grip force ($p = 0.0234$). No significant difference was observed in peak grip force ($p = 0.677$) and the number of faults for expert surgeons. Looking at the inter-subject variation, most subjects benefited from the presence of HFS, though the impact was less apparent than in novices.

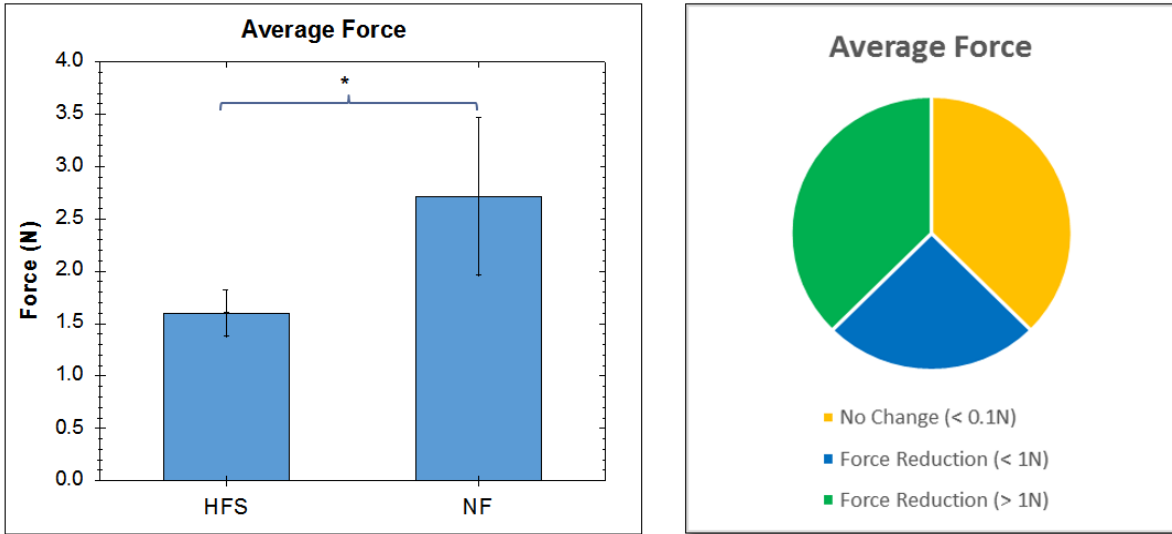


Figure 84: Comparison of Average Grip Force Between No Feedback and Kinesthetic-Tactile Feedback Condition During a Porcine Bowel Run and the Variation in Effectiveness of HFS in Expert Subjects in the Same Study

7.3.3.1.3 Discussion

The results of the ex-vivo studies show that in the bi-modal haptic feedback can help reduce the applied grip force, both in novices and experts. However, the results also show that such a feedback system can have a much more significant impact in the less experienced population. In fact, novices benefited significantly from the presence of feedback with regards to the applied peak grip force. On the other hand, for surgeons, the applied peak grip force was approximately 4N, with or without feedback. That is on par with the peak grip force in novices after feedback was provided. These results help highlight the importance of training and how expert robotic surgeons have

learned to compensate for the lack of feedback. Having said that, the average grip force data for expert surgeons under the no feedback conditions shows that there is still room for improvement. That is, even for experienced surgeons, without HFS, the applied average and peak forces are still high enough to induce tissue damage, making the multi-modal HFS valuable even for expert robotic surgeons.

7.4 A TRI-MODAL HAPTIC FEEDBACK SYSTEM

The investigations on the effectiveness of bi-modal haptic feedback systems in improving performance of subjects in various robotic surgical applications has clearly shown that multi-modal feedback, when implemented correctly, can have significant advantage over single-modality feedback. Despite these benefits, the investigated bi-modal feedback system simulates only a subsection of all the feedback modalities present in real human touch. The bi-modal pneumatic kinesthetic-tactile HFS was one of the most complete and optimized feedback solutions developed in this research project, because it built upon many years of research in normal force tactile feedback^{20,25,102,119,120}. Yet, in many cases, the peak forces and even average grip forces applied when picking up an object with the robotic surgical system are high enough to cause tissue damage. Looking at peak grip forces in nearly all HFS studies, even when haptic feedback is present, it is clear that subjects can often ignore the provided feedback and apply high forces. This is particularly true in novice users. Part of the reason is that subjects are often so immersed in the task that they begin to ignore the provided feedback.

Based on the understanding of vibration feedback gained in the previous studies of this research project, it is therefore feasible to consider using vibration feedback to draw the operator's attention to the applied excessive force. With this in mind, a tri-modal haptic feedback system was utilized to provide a third modality of feedback when applied forces move beyond a certain threshold. The goal of this investigation was to determine the potential benefits that a tri-modal HFS would have over the previously tested bi-modal kinesthetic-tactile feedback system, in reducing average and peak grip forces in RMIS tasks.

7.4.1 METHODS

The control system for a tri-modal feedback system was implemented by configuring the logic engine of the Haptics Manager software (Figure 85).

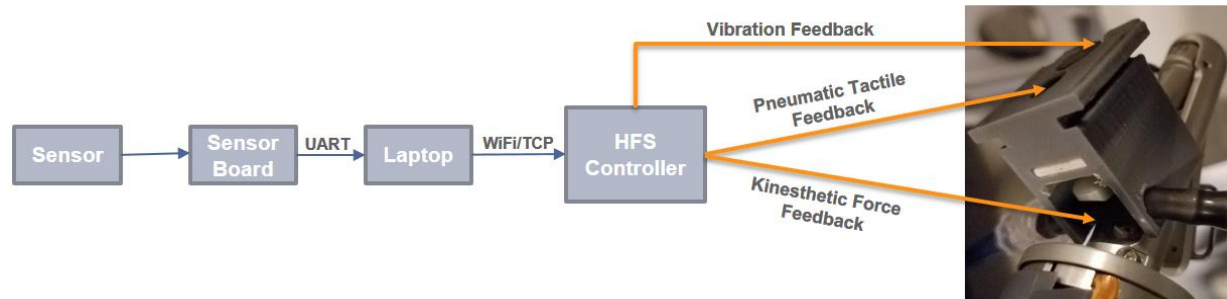


Figure 85: Control System for a Tri-Modal HFS

A total of 10 subjects were recruited to perform a two-handed peg transfer task using a da Vinci IS1200 surgical system. Two Cadere forceps were installed with FlexiForce B201 normal force sensors. On one hand the subject received bi-modal kinesthetic-tactile feedback while on the other, he/she received tri-modal feedback. The tri-modal feedback rules were the same as the bi-modal ones with the difference that vibration feedback was provided beyond level 3 of normal force tactile feedback ($\sim 2\text{N}$). A more intense vibration was provided beyond level 4 of normal force feedback ($\sim 3\text{N}$). To eliminate bias toward either hands, the hand receiving tri-modal feedback was switched for half of the subjects.

For all subjects, the study controlled for the utilization of the clutch by prohibiting subjects from using the clutch operation on the da Vinci. The proctor instead adjusted the controls such that no visual-perceptual mismatch was present and the subject could easily perform the tasks without needing access to the clutch operation.

Subjects were asked to perform four peg transfers. In each transfer, the subject would pick up the peg on one side of the field with the arm closest to the peg, pass it to the other arm, and then place

it back down on the other side of the field. The applied grip force and the number of peg drops with each hand was recorded throughout the trial. Statistical analysis was performed using a standard Student's paired t-test when normality assumption was met and a Wilcoxon Signed Rank test when the data was not normally distributed.

7.4.2 RESULTS

The results of the study (Figure 86) show a significant reduction in average grip force when the tri-modal HFS is used compared to the bi-modal kinesthetic-tactile feedback ($p = 0.00039$). The same patterned followed with the peak grip force where the tri-modal feedback system showed a lower peak grip force compared to the bi-modal HFS ($p = 0.0049$). Figure 86 also shows the average and peak grip forces for peg-transfers using human hands in green overlaid on top of the data for this study as a point of comparison.

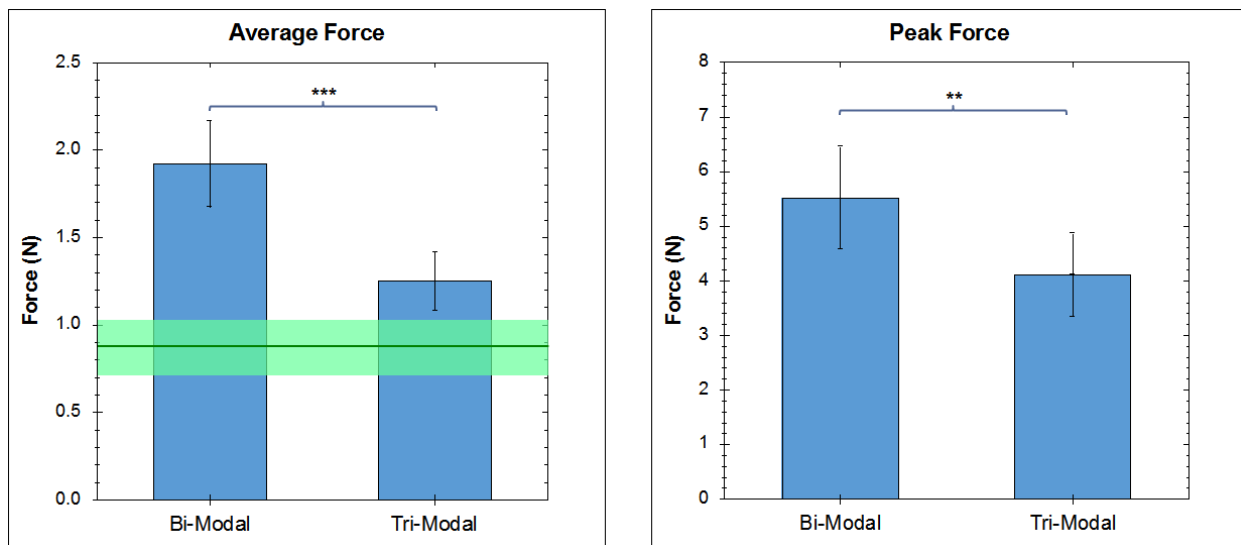


Figure 86: Comparison of Average and Peak Grip Force in a Peg-Transfer Study Using Bi-Modal and Tri-Modal HFS

7.4.3 DISCUSSION

The results of this investigation shows the benefits that the addition of vibration feedback can have on reducing grip-forces. This data further highlights the value of multi-modal haptic feedback systems and how addition of each modality of feedback, when used in a synergistic way, can improve the overall performance of the system.

The overlaid data from the peg-transfers performed by human hands also tells an interesting story. These simple bench top tests which were performed on a few subjects where the same FlexiForce B201 sensor was attached to an individual's thumb. This data shows that average grip force when performing a peg-transfer with a human hand was a mere 0.88N with a standard deviation of 0.15N. The data also shows how close the multi-modal haptic feedback system has come to achieving what may be considered the ideal grip force. Of course, peak grip forces are still significantly higher, even with the haptic feedback system, clearly showing that there is plenty of room for further investigation and optimization of multi-modal HFS in robotic surgery.

8 CONCLUSION

The goal of this research project was to develop and evaluate a multi-modal haptic feedback system for application in robotic surgical procedures. More specifically, this investigation aimed to determine the potential benefits that a multi-modal feedback solution has over traditional unimodal haptic feedback systems. To this end, the primary research aims focused on a better understanding of existing tactile feedback systems, improvement of various aspects of pneumatic tactile feedback, development of a multi-modal HFS and its evaluation in various RMIS applications.

Investigations conducted regarding the presence of large inter-subject variations in haptic feedback studies, led to a better understanding of the Visual-Perceptual Mismatch phenomenon, and the impact of haptics on subject performance. These experiments showed that haptic feedback has the potential to improve time-to-completion and reduce errors in robotic surgical tasks. They also helped highlight an important factor that must be considered when designing experiments for evaluating haptic feedback systems. More specifically, results showed that the utilization of the Clutch operation in surgical robotic systems must be controlled for in robotic studies, particularly in tasks involving coordination between the two arms.

Further research was also conducted on various aspects of CASIT's normal force tactile feedback system. Improvements were made to the sensor board to provide support for a larger variety, and number of sensors. The sensing technology itself was also improved with the design and development of shear sensors capable of being installed on da Vinci instruments and detecting shear forces on the end effectors of the robotic system. Pneumatic actuators were also improved by introducing depressed-membrane designs that were easier to manufacture, and performed better than the original, flat PDMS-based actuators. More importantly these actuators helped eliminate

sensory desensitization, therefore maintaining effectiveness of the feedback system even in long running surgical tasks.

The development of the multi-modal HFS itself required a complete redesign of the system architecture inherited from the original tactile feedback system. Low latency wireless communication modules were developed that would allow all components of the haptic feedback system from being accessed across the internet. The core filtering and control engine was developed in software and optimized to provide processing times of $< 1\text{ms}/\text{packet}$. The software was further enhanced to allowed support for a variety of sensors and actuators, and provide seamless configuration of haptic feedback control systems for use in a variety of RMIS applications.

Additional modalities of feedback were also introduced by engineering technologies that provide kinesthetic force feedback and vibration feedback. These technologies were designed with considerations for behaviors of the human neuromuscular and somatosensory systems and extensively optimized to provide fast response times.

Finally, the developed multi-modal HFS was evaluated through application in several different robotic surgical tasks. A suture breakage warning system utilizing shear sensors and the vibration feedback modality showed that feedback could help reduce instances of suture failure, while simultaneously improving knot quality. A hybrid vibro-tactile feedback system was used to highlight the benefits of the multi-modal HFS in identifying structures such as vessels and tumors in soft tissue. Bi-modal and tri-modal haptic feedback systems were also used to show the benefits of multi-modal HFS in reduction of grip force, both in robotic peg transfer tasks and in ex-vivo bowel run experiments.

Together the results of these investigations highlight the importance and impact that multi-modal haptic feedback systems can have in reducing risk of tissue damage and improving performance in robotic surgery. The benefit of multi-modal HFS over single-modality feedback lies in its ability to target and recruit a variety of mechanoreceptors in the skin and the muscles, therefore better simulating real human touch. This investigation can therefore serve as the foundation for further research into multi-modal haptic feedback systems and their potential in developing the future of haptics in robotic surgery.

9 FUTURE WORK

Even though significant advances have been made in haptic feedback technologies and their application for robotic minimally invasive surgery, there are still many areas of research that remain unexplored. Based on the results of this work, the following sections aim to highlight potential avenues for advancements in this field.

9.1 ADAPTIVE HAPTIC FEEDBACK

The pneumatic tactile and kinesthetic feedback systems developed and evaluated throughout this investigation have relied on predefined pressure levels. This means that every subject received the same feedback in response to some force applied to the tissue. Due to significant variation in the skin sensitivity and muscle strength of different individuals, feedback systems can, in some rare situations, have a negative impact on the performance of some subjects (Section 7.3.2). In most cases, this is resolved through additional training with the feedback system. However in reality, the best solution would be to develop an adaptive feedback system that can learn the user's behavior and adjust feedback levels accordingly.

The current multi-modal HFS already provides the ability to export the configuration of the logic engine as a user/controller profile. Expanding the current logic engine to allow the system to automatically adjust the parameters of various feedback rules to improve the performance of the user is therefore feasible. Such a system can potentially lead to a much more natural feeling HFS that would be optimized for each user and require little to no training at all.

9.2 BI-AXIAL SHEAR SENSING

The development of uni-axial shear sensors (Section 5.4) and their application in a suture breakage warning system (Section 7.1) showed the potential benefits of HFS in improving outcomes of knot tying tasks for RMIS. In real world surgical conditions, uni-axial shear sensors are not sufficient to detect all the forces applied to a suture. This is because a suture is rarely ever pulled only in the same axis that the sensor can detect shear. Therefore, the development of a bi-axial shear sensor can be critical for this technology to be applied to real-world clinical conditions.

As a proof of concept, a bi-axial variant of the uni-axial shear sensor was investigated, though not fabricated, due to limitations in the resolution of 3D printing technology. This bi-axial sensor design relies on the same two piezoresistive sensors, however it utilizes a slight modification to the inner chamber of the sensor's outer shell and a differential technique to identify shear in two axis. An overview of this design concept can be seen in Figure 87.

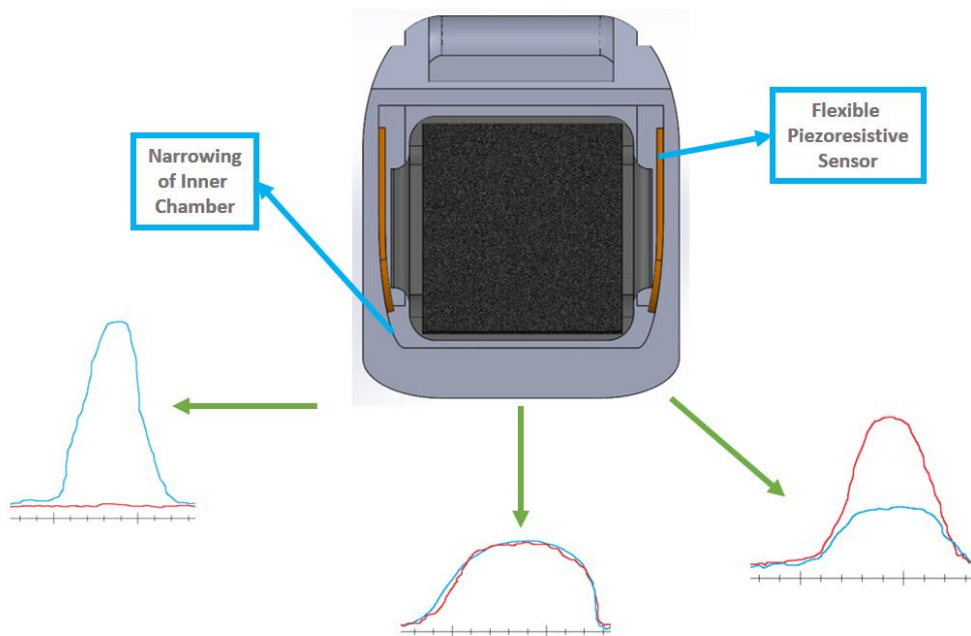


Figure 87: Bi-Axial Shear Sensing Concept Based on Differential Sensing Methods.

9.3 TRI-AXIAL TACTILE FEEDBACK ACTUATORS

The investigation of the suture breakage warning system which utilizes shear sensors to improve outcomes of knot tying tasks in RMIS, relies on vibration feedback for conveying information about shear sensors. While effective as a warning mechanism, in reality, vibration motors are not the ideal method for conveying shear forces. The sense of shear results from deformations in the surface of the skin while the sense of slipping involves a combination of skin deformation and activation of fast acting mechanoreceptors in the skin (normally also involved in detecting vibration).

The development of a tri-axial tactile feedback actuator that can not only provide normal force tactile feedback, but also convey bi-axial shear forces, and sense of slippage, can be the next step in bringing multi-modal HFS one step closer to real touch. Skin deformation as a feedback modality has previously been discussed in literature⁸⁸. Such an actuator would build up upon the work performed on the pneumatic normal force tactile feedback, vibration feedback and skin deformation feedback to help develop a multi-modal tactile actuator.

9.4 PRE-CLINICAL EVALUATION OF MULTI-MODAL HFS

The evaluation of the tri-modal feedback system and the ex-vivo studies performed highlight the benefits of multi-modal HFS in RMIS tasks involving tissue manipulation. The next step is to perform an in-vivo evaluation of the multi-modal haptic feedback system. Robot-assisted laparoscopic Total Mesorectal Excision (TME) is one possible procedure that can benefit from

HFS. Such an investigation would focus on the benefits of HFS in reducing risk of pelvic autonomic nerve injury by enabling surgeons to perform the dissection with less force.

10 REFERENCES

1. Lau WY, Leow CK LA. History of endoscopic and laparoscopic surgery. *World J Surg.* 1997;21:444-453.
2. Jacobs JK, Goldstein RE, Geer RJ. *Laparoscopic Adrenalectomy. A New Standard of Care.* Vol 225.; 1997.
3. Lum MJH, Friedman DCW, King HHI, et al. Teleoperation of a surgical robot via airborne wireless radio and transatlantic internet links. In: *Springer Tracts in Advanced Robotics.* Vol 42. ; 2008:305-314. doi:10.1007/978-3-540-75404-6_29.
4. Madhani AJ, Niemeyer G, Salisbury JK. J. The Black Falcon: a teleoperated surgical instrument for minimallyinvasive surgery. *Proceedings 1998 IEEE/RSJ Int Conf Intell Robot Syst Innov Theory, Pract Appl (Cat No98CH36190).* 1998;2. doi:10.1109/IROS.1998.727320.
5. Taylor R. A Steady-Hand Robotic System for Microsurgical Augmentation. *Int J Rob Res.* 1999;18:1201-1210. doi:10.1177/02783649922067807.
6. Çavuşoğlu MC, Tendick F, Cohn M, Sastry SS. A laparoscopic telesurgical workstation. *IEEE Trans Robot Autom.* 1999;15:728-739. doi:10.1109/70.782027.
7. Das H, Zak H, Johnson J, Crouch J, Frambach D. Evaluation of a telerobotic system to assist surgeons in microsurgery. *Comput Aided Surg.* 1999;4:15-25. doi:10.1002/(SICI)1097-0150(1999)4:1<15::AID-IGS2>3.0.CO;2-0.
8. McBeth PB, Louw DF, Rizun PR, Sutherland GR. Robotics in neurosurgery. *Am J Surg.* 2004;188. doi:10.1016/j.amjsurg.2004.08.004.
9. Buess GF, Schurr MO, Fischer SC. Robotics and allied technologies in endoscopic surgery.

- Arch Surg.* 2000;135:229-235. doi:10.1001/archsurg.135.2.229.
10. Brown JD, Rosen J, Chang L, Sinanan MN, Hannaford B. Quantifying surgeon grasping mechanics in laparoscopy using the blue DRAGON system. In: *Studies in Health Technology and Informatics*. Vol 98. ; 2004:34-36. doi:10.3233/978-1-60750-942-4-34.
 11. Strong VE, Devaud N, Allen PJ, Gonen M, Brennan MF, Coit D. Laparoscopic versus open subtotal gastrectomy for adenocarcinoma: a case-control study. *Ann Surg Oncol.* 2009;16:1507-1513. doi:10.1245/s10434-009-0386-8.
 12. Dageforde LA, Moore DR, Landman MP, et al. Comparison of open live donor nephrectomy, laparoscopic live donor nephrectomy, and hand-assisted live donor nephrectomy: A cost-minimization analysis. *J Surg Res.* 2012;176. doi:10.1016/j.jss.2011.12.013.
 13. Sackier JM, Wang Y. Robotically assisted laparoscopic surgery. *Surg Endosc.* 1994;8(1):63-66. doi:10.1007/BF02909496.
 14. Shah J, Buckley D, Frisby J, Darzi A. Depth cue reliance in surgeons and medical students. *Surg Endosc Other Interv Tech.* 2003;17(9):1472-1474. doi:10.1007/s00464-002-9178-y.
 15. Cartmill JA, Shakeshaft AJ, Walsh WR, Martin CJ. HIGH PRESSURES ARE GENERATED AT THE TIP OF LAPAROSCOPIC GRASPERS. *ANZ J Surg.* 1999;69(2):127-130. doi:10.1046/j.1440-1622.1999.01496.x.
 16. Heijnsdijk EAM, van der Voort M, de Visser H, Dankelman J, Gouma DJ. Inter- and intraindividual variabilities of perforation forces of human and pig bowel tissue. *Surg Endosc.* 2003;17(12):1923-1926. doi:10.1007/s00464-003-9002-3.
 17. De S, Rosen J, Dagan a., Hannaford B, Swanson P, Sinanan M. Assessment of Tissue Damage due to Mechanical Stresses. *Int J Rob Res.* 2007;26(11-12):1159-1171.

doi:10.1177/0278364907082847.

18. Anup R, Balasubramanian K a. Surgical stress and the gastrointestinal tract. *J Surg Res.* 2000;92(2):291-300. doi:10.1006/jsre.2000.5874.
19. Culjat MO, King C-H, Franco ML, et al. A tactile feedback system for robotic surgery. *Conf Proc IEEE Eng Med Biol Soc.* 2008;2008:1930-1934. doi:10.1109/IEMBS.2008.4649565.
20. CR. W. An investigation into the benefits of tactile feedback for laparoscopic, robotic, and remote surgery. 2013. <https://escholarship.org/uc/item/7w74q3wh.pdf>.
21. van der Meijden OA, Schijven MP. The value of haptic feedback in conventional and robot-assisted minimal invasive surgery and virtual reality training: a current review. *Surg Endosc.* 2009;23(6):1180-1190. doi:10.1007/s00464-008-0298-x.
22. Schoonmaker RE, Cao CGL. Vibrotactile force feedback system for minimally invasive surgical procedures. *2006 IEEE Int Conf Syst Man Cybern.* 2006;3(September):2464-2469. doi:10.1109/ICSMC.2006.385233.
23. Pacchierotti C, Meli L, Chinello F, Malvezzi M, Prattichizzo D. Cutaneous haptic feedback to ensure the stability of robotic teleoperation systems. *Int J Rob Res.* 2015:1-14. doi:10.1177/0278364915603135.
24. AKAMATSU M, MACKENZIE IS, HASBROUCQ T. A comparison of tactile, auditory, and visual feedback in a pointing task using a mouse-type device. *Ergonomics.* 1995;38(4):816-827. doi:10.1080/00140139508925152.
25. Wottawa CR, Genovese B, Nowroozi BN, et al. Evaluating tactile feedback in robotic surgery for potential clinical application using an animal model. *Surg Endosc.* 2016;30(8):3198-3209. doi:10.1007/s00464-015-4602-2.
26. Cullen KA, Hall MJ, Golosinskiy A. Ambulatory surgery in the United States, 2006. *Natl*

- Health Stat Report*. 2009;1-25. doi:5/9/2013.
27. Gould JC, Kent KC, Wan Y, Rajamanickam V, Levenson G, Campos GM. Perioperative safety and volume: Outcomes relationships in bariatric surgery: A study of 32,000 patients. *J Am Coll Surg*. 2011;213:771-777. doi:10.1016/j.jamcollsurg.2011.09.006.
 28. Niebisch S, Peters JH. Update on fundoplication for the treatment of GERD. *Curr Gastroenterol Rep*. 2012;14:189-196. doi:10.1007/s11894-012-0256-6.
 29. Jacoby VL, Autry A, Jacobson G, Domush R, Nakagawa S, Jacoby A. Nationwide use of laparoscopic hysterectomy compared with abdominal and vaginal approaches. *Obstet Gynecol*. 2009;114:1041-1048. doi:10.1097/AOG.0b013e3181b9d222.
 30. Mamidanna R, Burns EM, Bottle A, et al. Reduced Risk of Medical Morbidity and Mortality in Patients Selected for Laparoscopic Colorectal Resection in England: A Population-Based Study. *Arch Surg*. 2012;147:219-227. doi:10.1001/archsurg.2011.311.
 31. Gelmini R, Franzoni C, Spaziani A, Patrìti A, Casciola L, Saviano M. Laparoscopic splenectomy: conventional versus robotic approach--a comparative study. *J Laparoendosc Adv Surg Tech A*. 2011;21:393-398. doi:10.1089/lap.2010.0564.
 32. Grena. Endo instruments. [https://www.grena.co.uk/images/products/Endo instruments.jpg](https://www.grena.co.uk/images/products/Endo_instruments.jpg). Accessed May 2, 2017.
 33. UPMC. Laparoscopic liver surgery at UPMC. <https://www.youtube.com/watch?v=BsCssx4nsiQ>. Accessed May 2, 2017.
 34. Tsui C, Klein R, Garabrant M. Minimally invasive surgery: National trends in adoption and future directions for hospital strategy. *Surg Endosc Other Interv Tech*. 2013;27(7):2253-2257. doi:10.1007/s00464-013-2973-9.
 35. Lanfranco AR, Castellanos AE, Desai JP, Meyers WC. Robotic surgery: a current

- perspective . *Ann Surg.* 2004;239(1):14-21. doi:10.1097/01.sla.0000103020.19595.7d [doi].
36. Satava RM. Surgical robotics: the early chronicles: a personal historical perspective. *Surg Laparosc Endosc Percutan Tech.* 2002;12(1):6-16. doi:10.1097/00129689-200202000-00002.
 37. Schurr MO, Arezzo A, Buess GF. Robotics and systems technology for advanced endoscopic procedures: Experiences in general surgery. In: *European Journal of Cardio-Thoracic Surgery.* Vol 16. ; 1999. doi:10.1016/S1010-7940(99)00281-X.
 38. Berkelman PJ, Whitcomb LL, Taylor RH, Jensen P. A Miniature Microsurgical Instrument Tip Force Sensor for Enhanced Force Feedback During Robot-Assisted Manipulation. *IEEE Trans Robot Autom.* 2003;19(5):917-922. doi:10.1109/TRA.2003.817526.
 39. Louw DF, Fielding T, McBeth PB, et al. Surgical robotics: A review and neurosurgical prototype development. *Neurosurgery.* 2004;54(3):525-537. doi:10.1227/01.NEU.0000108638.05274.E9.
 40. Jacob BP, Gagner M. Robotics and general surgery. *Surg Clin North Am.* 2003;83(6):1405-1419. doi:10.1016/S0039-6109(03)00159-2.
 41. Moorthy K, Munz Y, Dosis a, et al. Dexterity enhancement with robotic surgery. *Surg Endosc.* 2004;18(5):790-795. doi:10.1007/s00464-003-8922-2.
 42. Munz Y, Moorthy K, Dosis a, et al. The benefits of stereoscopic vision in robotic-assisted performance on bench models. *Surg Endosc.* 2004;18(4):611-616. doi:10.1007/s00464-003-9017-9.
 43. Jourdan IC, Dutson E, Garcia A, et al. Stereoscopic vision provides a significant advantage for precision robotic laparoscopy. *Br J Surg.* 2004;91(7):879-885. doi:10.1002/bjs.4549.

44. Ijsselsteijn WA, De Ridder H, Vliegen J. Subjective evaluation of stereoscopic images: Effects of camera parameters and display duration. *IEEE Trans Circuits Syst Video Technol.* 2000;10(2):225-233. doi:10.1109/76.825722.
45. Alemzadeh H, Iyer RK, Kalbarczyk Z, Leveson N, Raman J. Adverse Events in Robotic Surgery: A Retrospective Study of 14 Years of FDA Data. *CoRR.* 2015;(January):1-30. doi:10.1371/journal.pone.0151470.
46. Schluender S, Conrad J, Divino CM, Gurland B. Robot-assisted laparoscopic repair of ventral hernia with intracorporeal suturing: An experimental study. *Surg Endosc Other Interv Tech.* 2003;17(9):1391-1395. doi:10.1007/s00464-002-8795-9.
47. Kang CM, Kim DH, Lee WJ, Chi HS. Conventional laparoscopic and robot-assisted spleen-preserving pancreatectomy: Does da Vinci have clinical advantages? *Surg Endosc Other Interv Tech.* 2011;25(6):2004-2009. doi:10.1007/s00464-010-1504-1.
48. Beutler WJ, Peppelman WC, DiMarco LA. The da Vinci Robotic Surgical Assisted Anterior Lumbar Interbody Fusion. *Spine (Phila Pa 1976).* 2013;38(4):356-363. doi:10.1097/BRS.0b013e31826b3d72.
49. Herron DM, Marohn M. A consensus document on robotic surgery. *Surg Endosc.* 2008;22(2):313-325. doi:10.1007/s00464-007-9727-5.
50. Corcione F, Esposito C, Cuccurullo D, et al. Advantages and limits of robot-assisted laparoscopic surgery: Preliminary experience. *Surg Endosc Other Interv Tech.* 2005;19(1):117-119. doi:10.1007/s00464-004-9004-9.
51. Cestari A, Ferrari M, Zanoni M, et al. Side docking of the da Vinci robotic system for radical prostatectomy: advantages over traditional docking. *J Robot Surg.* 2015;9(3):243-247. doi:10.1007/s11701-015-0523-2.

52. Hong WC, Tsai JC, Chang SD, Sorger JM. Robotic skull base surgery via supraorbital keyhole approach: A cadaveric study. *Neurosurgery*. 2013;72(SUPPL. 1):33-38. doi:10.1227/NEU.0b013e318270d9de.
53. Marcus HJ, Hughes-Hallett A, Cundy TP, Yang GZ, Darzi A, Nandi D. da Vinci robot-assisted keyhole neurosurgery: a cadaver study on feasibility and safety. *Neurosurg Rev*. 2015;38(2):367-371. doi:10.1007/s10143-014-0602-2.
54. Bethea BT, Okamura AM, Kitagawa M, et al. Application of haptic feedback to robotic surgery. *J Laparoendosc Adv Surg Tech A*. 2004;14(3):191-195. doi:10.1089/1092642041255441.
55. Koehn JK, Kuchenbecker KJ. Surgeons and non-surgeons prefer haptic feedback of instrument vibrations during robotic surgery. *Surg Endosc Other Interv Tech*. 2015;29(10):2970-2983. doi:10.1007/s00464-014-4030-8.
56. McMahan W, Gomez ED, Chen L, et al. A practical system for recording instrument interactions during live robotic surgery. *J Robot Surg*. 2013;7(4):351-358. doi:10.1007/s11701-013-0399-y.
57. Kitagawa M, Dokko D, Okamura AM, Yuh DD. Effect of sensory substitution on suture-manipulation forces for robotic surgical systems. *J Thorac Cardiovasc Surg*. 2005;129(1):151-158. doi:10.1016/j.jtcvs.2004.05.029.
58. King CH, Culjat MO, Franco ML, et al. Tactile feedback induces reduced grasping force in robot-assisted surgery. *IEEE Trans Haptics*. 2009;2:103-110. doi:10.1109/TOH.2009.4.
59. Okamura AM. Haptic feedback in robot-assisted minimally invasive surgery. *Curr Opin Urol*. 2009;19(1):102-107. doi:10.1097/MOU.0b013e32831a478c.
60. Enayati N, De Momi E, Ferrigno G. Haptics in robot-assisted surgery: Challenges and

- benefits. *IEEE Rev Biomed Eng.* 2016;9:49-65. doi:10.1109/RBME.2016.2538080.
61. Okamura AM, Verner LN, Reiley CE, Mahvash M. Haptics for robot-assisted minimally invasive surgery. In: *Springer Tracts in Advanced Robotics*. Vol 66. ; 2010:361-372. doi:10.1007/978-3-642-14743-2_30.
 62. Westebring-van der Putten EP, Goossens RHM, Jakimowicz JJ, Dankelman J. Haptics in minimally invasive surgery--a review. *Minim Invasive Ther Allied Technol.* 2008;17(1):3-16. doi:10.1080/13645700701820242.
 63. Reiley CE, Akinbiyi T, Burschka D, Chang DC, Okamura AM, Yuh DD. Effects of visual force feedback on robot-assisted surgical task performance. *J Thorac Cardiovasc Surg.* 2008;135(1):196-202. doi:10.1016/j.jtcvs.2007.08.043.
 64. Coratti A, Annecchiarico M. Robotics in general surgery: Current status and critical review. *OA Robot Surg.* 2013;01;1(1):5.
 65. Bach-y-Rita P, W. Kercel S. Sensory substitution and the human-machine interface. *Trends Cogn Sci.* 2003;7(12):541-546. doi:10.1016/j.tics.2003.10.013.
 66. Schostek S, Schurr MO, Buess GF. Review on aspects of artificial tactile feedback in laparoscopic surgery. *Med Eng Phys.* 2009;31(8):887-898. doi:10.1016/j.medengphy.2009.06.003.
 67. VITENSE HS, JACKO JA, EMERY VK. Multimodal feedback: an assessment of performance and mental workload. *Ergonomics.* 2003;46(1-3):68-87. doi:10.1080/00140130303534.
 68. Giabbiconi C-M, Trujillo-Barreto NJ, Gruber T, Müller MM. Sustained spatial attention to vibration is mediated in primary somatosensory cortex. *Neuroimage.* 2007;35(1):255-262. doi:http://doi.org/10.1016/j.neuroimage.2006.11.022.

69. Lécuyer A, Coquillart S, Kheddar A, Richard P, Coiffet P. Pseudo-Haptic Feedback: Can Isometric Input Devices Simulate Force Feedback? *Proc IEEE Virtual Real Conf.* 2000:83-90. doi:10.1109/VR.2000.840369.
70. Prochazka A. Proprioceptive Feedback and Movement Regulation. In: *Comprehensive Physiology*. John Wiley & Sons, Inc.; 2010. doi:10.1002/cphy.cp120103.
71. Mirbagheri A, Dargahi J, Najarian S, Ghomshe FT. Design, fabrication, and testing of a membrane piezoelectric tactile sensor with four sensing elements. *Am J Appl Sci.* 2007;4(9):645-652.
72. Grundfest WS, Culjat MO, King C-H, et al. Development and testing of a tactile feedback system for robotic surgery. *Stud Health Technol Inform.* 2009;142:103-108. doi:10.3233/978-1-58603-964-6-103.
73. Covidien. Covidien Trocar. <https://abm-website-assets.s3.amazonaws.com/surgicalproductsmag.com/s3fs-public/Covidien.jpg>. Accessed May 2, 2017.
74. Intuitive Surgical. Cadiere Single Straight up. https://www.intuitivesurgical.com/test-drive/assets/images/instruments/Cadiere_Single_Straight_up.jpg. Accessed May 2, 2017.
75. CH King. Cadiere graspers with pressure sensor. <http://doi.ieeecomputersociety.org/cms/Computer.org/dl/trans/th/2009/02/figures/tth20090201031.gif>. Accessed May 2, 2017.
76. Tekscan. flexiforce-a101-force-sensor. https://www.tekscan.com/sites/default/files/styles/product_image/public/flexiforce-a101-force-sensor-275-275_0.jpg?itok=x_fMT5ZT. Accessed May 2, 2017.
77. Tekscan. Flexiforce 1lb sensor. <https://www.parallax.com/sites/default/files/styles/full->

- size-product/public/30056.png?itok=djgKmaM1. Accessed May 2, 2017.
78. Tekscan. flexiforce-circuit. <https://www.tekscan.com/sites/default/files/flexiforce-circuit.jpg>. Accessed May 2, 2017.
 79. Tekscan. a101-force-resistance-conductance-chart. <https://www.tekscan.com/sites/default/files/a101-force-resistance-conductance-chart-2.png>. Accessed May 2, 2017.
 80. Leineweber M, Pelz G, Schmidt M, Kappert H, Zimmer G. New tactile sensor chip with silicone rubber cover. *Sensors Actuators A Phys.* 2000;84(3):236-245. doi:[https://doi.org/10.1016/S0924-4247\(00\)00310-1](https://doi.org/10.1016/S0924-4247(00)00310-1).
 81. Palasagaram JN, Ramadoss R. MEMS-capacitive pressure sensor fabricated using printed-circuit-processing techniques. *IEEE Sens J.* 2006;6(6):1374-1375. doi:10.1109/JSEN.2006.884430.
 82. Paydar O, Abiri A, Genovese B, Candler R, Grundfest W, Dutson E. Capacitive Sensors to Prevent Suture Breakage in Robotic Surgery. In: *SAGES 2016.* ; 2016.
 83. Dai Y, Paydar O, Abiri A, et al. Miniature Multi-axis Force Sensor for Haptic Feedback System in Robotic Surgery. In: *EMBC 2016.* ; 2016.
 84. Yuan Dai, Abiri A, Liu S, et al. Grasper Integrated Tri-Axial Force Sensor System for Robotic Minimally Invasive Surgery. In: *EMBC 2017.* ; 2017.
 85. Wettels N, Fishel JA, Loeb GE. Multimodal tactile sensor. *Springer Tracts Adv Robot.* 2014;95:405-405. doi:10.1007/978-3-319-03017-3_19.
 86. Dargahi J, Parameswaran M, Payandeh S. Micromachined piezoelectric tactile sensor for an endoscopic grasper - theory, fabrication and experiments. *J Microelectromechanical Syst.* 2000;9(3):329-335. doi:10.1109/84.870059.

87. Najarian S, Dargahi J, Mehrizi A. *Artificial Tactile Sensing in Biomedical Engineering*. McGraw-Hill Education; 2009. <https://books.google.com/books?id=RCXCA2YK9a0C>.
88. Quek ZF, Schorr SB, Nisky I, Provancher WR, Okamura AM. Sensory Substitution and Augmentation Using 3-Degree-of-Freedom Skin Deformation Feedback. *IEEE Trans Haptics*. 2015;8(2):209-221. doi:10.1109/TOH.2015.2398448.
89. Debus T, Becker T, Dupont P, Jang T, Howe R. Multichannel vibrotactile display for sensory substitution during teleoperation. *2001 SPIE Int Symp Intell Syst Adv Manuf*. 2001:28-31. doi:10.1117/12.454744.
90. Johansson RS, Riso R, Häger C, Bäckström L. Somatosensory control of precision grip during unpredictable pulling loads - I. Changes in load force amplitude. *Exp Brain Res*. 1992;89(1):181-191. doi:10.1007/BF00229015.
91. Macefield VG, Häger-Ross C, Johansson RS. Control of grip force during restraint of an object held between finger and thumb: responses of cutaneous afferents from the digits. *Exp Brain Res*. 1996;108(1):155-171. doi:10.1007/BF00242913.
92. Pacchierotti C, Prattichizzo D, Kuchenbecker KJ. Cutaneous feedback of fingertip deformation and vibration for palpation in robotic surgery. *IEEE Trans Biomed Eng*. 2016;63(2):278-287. doi:10.1109/TBME.2015.2455932.
93. Pryor AD, Tushar JR, DiBernardo LR. Single-port cholecystectomy with the TransEnterix SPIDER: Simple and safe. *Surg Endosc Other Interv Tech*. 2010;24(4):917-923. doi:10.1007/s00464-009-0695-9.
94. Diana M, Marescaux J. Robotic surgery. *Br J Surg*. 2015;102(2):e15-e28. doi:10.1002/bjs.9711.
95. Konietschke R, Hagn U, Nickl M, et al. The DLR MiroSurge - A robotic system for surgery.

- In: *2009 IEEE International Conference on Robotics and Automation.* ; 2009:1589-1590.
doi:10.1109/ROBOT.2009.5152361.
96. Science Daily. Better Surgery With New Surgical Robot With Force Feedback.
 97. Hannaford B, Rosen J, Friedman D, et al. Raven-II: an open platform for surgical roboticsresearch. *IEEE Trans Biomed Eng.* 2013;60(4):954-959.
doi:10.1109/TBME.2012.2228858.
 98. Graham JL, Manuel SG, Johannes MS, Armiger RS. Development of a multi-modal haptic feedback system for dexterous robotic telemanipulation. In: *Conference Proceedings - IEEE International Conference on Systems, Man and Cybernetics.* ; 2011:3548-3553.
doi:10.1109/ICSMC.2011.6084219.
 99. Kokkinara E, Slater M, López-Moliner J. The Effects of Visuomotor Calibration to the Perceived Space and Body, through Embodiment in Immersive Virtual Reality. *ACM Trans Appl Percept.* 2015;13(1):1-22. doi:10.1145/2818998.
 100. Proske U, Gandevia SC. The kinaesthetic senses. *J Physiol.* 2009;17:4139-4146.
doi:10.1113/jphysiol.2009.175372.
 101. Peters JH, Fried GM, Swanstrom LL, et al. Development and validation of a comprehensive program of education and assessment of the basic fundamentals of laparoscopic surgery. *Surgery.* 2004;135(1):21-27. doi:10.1016/S0039-6060(03)00156-9.
 102. Franco ML, King CH, Culjat MO, et al. An integrated pneumatic tactile feedback actuator array for robotic surgery. *Int J Med Robot Comput Assist Surg.* 2009;5:13-19.
doi:10.1002/rcs.224.
 103. Abiri A, Tao A, LaRocca M, et al. Visual--perceptual mismatch in robotic surgery. *Surg Endosc.* 2016:1-8. doi:10.1007/s00464-016-5358-z.

104. Rank M, Shi Z, Müller HJ, Hirche S. Perception of Delay in Haptic Telepresence Systems. *Presence*. 2010;19(5):389-399. doi:10.1162/pres_a_00021.
105. Marsden CD, Merton PA, Morton HB. Stretch reflex and servo action in a variety of human muscles. *J Physiol*. 1976;259(2):531-560. doi:10.1113/jphysiol.1976.sp011481.
106. César Roberto de Souza. Accord.NET. <http://accord-framework.net/index.html>. Accessed May 6, 2017.
107. CodePlex. R.NET. <https://rdotnet.codeplex.com/team/view>. Accessed May 6, 2017.
108. Gentleman R, Ihaka R. R: The R Project for Statistical Computing. <https://www.r-project.org/>. Accessed May 6, 2017.
109. R-Project. Kickstarting R - Repeated Measures. https://cran.r-project.org/doc/contrib/Lemon-kickstart/kr_repms.html. Accessed May 6, 2017.
110. Tal Galili. Post hoc analysis for Friedman's Test. <https://www.r-statistics.com/2010/02/post-hoc-analysis-for-friedmans-test-r-code/>. Accessed May 6, 2017.
111. Thom Baguley. Beware the Friedman test. <https://seriousstats.wordpress.com/2012/02/14/friedman/>. Accessed May 6, 2017.
112. Salvatore S. Mangiafico. R Handbook: One-way Repeated Ordinal ANOVA with CLMM. http://rcompanion.org/handbook/G_08.html. Accessed May 6, 2017.
113. Bionics Lab. Raven Surgical Console. <https://i.ytimg.com/vi/Wn1IZV398UM/maxresdefault.jpg>. Accessed May 7, 2017.
114. Lindeman R, Yanagida Y, Sibert JL, Lavine R. Effective vibrotactile cueing in a visual search task. *Proc ninth IFIP TC13 Int Conf Human-computer Interact (INTERACT 2003)*. 2003:89-96.

http://books.google.com/books?hl=en&lr=&id=PTg0fVYqgCcC&oi=fnd&pg=PA89&dq=Effective+Vibrotactile+Cueing+in+a+Visual+Search+Task&ots=O8SKwzlyA_&sig=zW0TJW7PWU_5qhyYRH6QPBVjscI
<http://books.google.com/books?hl=en&lr=&id=PTg0fVYqgCcC&oi=fnd&pg=PA89&dq=Effec>.

115. Ho C, Tan HZ, Spence C. Using spatial vibrotactile cues to direct visual attention in driving scenes. *Transp Res Part F Traffic Psychol Behav.* 2005;8(6):397-412. doi:10.1016/j.trf.2005.05.002.
116. von Fraunhofer J a, Storey RS, Stone IK, Masterson BJ. Tensile strength of suture materials. *J Biomed Mater Res.* 1985;19(5):595-600. doi:10.1002/jbm.820190511.
117. Diks J, Nio D, Linsen MA, Rauwerda JA, Wisselink W. Suture damage during robot-assisted vascular surgery: is it an issue? *Surg Laparosc Endosc Percutan Tech.* 2007;17(6):524-527. doi:10.1097/SLE.0b013e318150e590.
118. Abiri A, Paydar O, Tao A, et al. Tensile strength and failure load of sutures for robotic surgery. *Surg Endosc.* 2017.
119. Culjat MO, King C-H, Franco ML, et al. A tactile feedback system for robotic surgery. *Conf Proc Int Conf IEEE Eng Med Biol Soc.* 2008;2008:1930-1934. <http://www.ncbi.nlm.nih.gov/pubmed/19377124>.
120. King C-H, Culjat MO, Franco ML, et al. A Multielement Tactile Feedback System for Robot-Assisted Minimally Invasive Surgery. *IEEE Trans Haptics.* 2009;2:52-56. doi:10.1109/TOH.2008.19.